Cosmology from the Abundance of SPT Clusters with DES and HST Weak Lensing

Sebastian Bocquet, LMU Munich

with Sebastian Grandis, Lindsey Bleem, Matthias Klein, Joe Mohr, Tim Schrabback
and the *South Pole Telescope* (SPT) and *Dark Energy Survey* (DES) collaborations

Image credit: SPT 2024 winter-overs Josh + Kevin

Cosmology

From the Big Bang to today

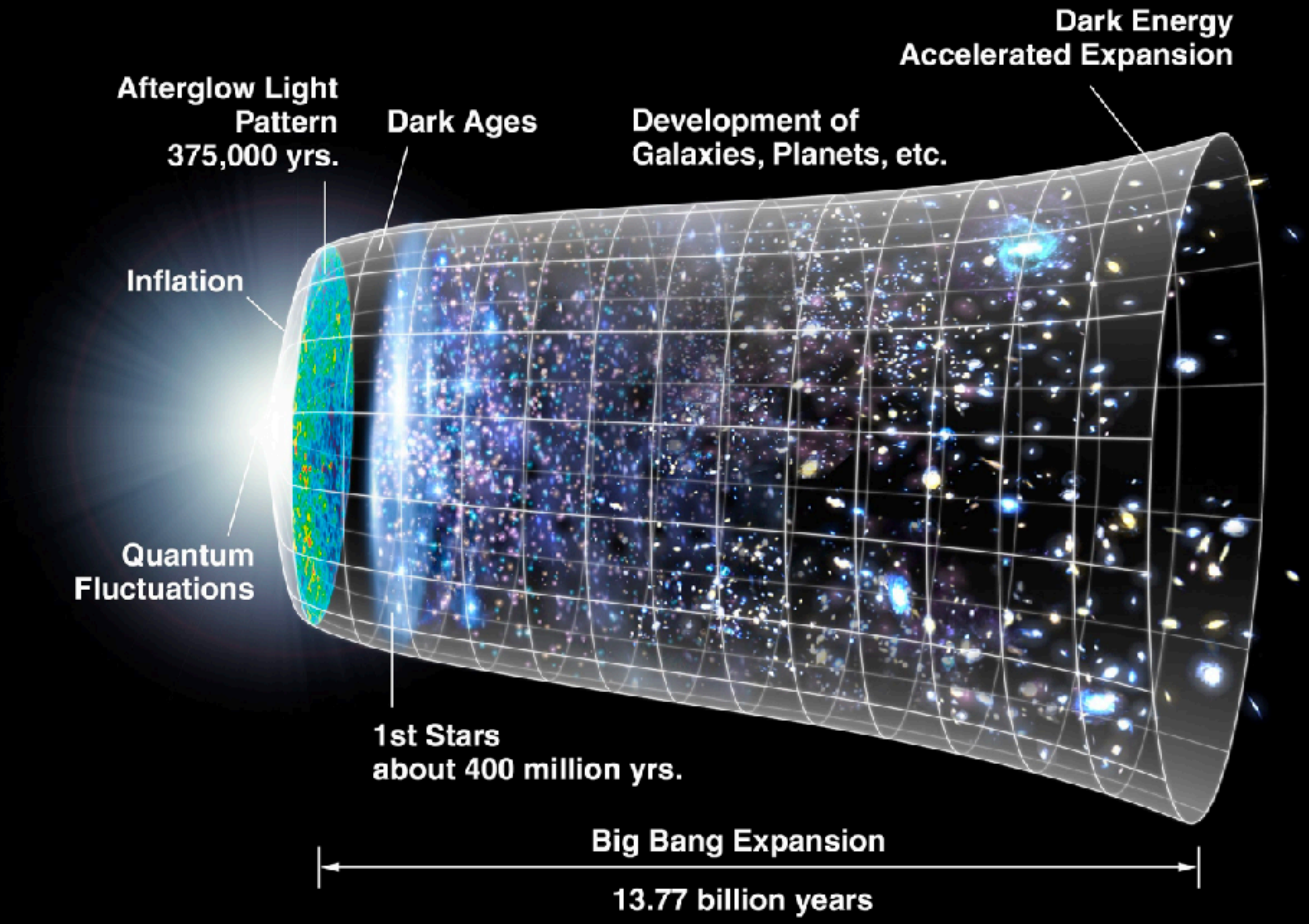

Cosmology

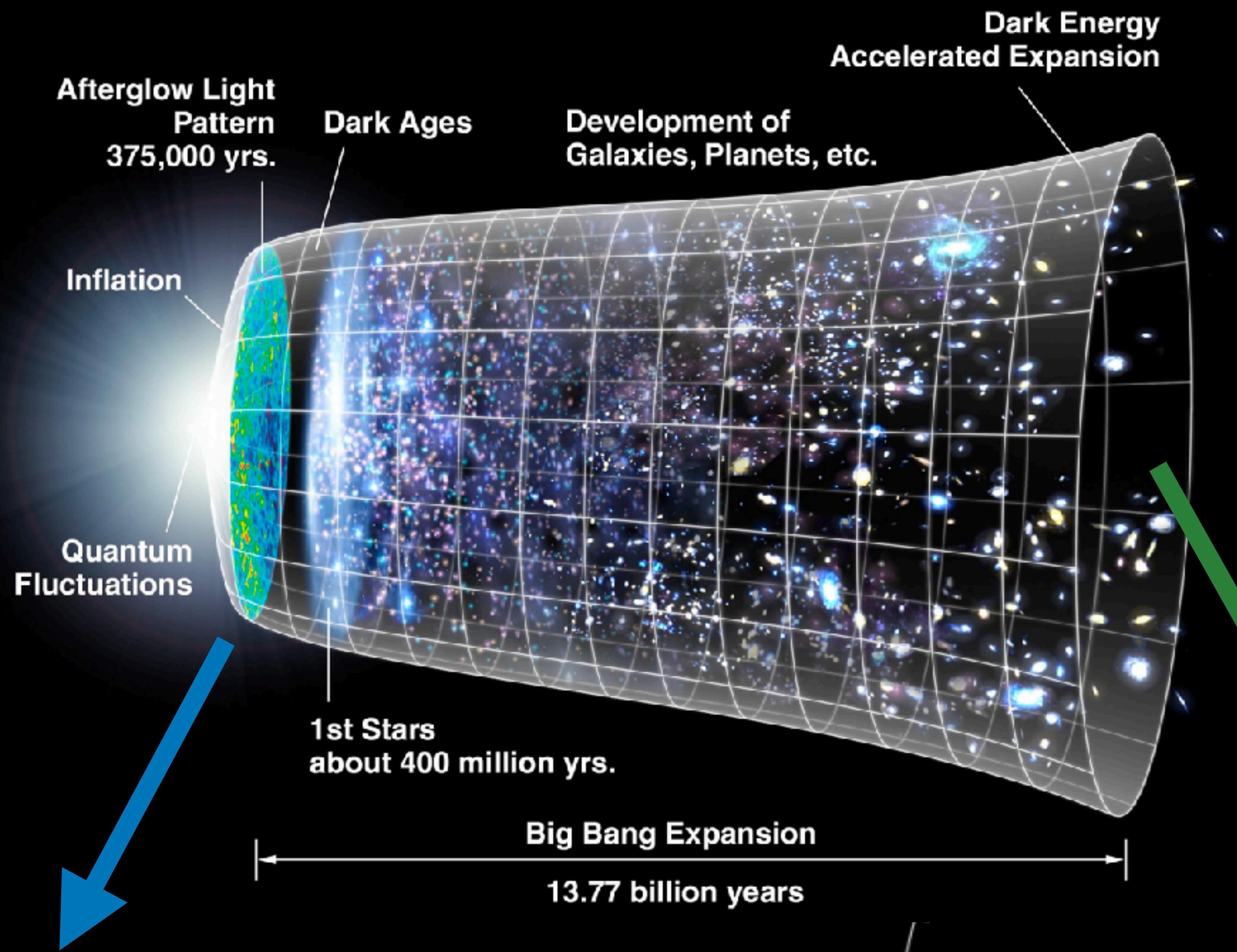
Dark Energy
Accelerated Expansion
Afterglow Light
Pattern
375,000 yrs.
Dark Ages
Development of
Galaxies, Planets, etc.
Inflation
Quantum
Fluctuations
1st Stars
about 400 million yrs.
Big Bang Expansion
13.77 billion years

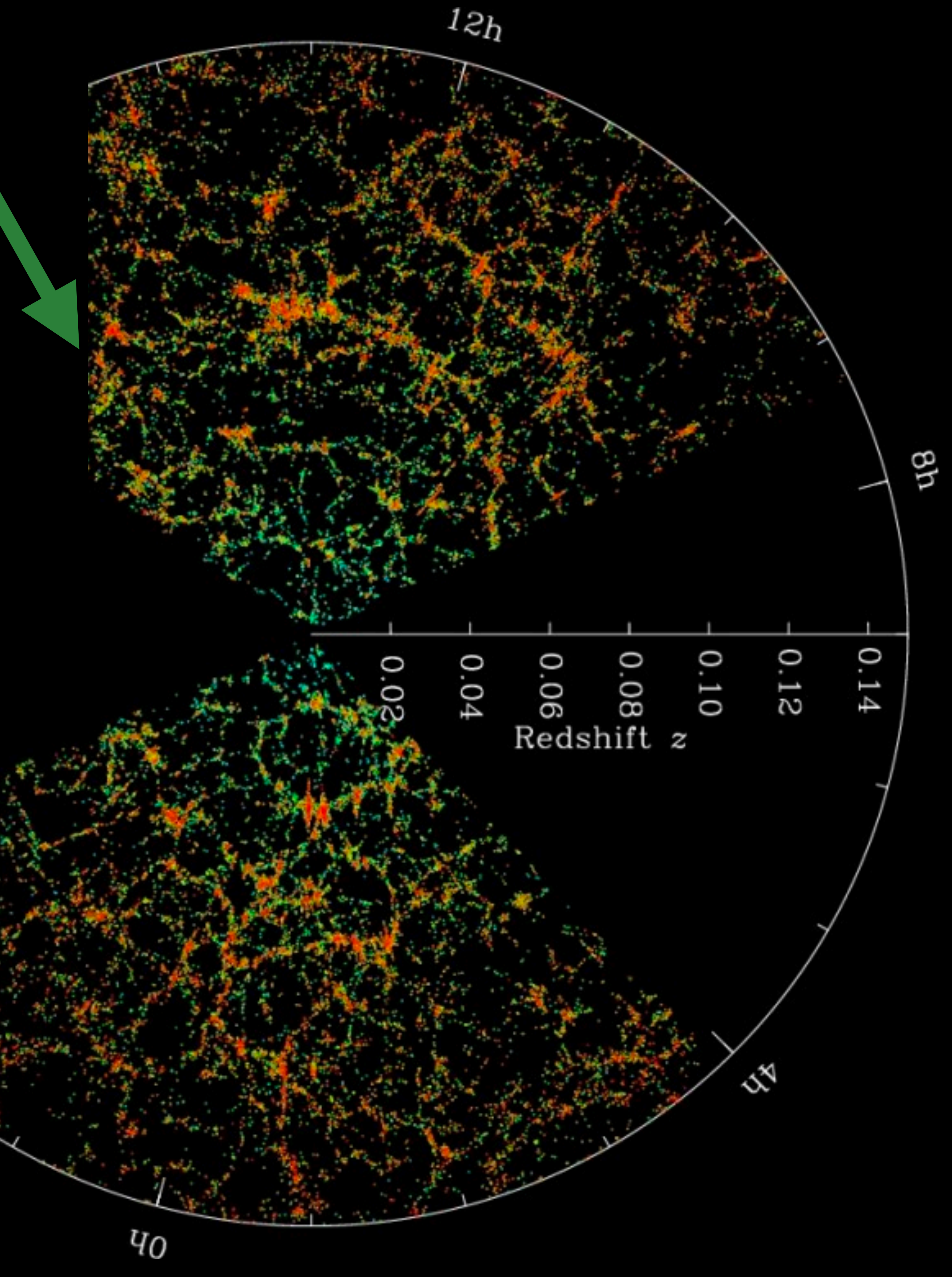
12h
8h
4h
0h
20h
0.02
0.04
0.06
0.08
0.10
0.12
0.14
Redshift z

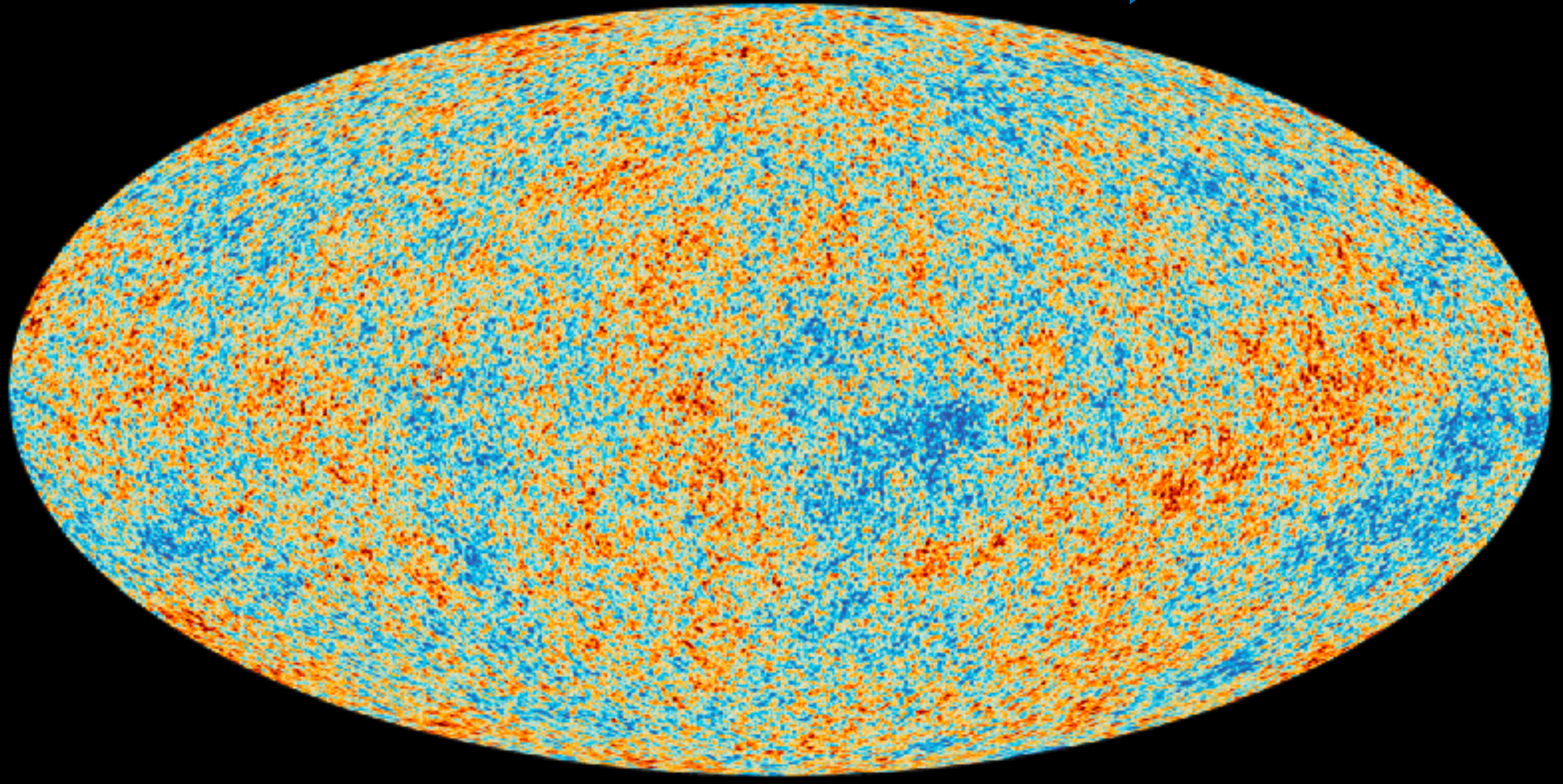

Cosmology

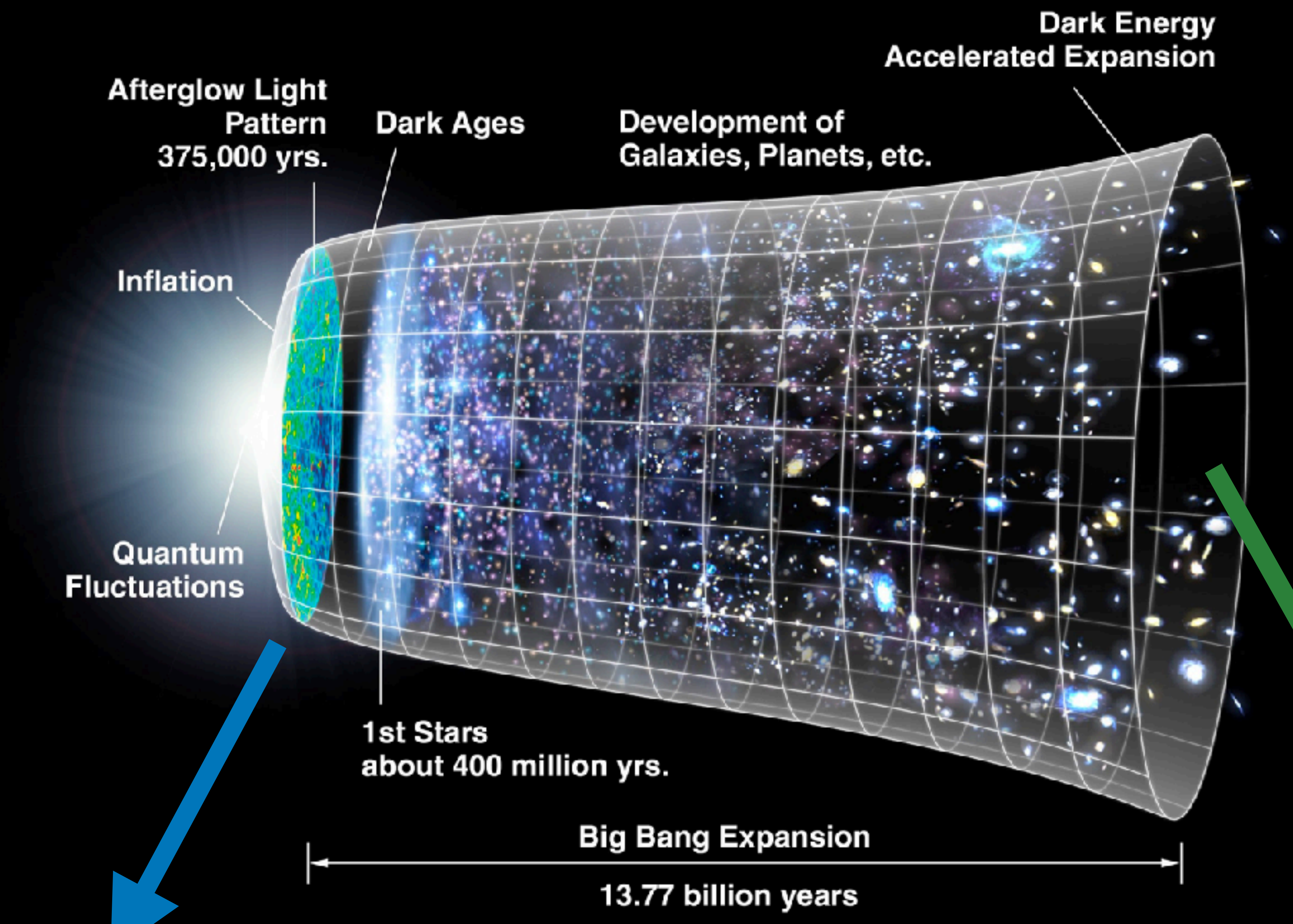

Dark Energy Accelerated Expansion
Afterglow Light Pattern 375,000 yrs.
Dark Ages
Development of Galaxies, Planets, etc.
Inflation
Quantum Fluctuations
1st Stars about 400 million yrs.
Big Bang Expansion
13.77 billion years

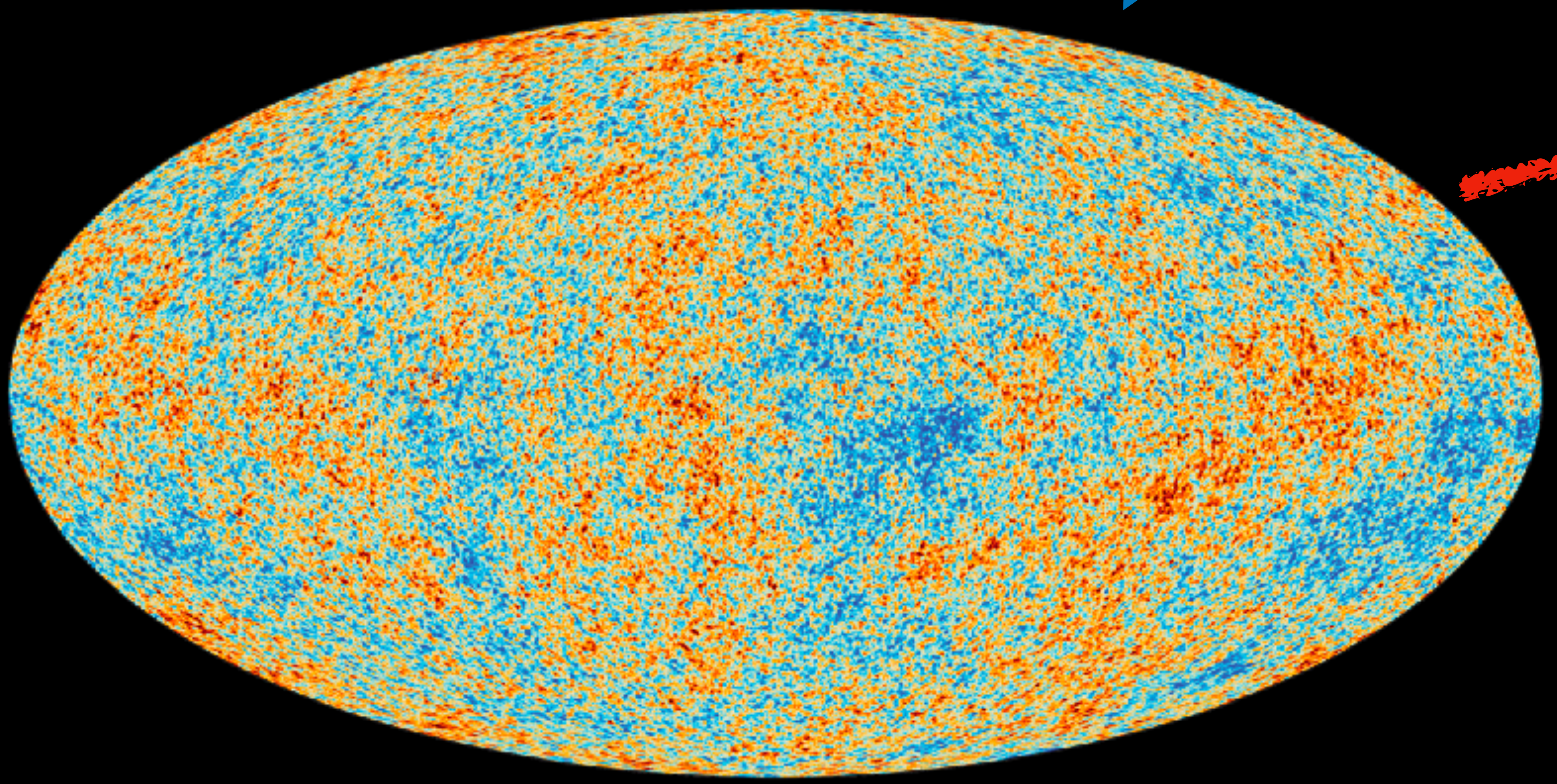

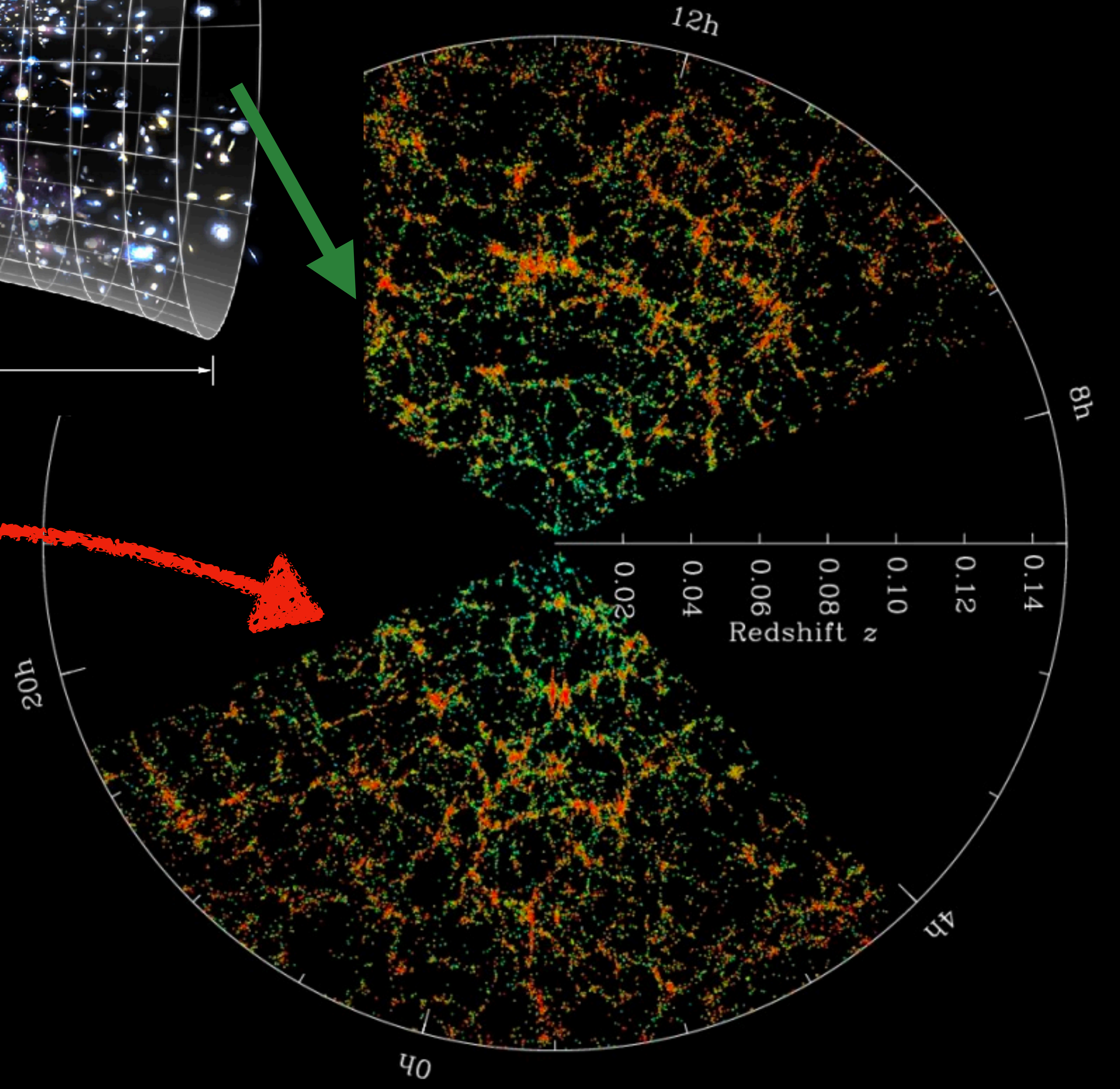

12h
8h
4h
0h
20h
0.02
0.04
0.06
0.08
0.10
0.12
0.14
Redshift z

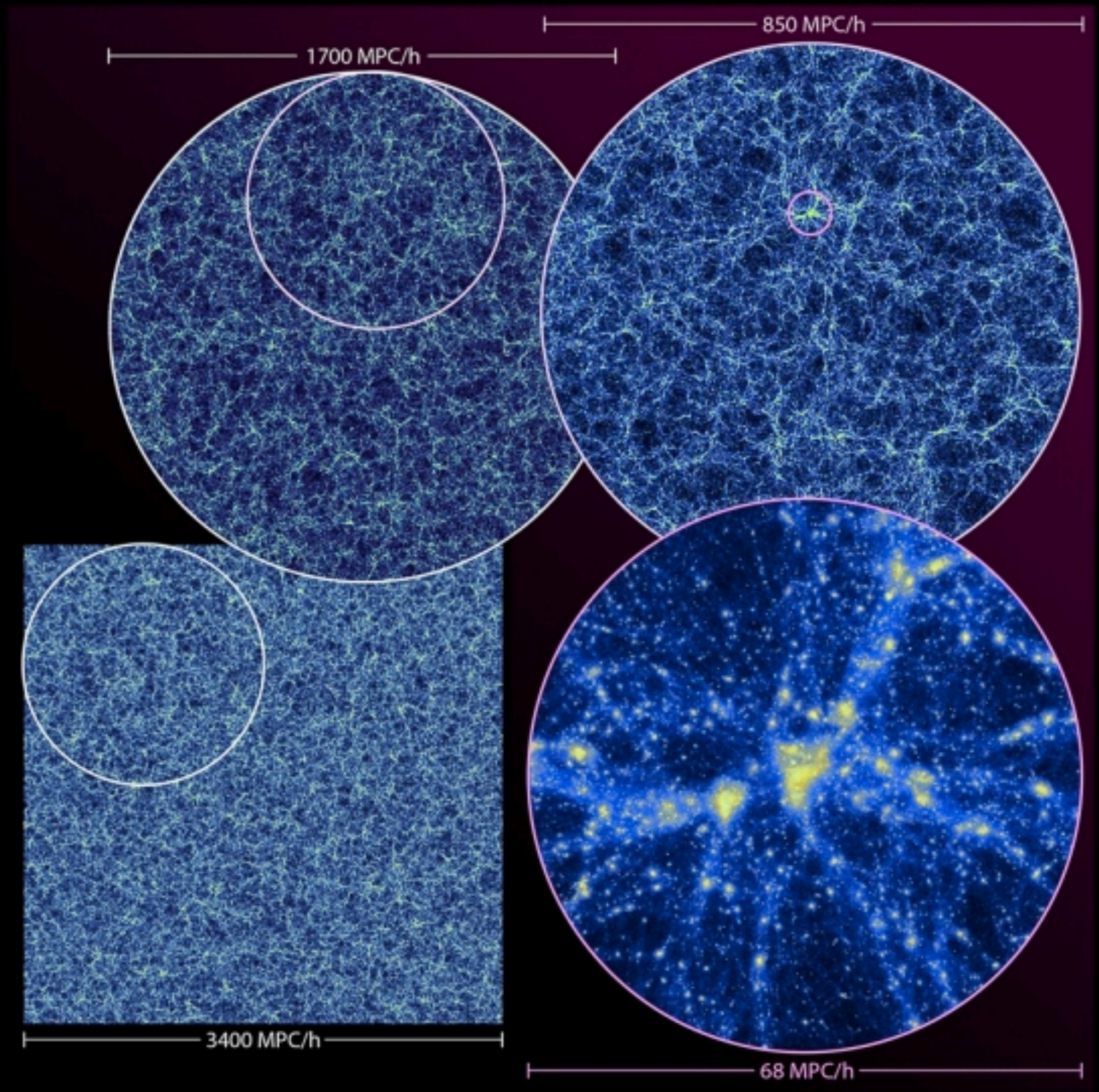

Last Journey (on Mira supercomputer)

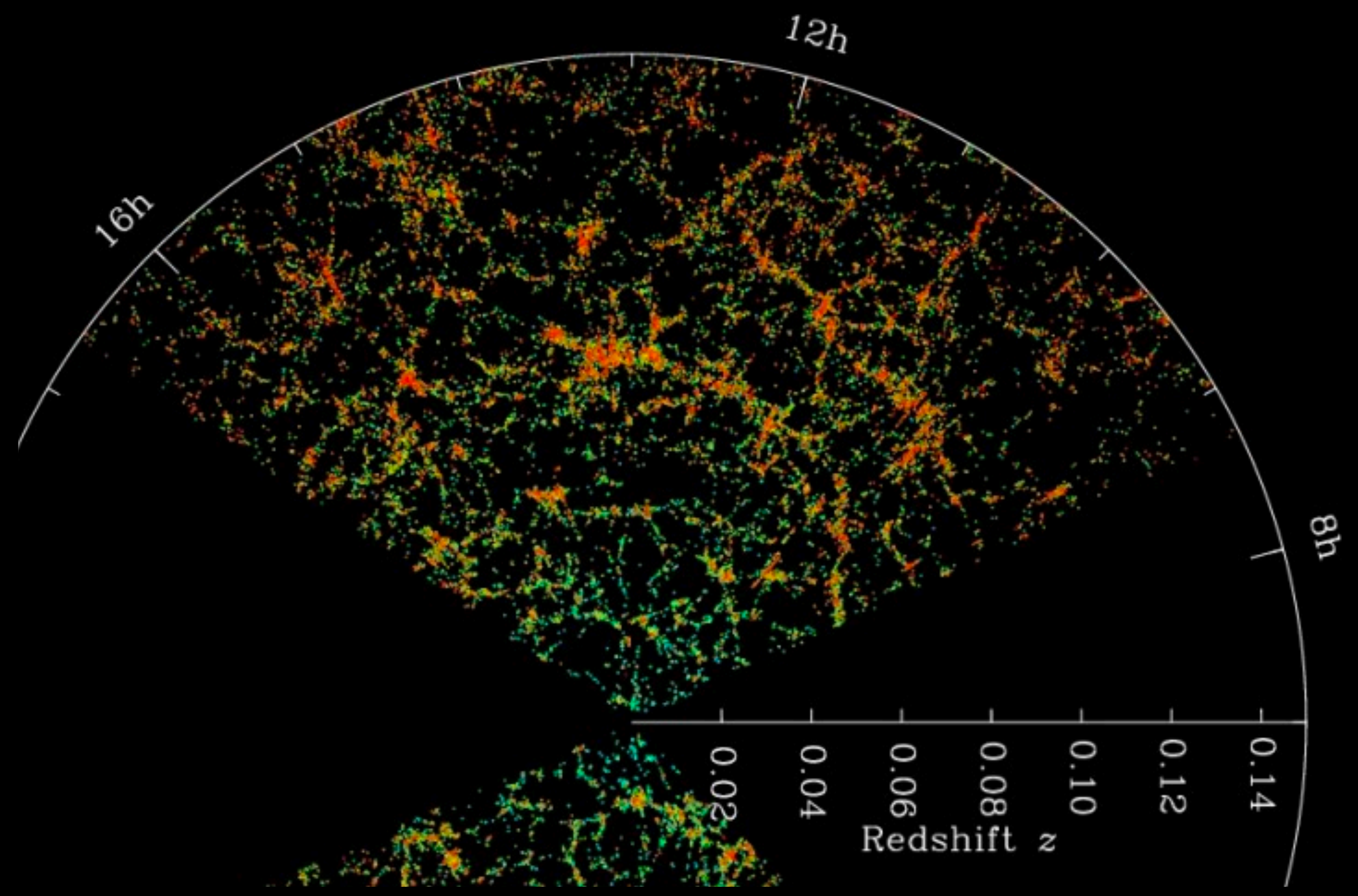

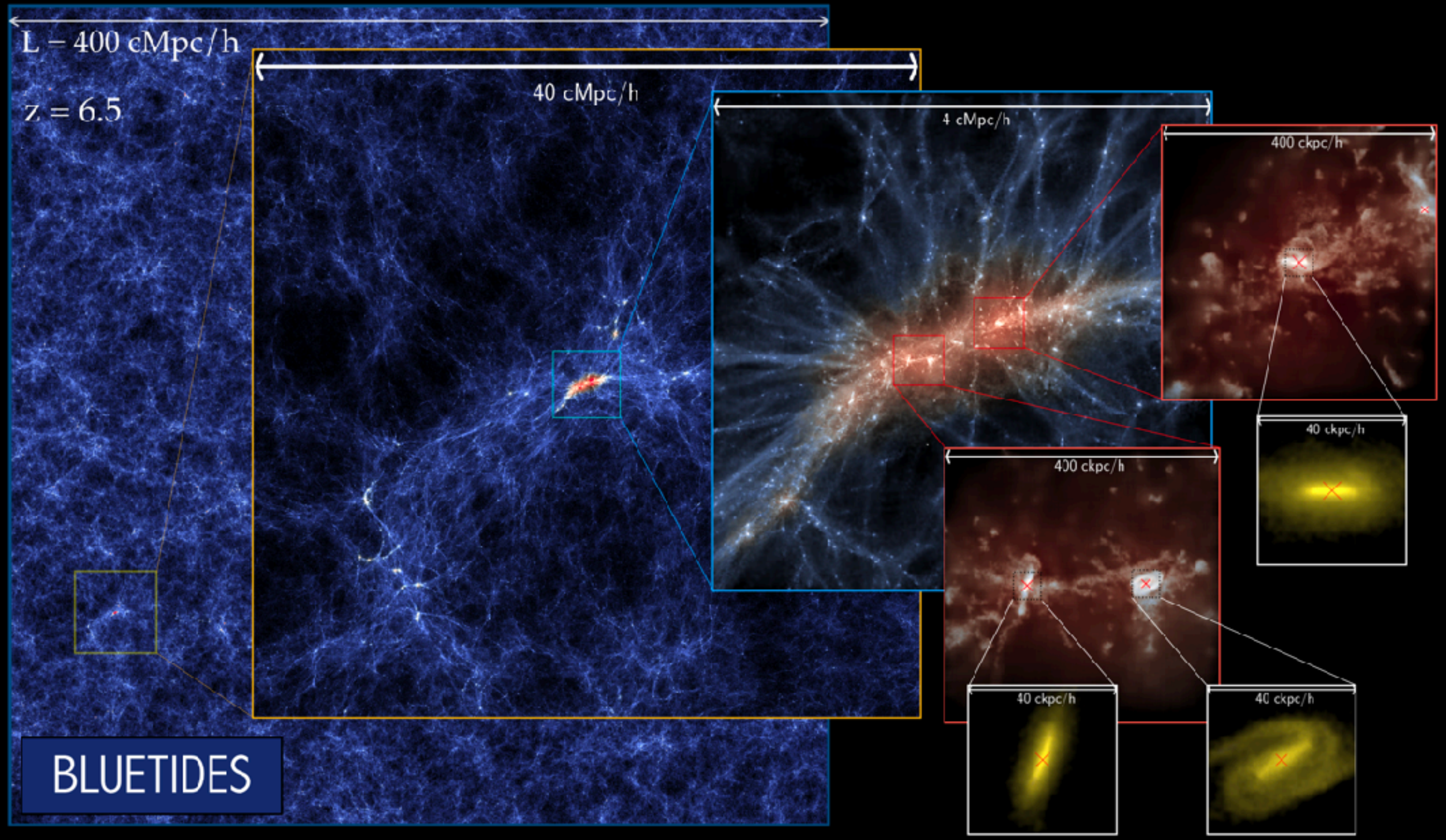

Cluster Cosmology

Why do we measure parameters?

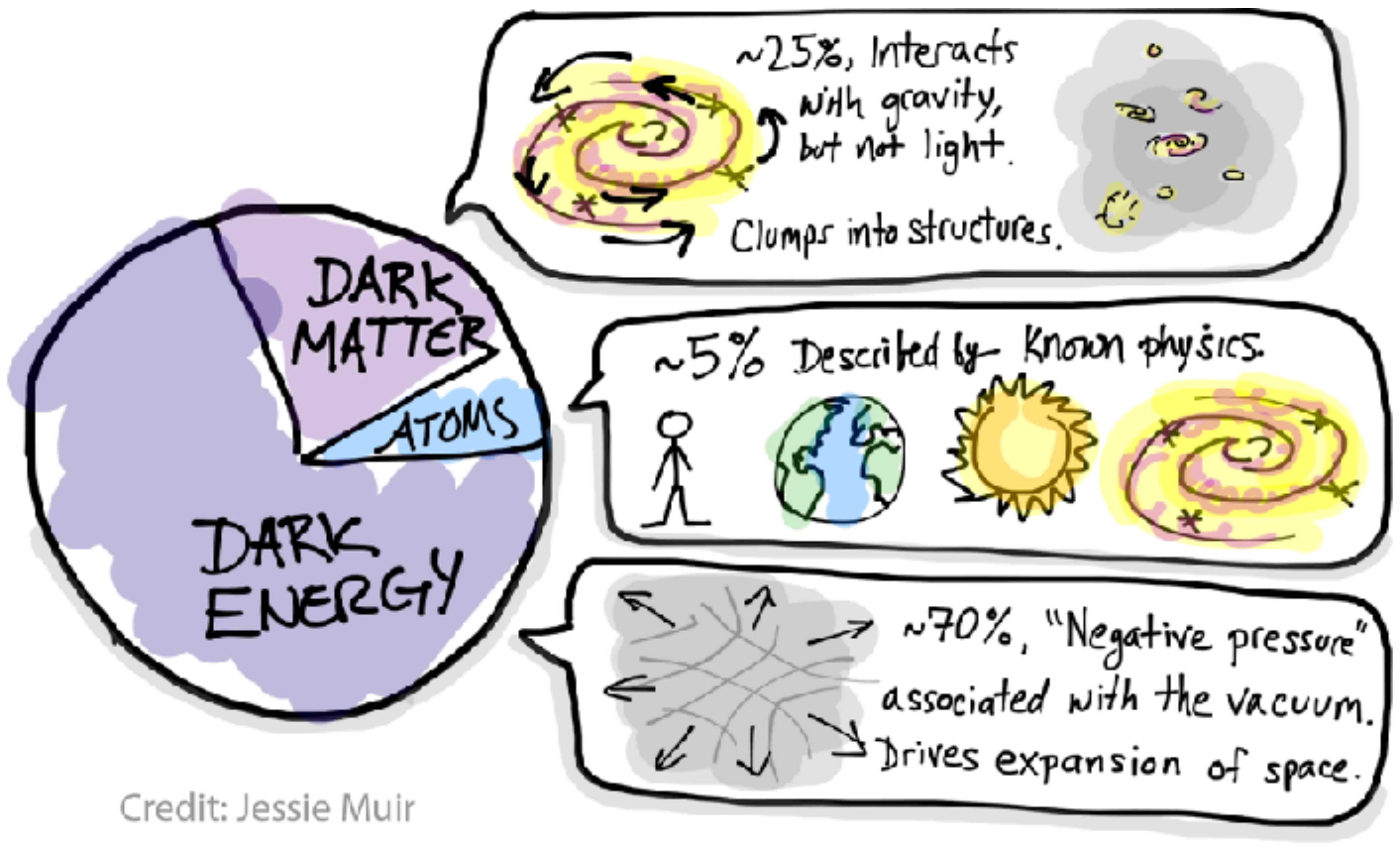

Credit: Jessie Muir

- Understand the accelerated expansion & dark matter by testing the ΛCDM model (this talk)
  - Evolution from high-redshift to low-redshift universe. (No) S_8 tension?
  - Hubble parameter H_0 tension? (not this talk)
- Understand neutrinos (e.g., hierarchy) through their imprint on large-scale structure
- Understand inflation by measuring tensor-to-scalar ratio r via BB mode in CMB
- Understand the formation of first stars/reionization

Cluster Cosmology

Why do we measure parameters?

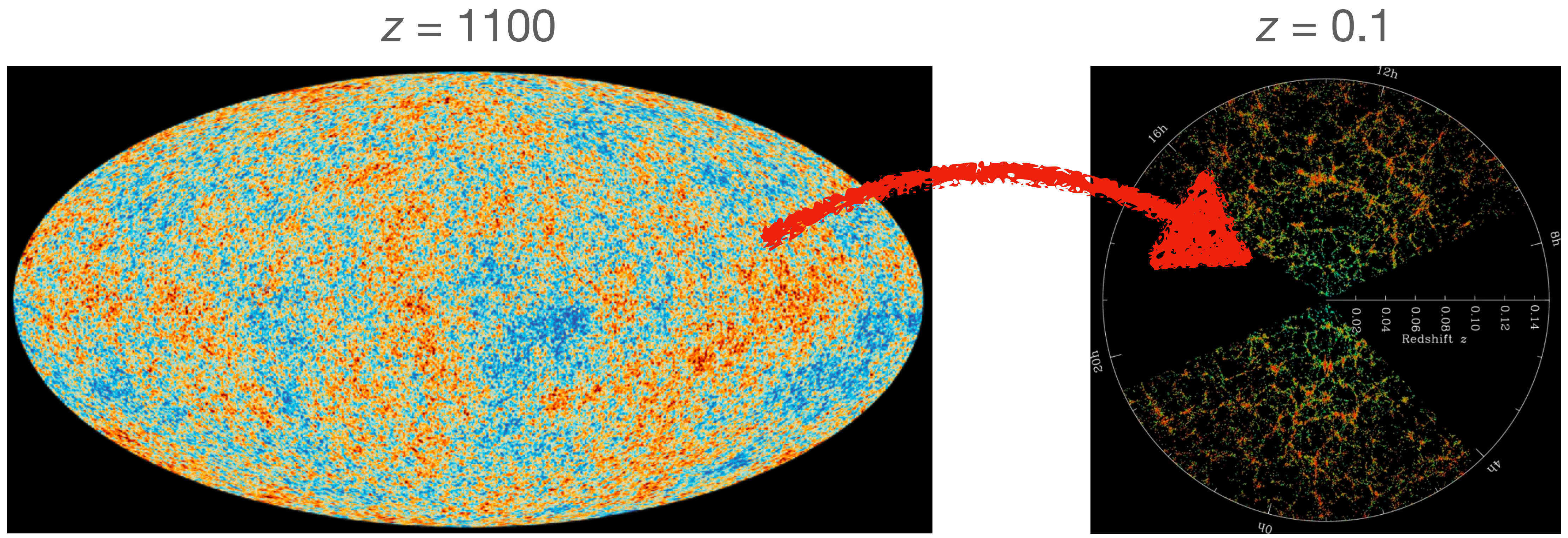

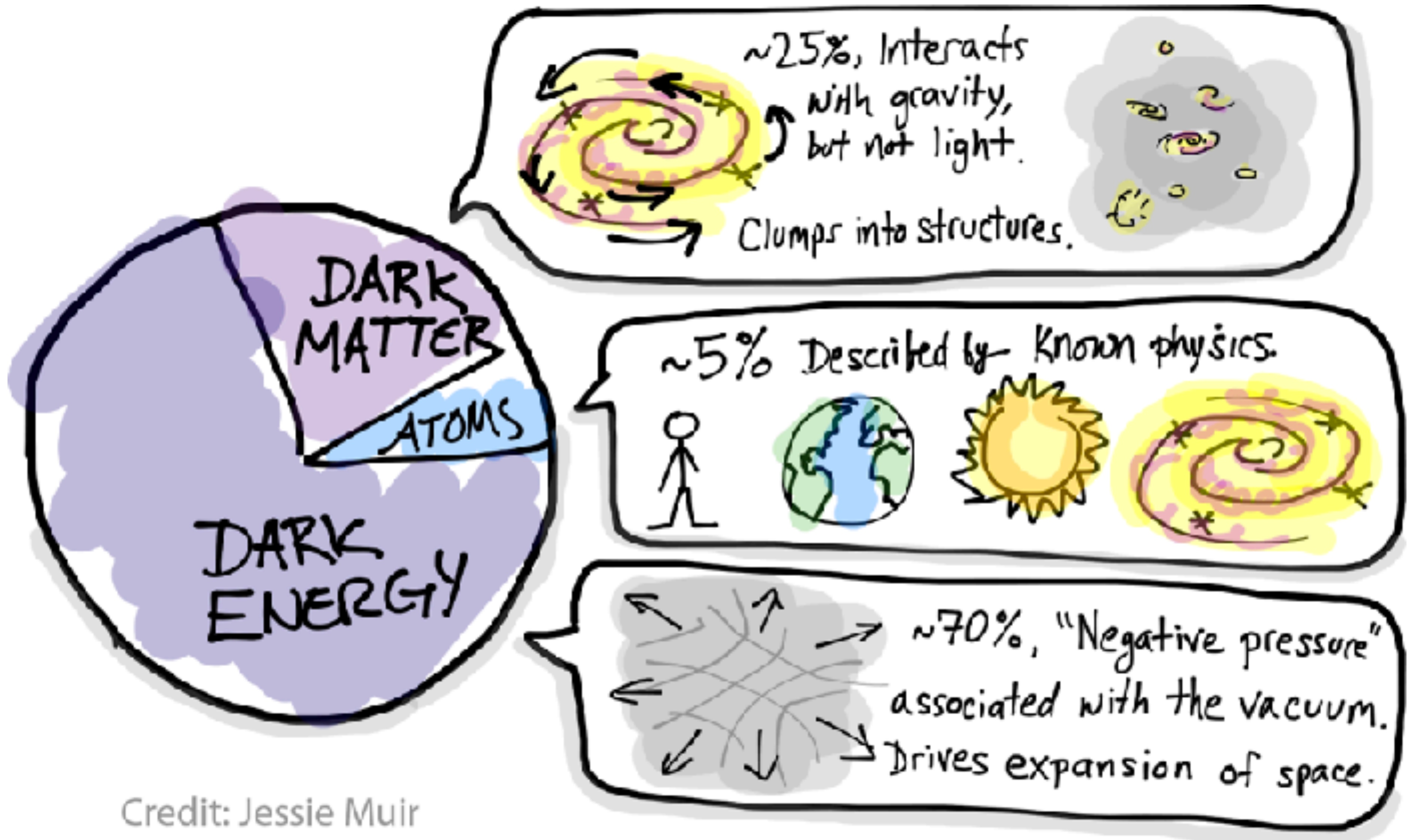

Credit: Jessie Muir

- Understand the accelerated expansion & dark matter by testing the ΛCDM model (this talk)
  - Evolution from high-redshift to low-redshift universe. (No) S_8 tension?
  - Hubble parameter H_0 tension? (not this talk)
- Understand neutrinos (e.g., hierarchy) through their imprint on large-scale structure
- Understand inflation by measuring tensor-to-scalar ratio r via BB mode in CMB
- Understand the formation of first stars/reionization

Cluster Cosmology

The most massive collapsed objects $\gtrsim 10^{14}\ M_\odot$

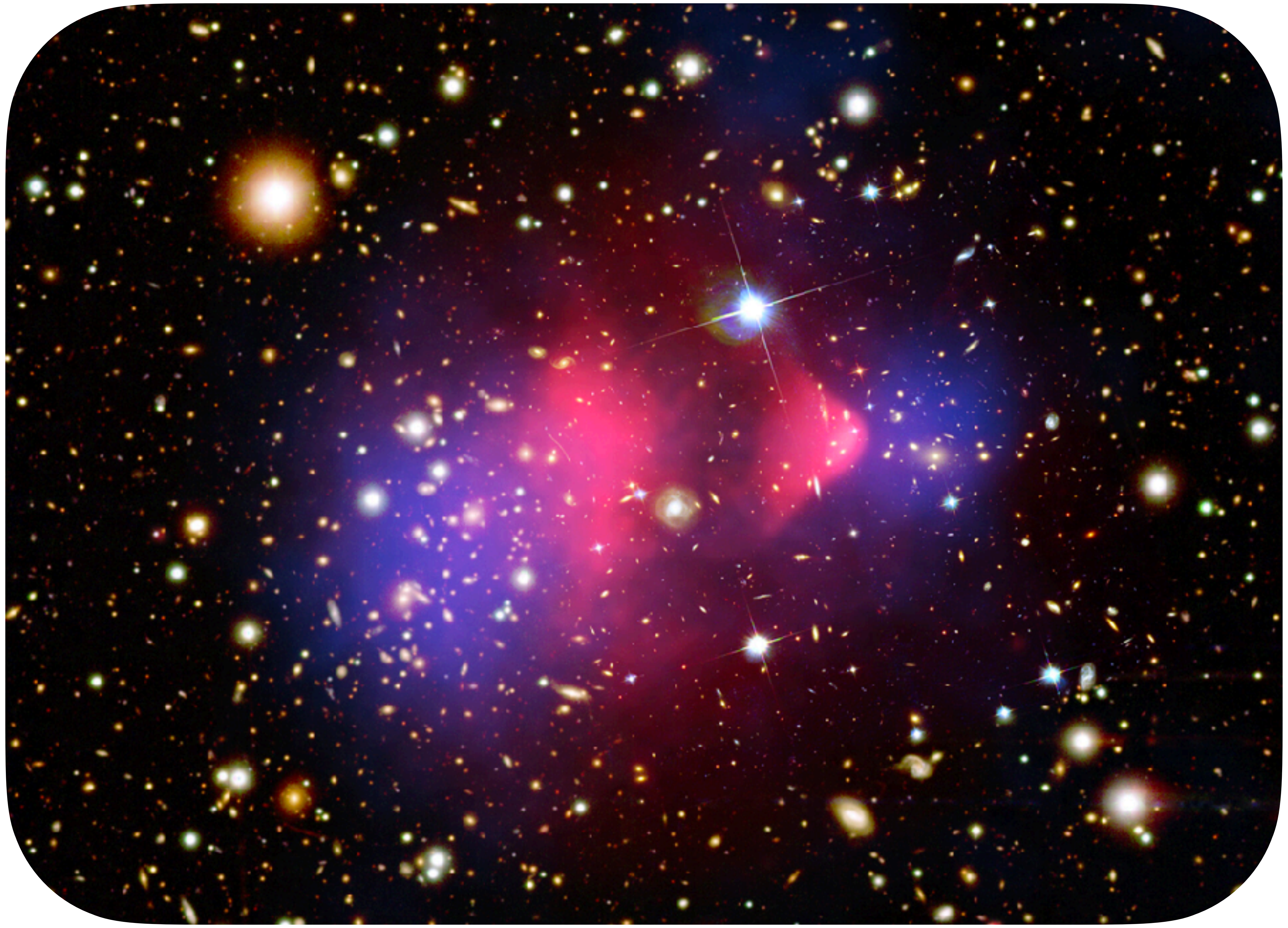

Bullet Cluster. X-ray: NASA/CXC/CfA/M.Markevitch, Optical and lensing map: NASA/STScI, Magellan/U.Arizona/D.Clowe, Lensing map: ESO WFI

- Composition
  - 85—90% dark matter
  - 10—15% ordinary matter, of which
    - ~ 75% (gravitationally heated) gas
    - ~ 25% galaxies/stars
- Somewhat arbitrary (but useful) definition
  - Halo ≡ *entire* thing
  - Cluster ≡ galaxies & gas (what we see)

Large-Scale Structure and Cosmology

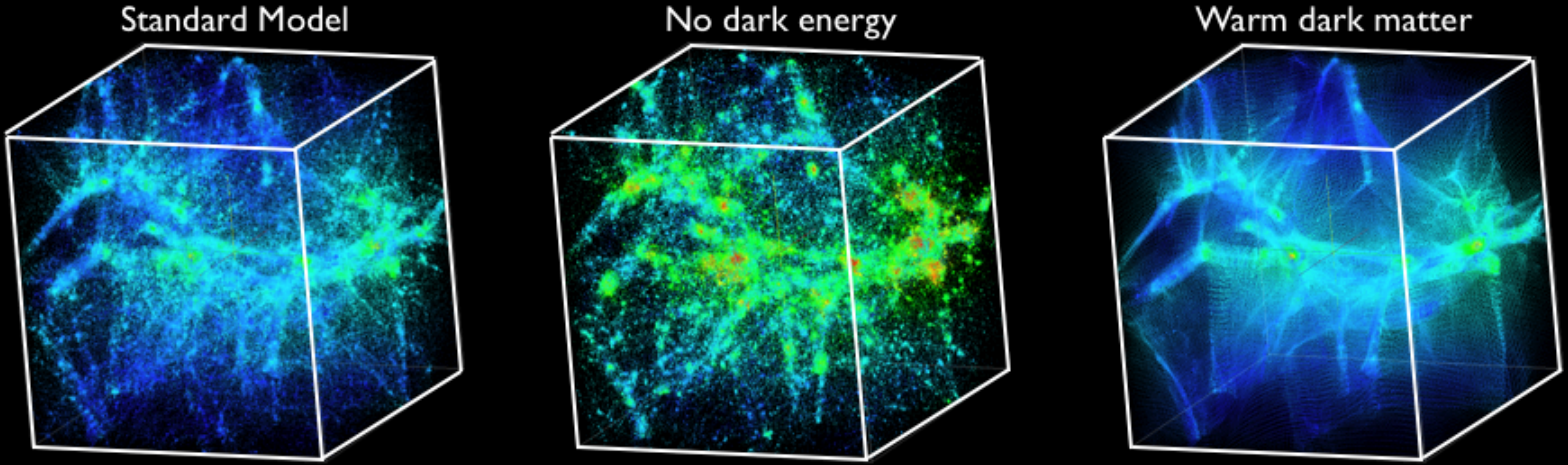

Credit: Katrin Heitmann

Halo Mass Function

d*N(z)*/dln*M* — vanilla ΛCDM cosmology

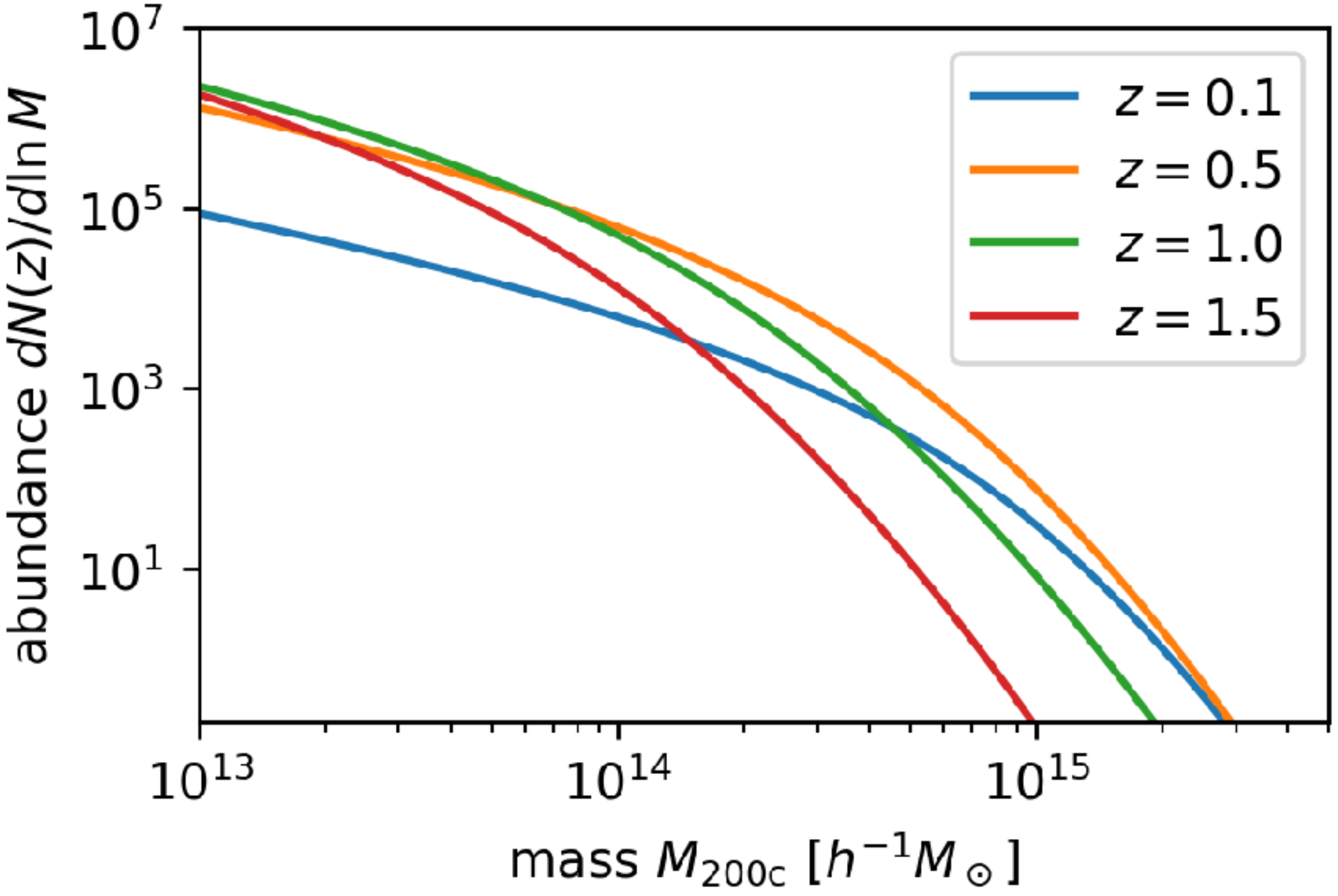

Halo Mass Function

d$N(z)$/dln$M$ — now w = -1.1 (instead of -1)

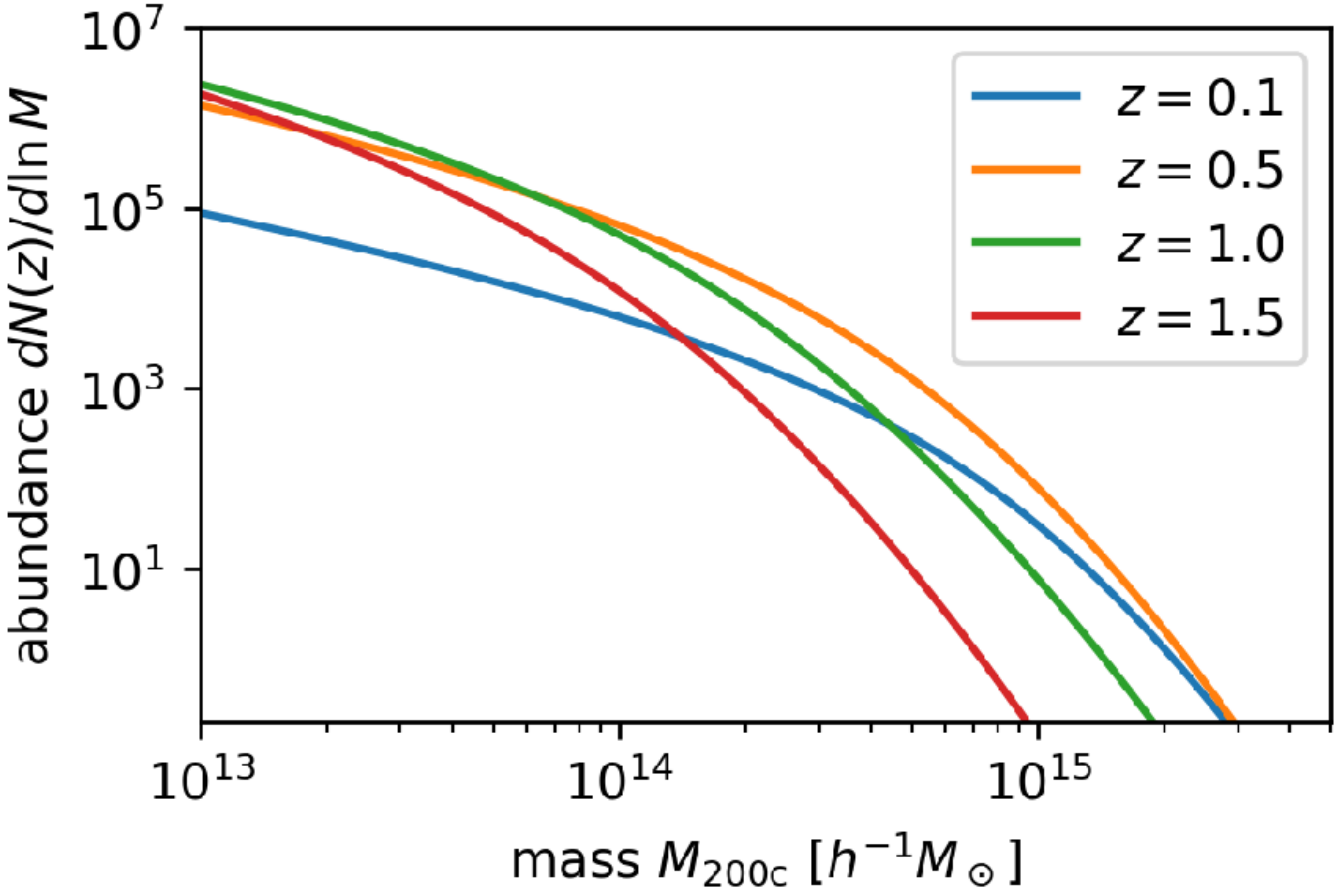

Halo Mass Function

Impact of changing dark energy equation of state parameter by 0.1

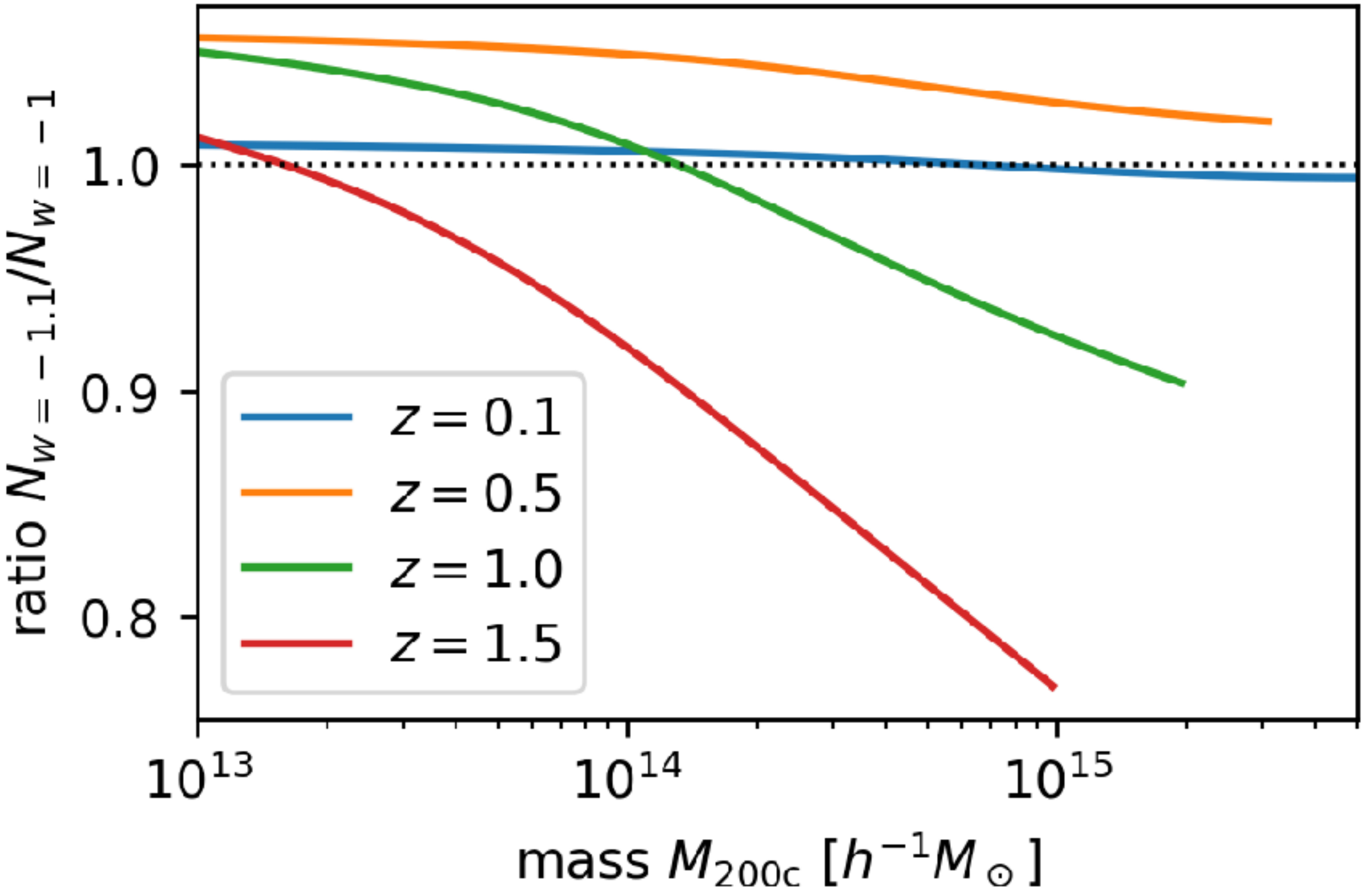

Back to reality

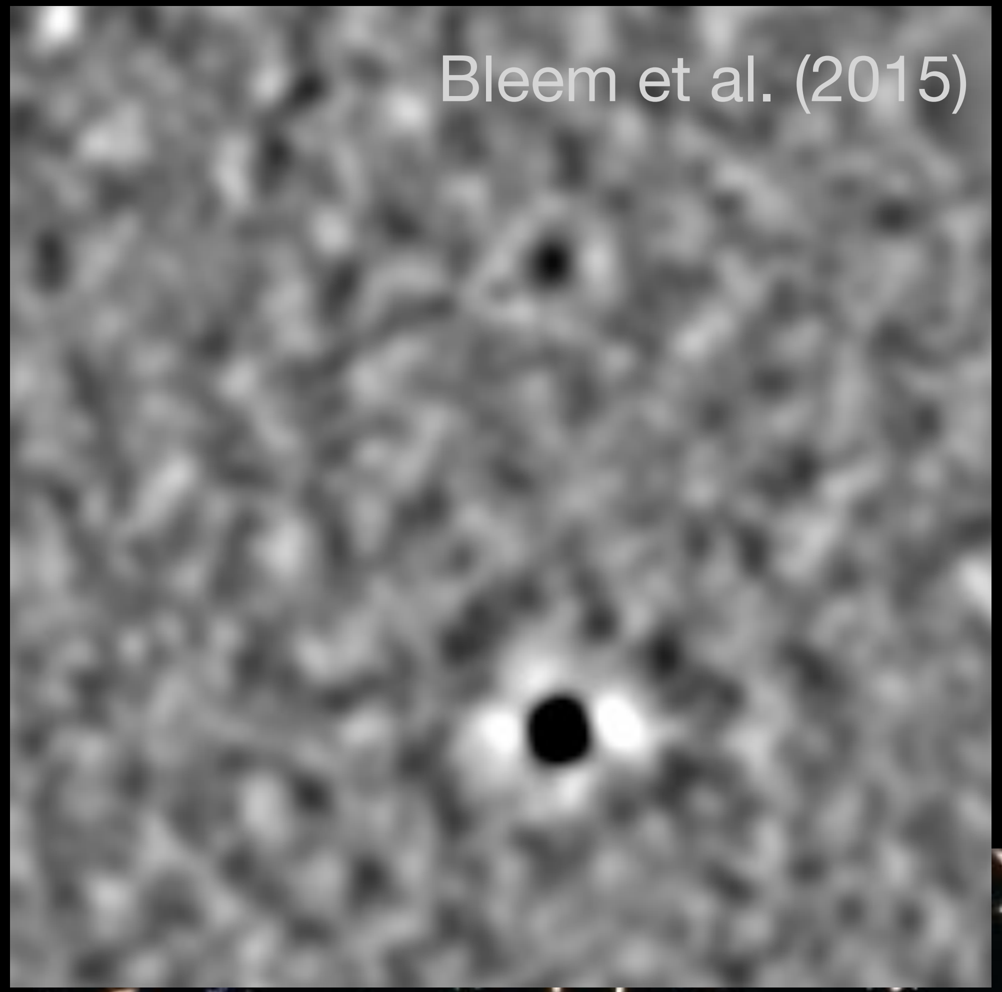

Bleem et al. (2015)

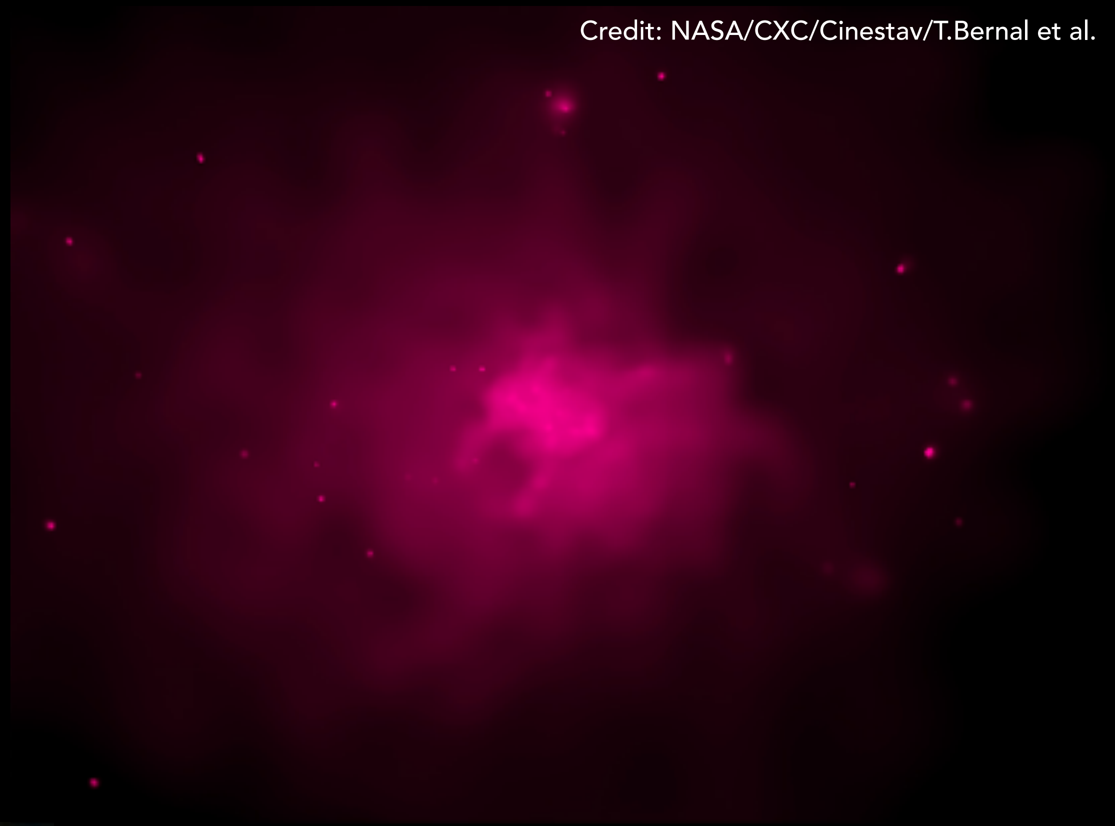

Credit: NASA/CXC/Cinestav/T.Bernal et al.

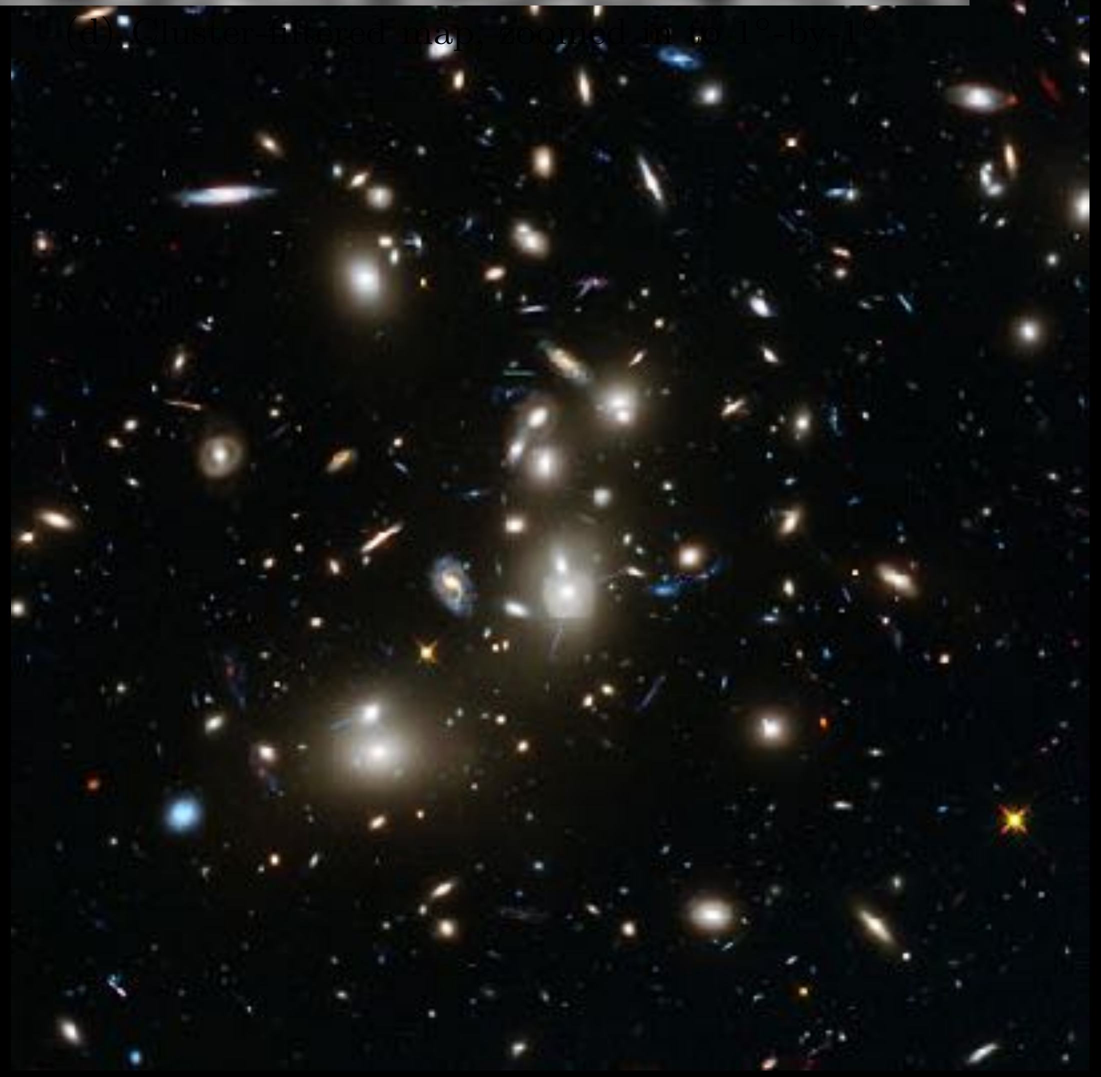

Credit: NASA, ESA, and J. Lotz, M. Mountain, A. Koekemoer, and the HFF Team (STScI) http://www.spacetelescope.org/images/heic1401a/

Credit: NASA, ESA, the Hubble Heritage Team (STScI/AURA), J. Blakeslee (NRC Herzberg Astrophysics Program, Dominion Astrophysical Observatory), and H. Ford (JHU) http://www.spacetelescope.org/images/heic1317a

Back to reality

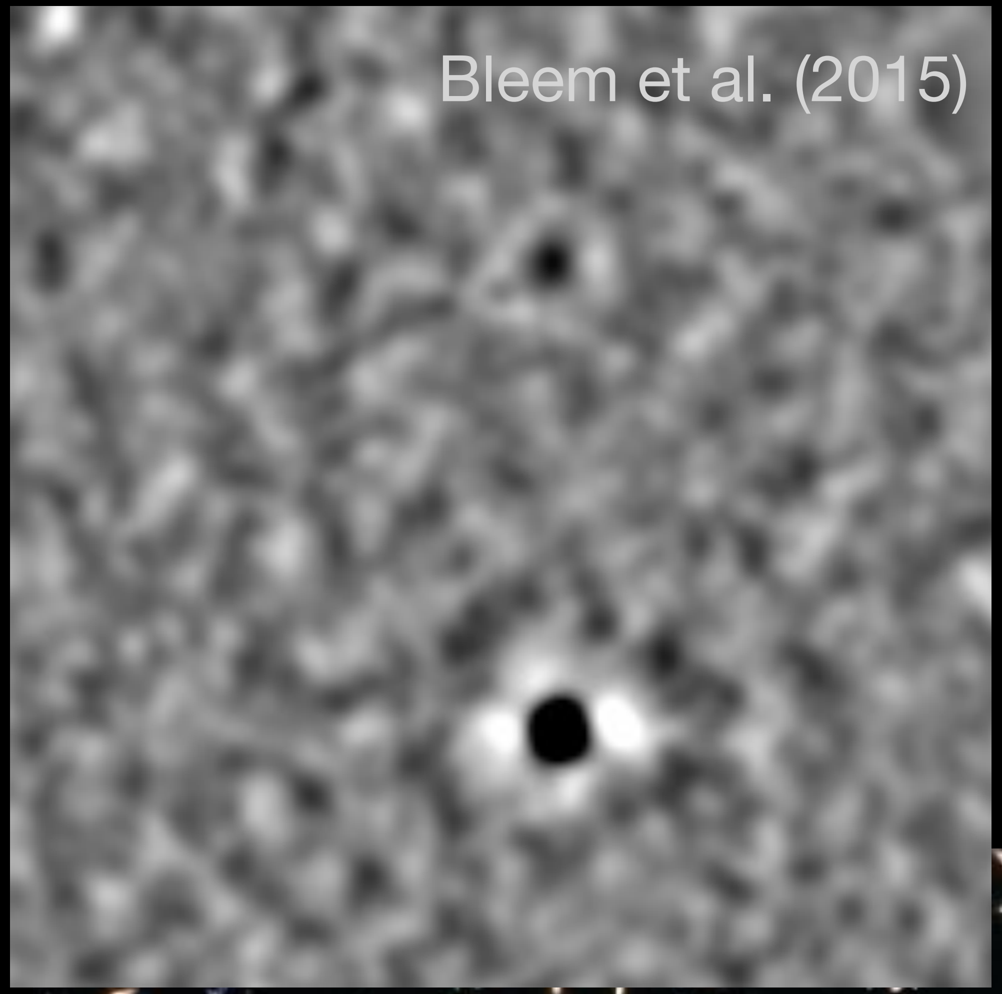

Bleem et al. (2015)

“Halo Observable Function”

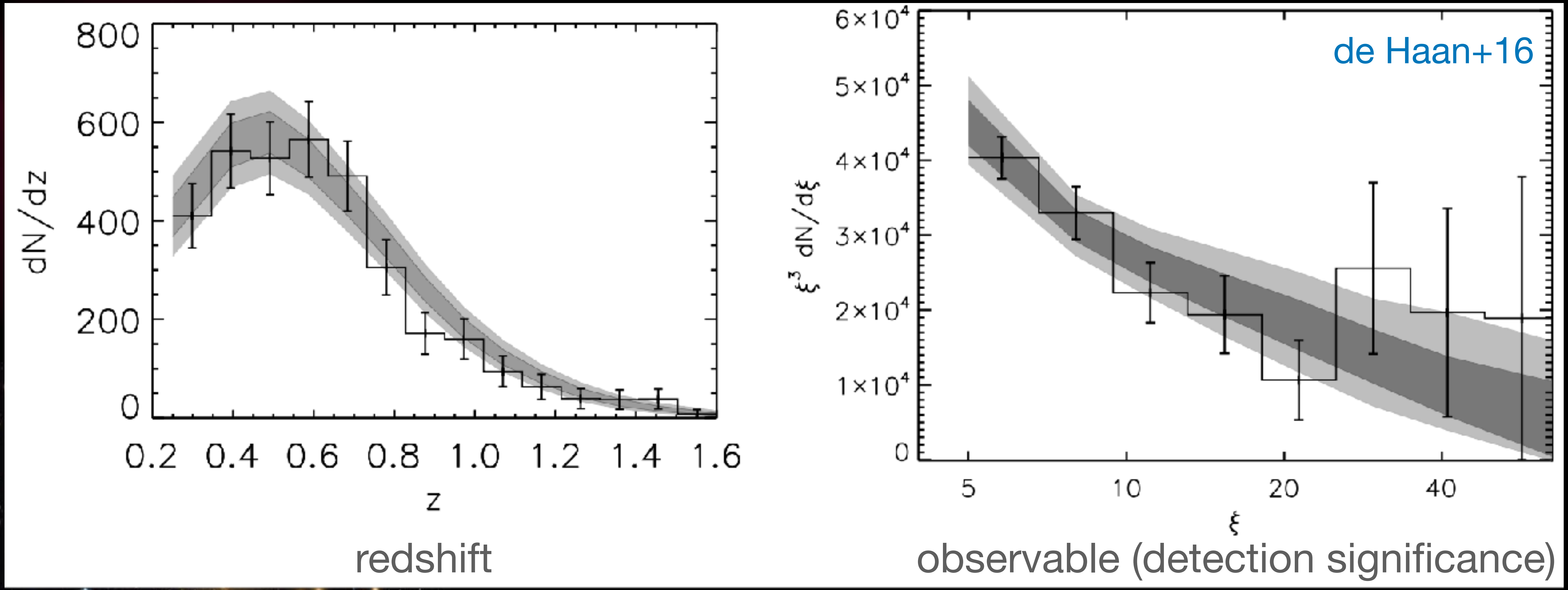

de Haan+16

redshift

observable (detection significance)

Credit: NASA, ESA, and J. Lotz, M. Mountain, A. Koekemoer, and the HFF Team (STScI) http://www.spacetelescope.org/images/heic1401a/

Credit: NASA, ESA, the Hubble Heritage Team (STScI/AURA), J. Blakeslee (NRC Herzberg Astrophysics Program, Dominion Astrophysical Observatory), and H. Ford (JHU) http://www.spacetelescope.org/images/heic1317a

Observable vs. Mass

halo observable function

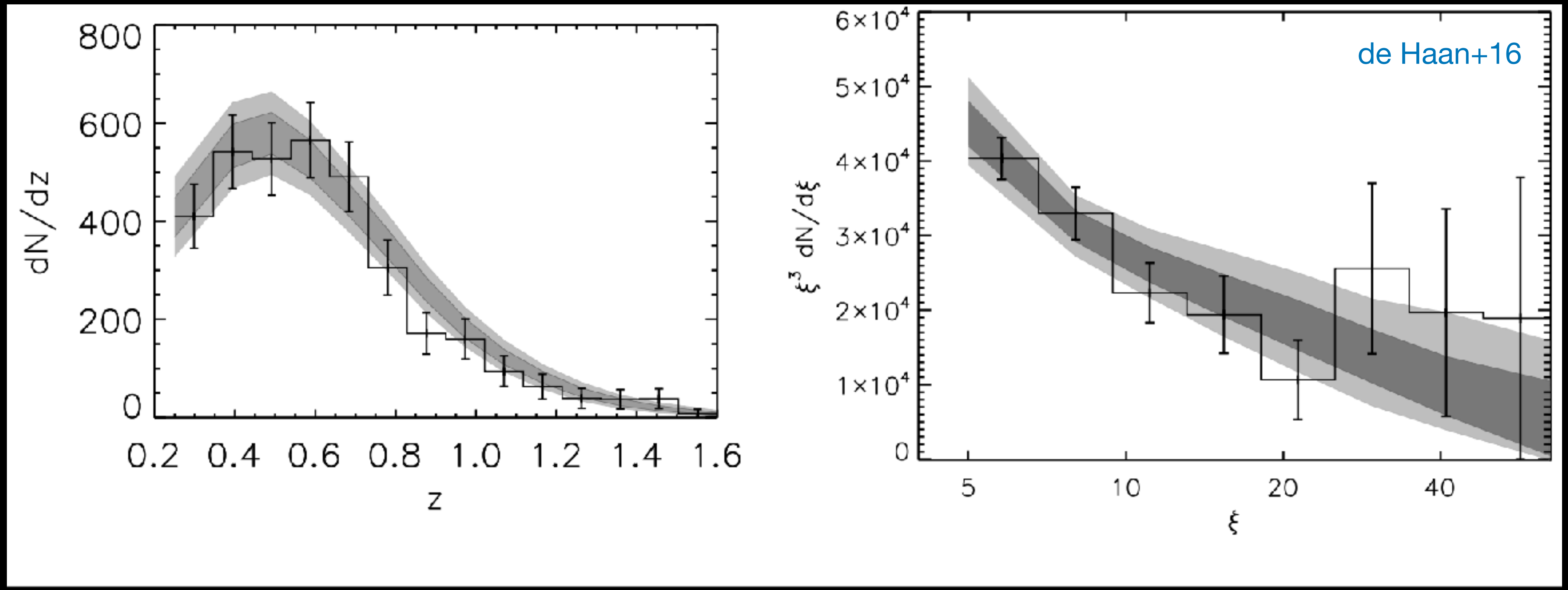

clusters

halos

halo mass function

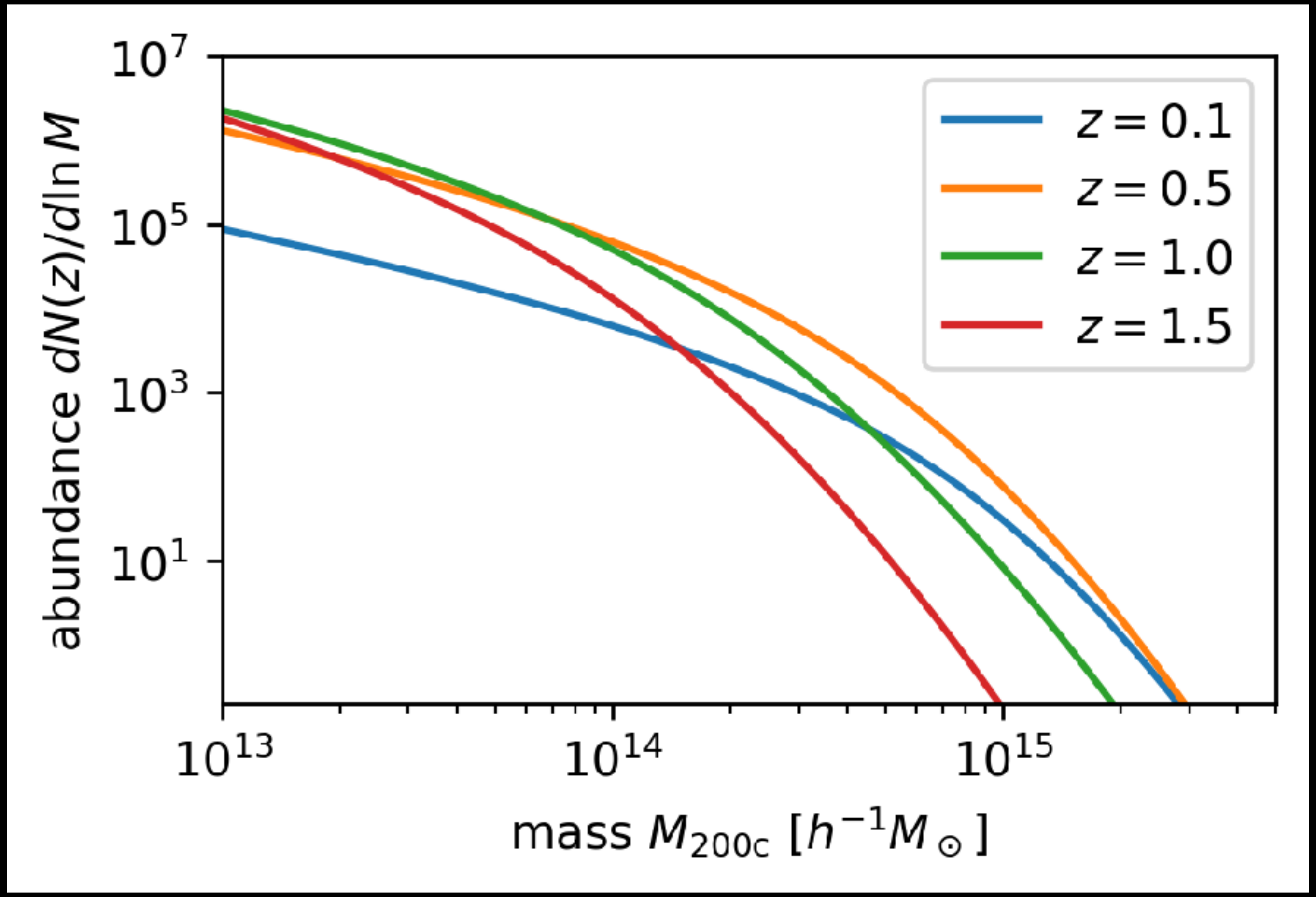

halo observable function

Observable vs. Mass

clusters

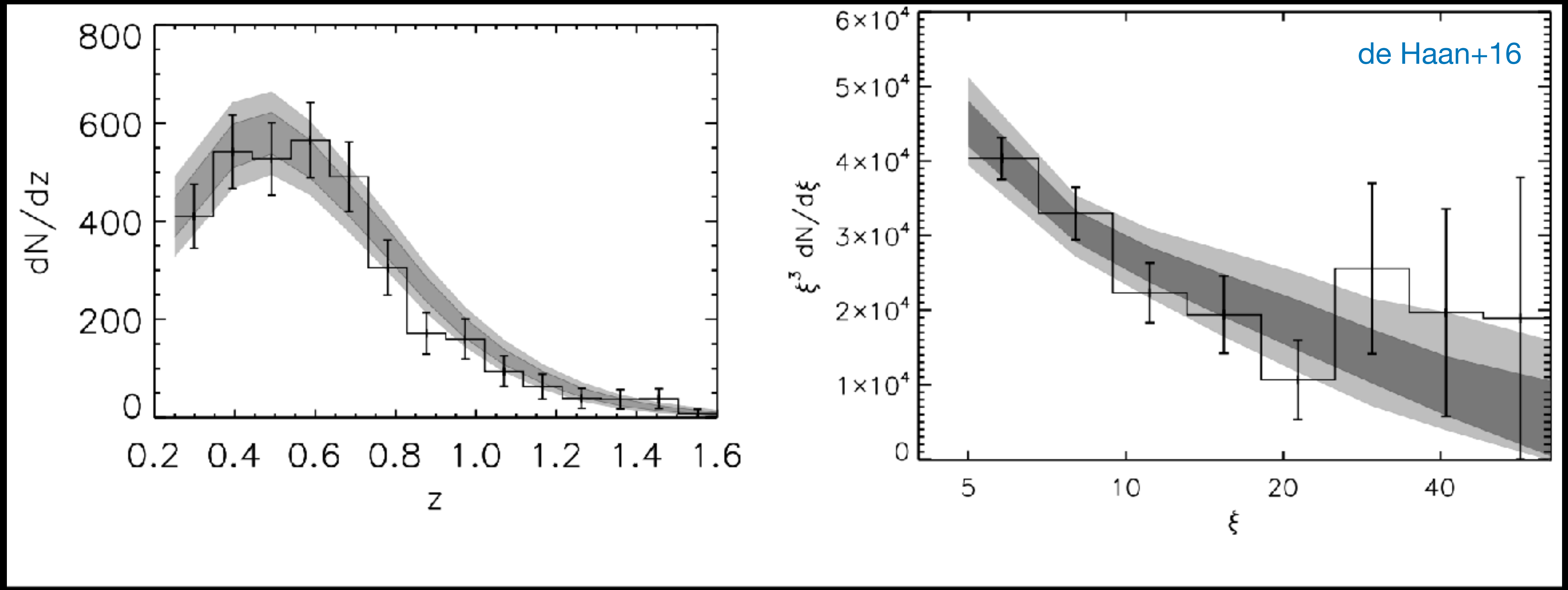

halo mass function

halos

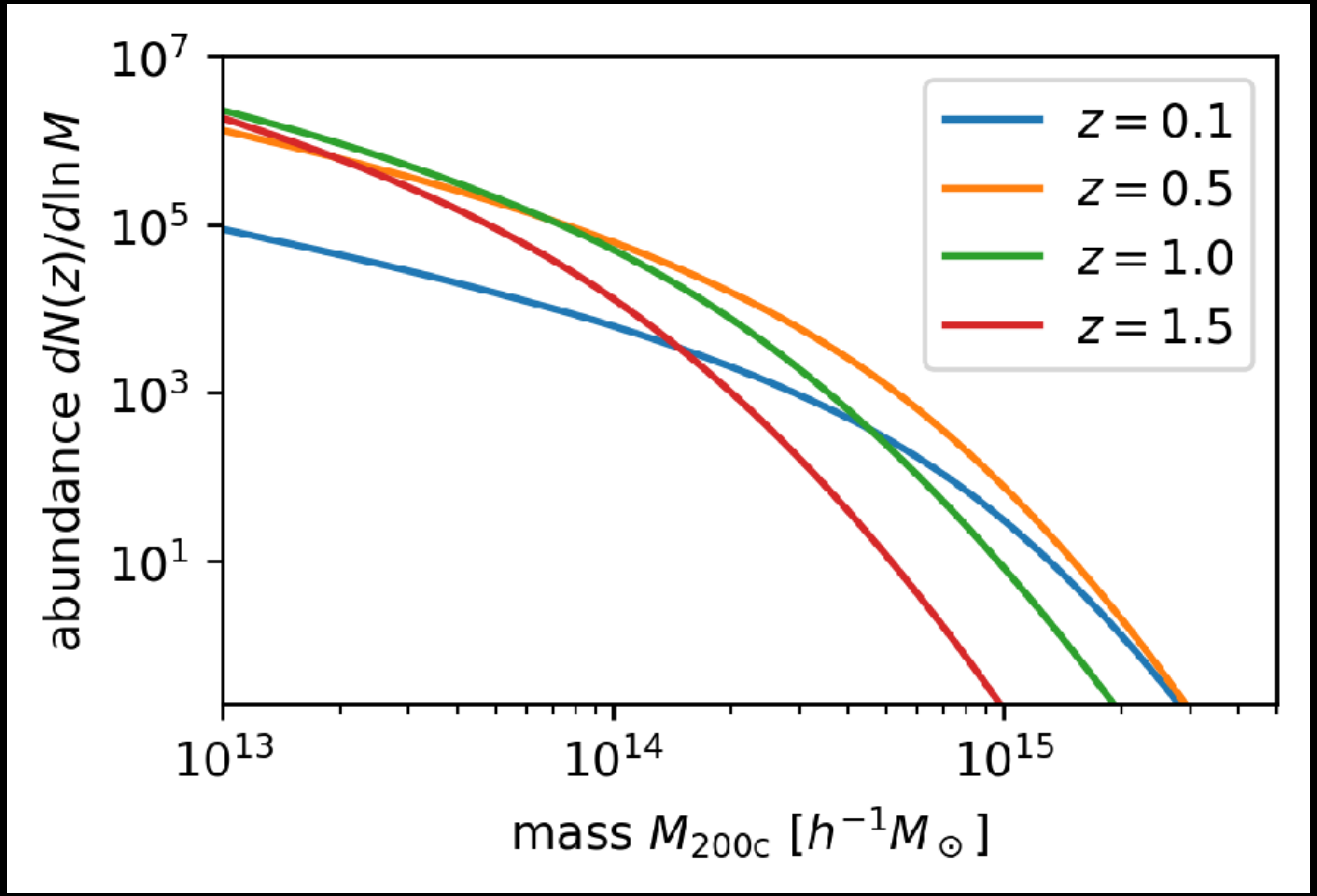

$$\frac{dN}{d\mathrm{obs}} = \int dM \, P(\mathrm{obs}\,|\,M) \, \frac{dN}{dM}$$

Observable vs. Mass

halo observable function

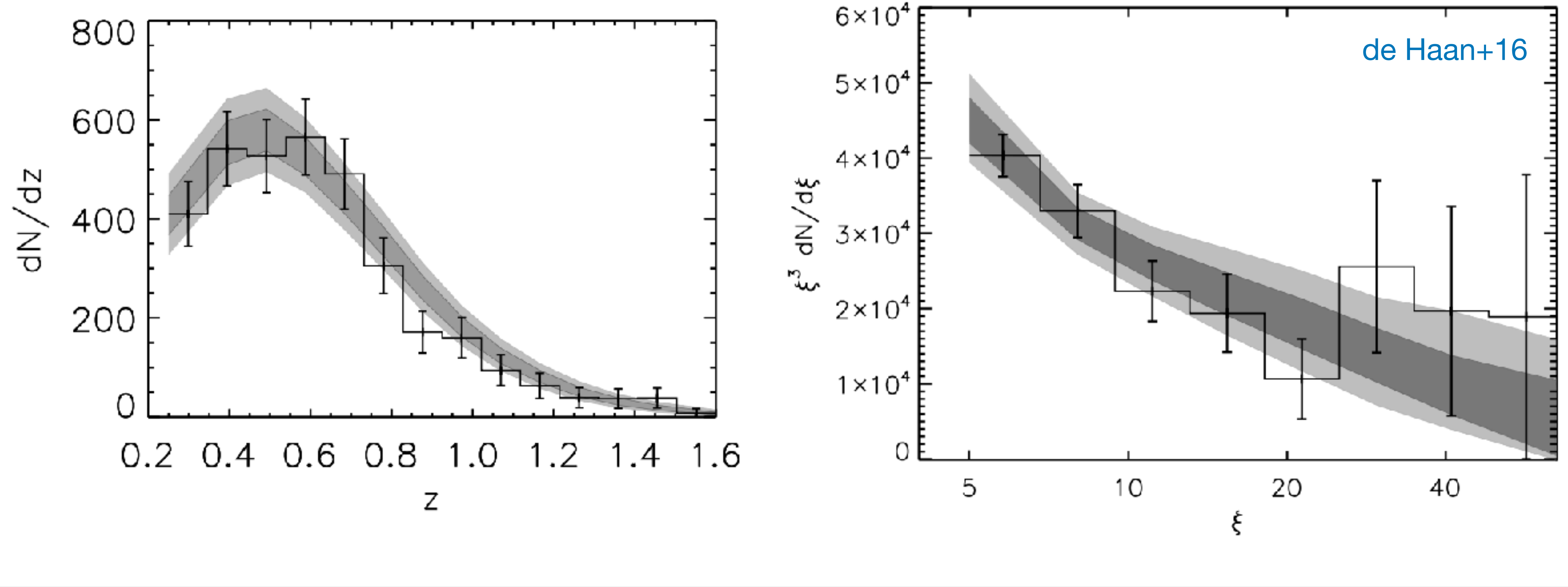

clusters

halos

halo mass function

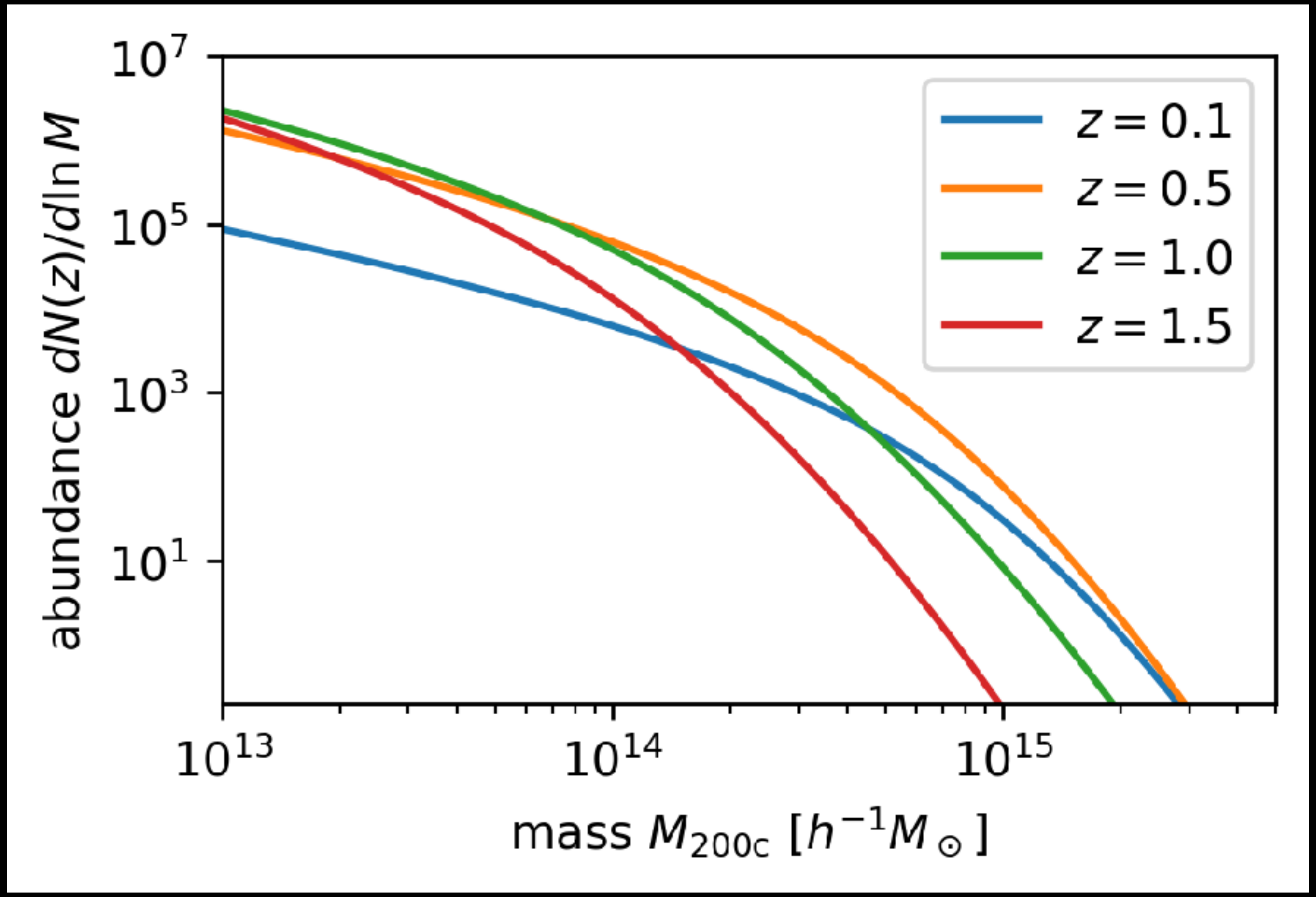

observable—mass relation

$$\frac{dN}{d\mathrm{obs}} = \int dM \, \boxed{P(\mathrm{obs}\,|\,M)} \, \boxed{\frac{dN}{dM}}$$

halo mass function

cluster cosmology = cluster selection + mass calibration

Modeling Framework

Observable — Mass Relations

- The bigger a halo, the stronger its SZ, X-ray, optical, lensing signal
  - Supported by theory and numerical simulations
  - These are average relations — there is intrinsic scatter, because no two objects are the same
- For the experts:
  - Halo morphology and evolution lead to correlated scatter among observables

Simulations (Angulo+12)

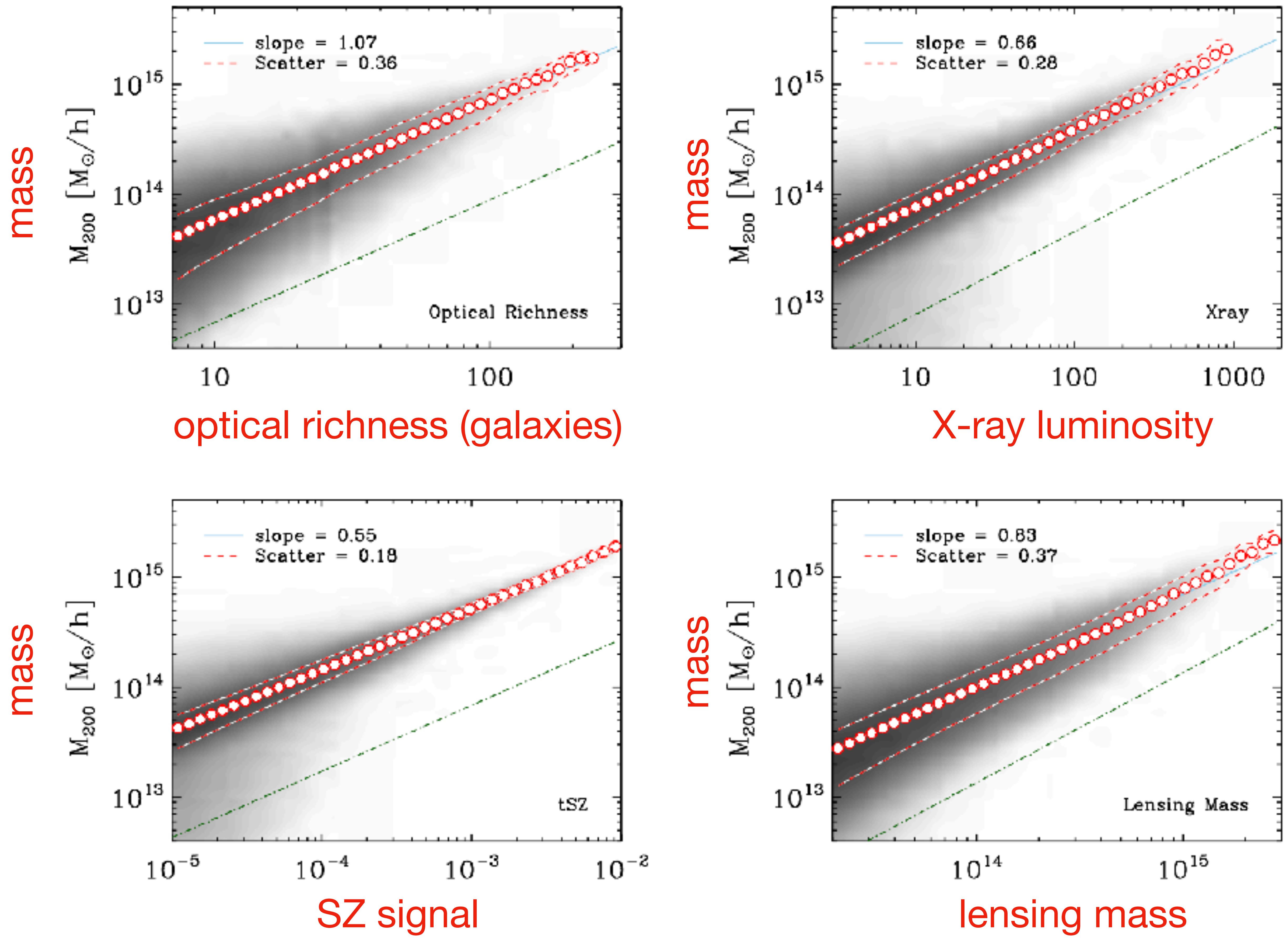

Mass Calibration

How do the observables relate to halo mass?

- We *could* use predictions from first principles (e.g., hydrostatic equilibrium) or numerical simulations

Mass Calibration

How do the observables relate to halo mass?

- We *could* use predictions from first principles (e.g., hydrostatic equilibrium) or numerical simulations
    - Systematically limited by uncertain astrophysics

Mass Calibration

How do the observables relate to halo mass?

- We *could* use predictions from first principles (e.g., hydrostatic equilibrium) or numerical simulations
    - Systematically limited by uncertain astrophysics
- Weak-lensing-to-mass relation is known within few percents

Idealized (exaggerated) situation

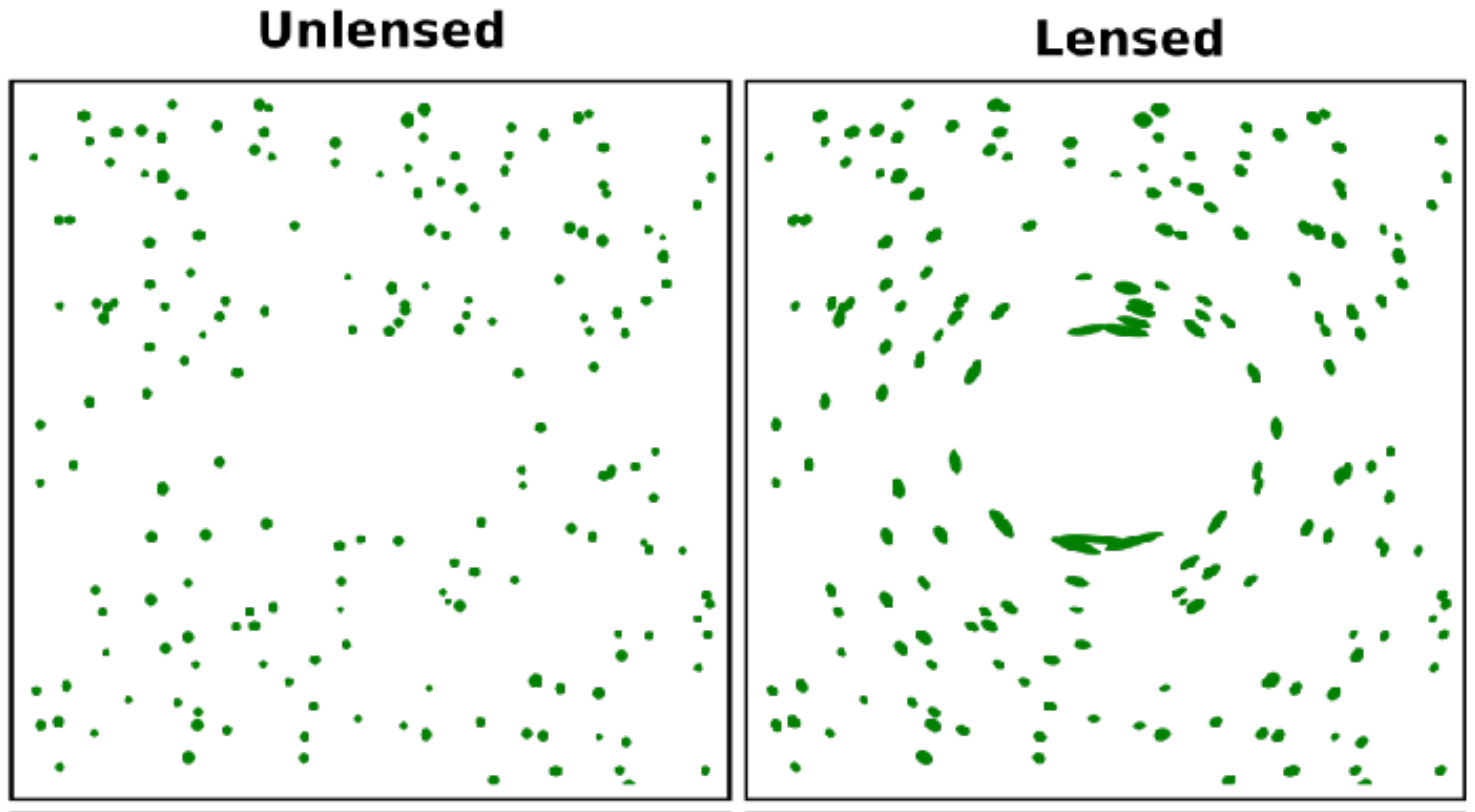

By TallJimbo - Own work, CC BY-SA 3.0, https://commons.wikimedia.org/w/index.php?curid=4150002

Mass Calibration

How do the observables relate to halo mass?

- We *could* use predictions from first principles (e.g., hydrostatic equilibrium) or numerical simulations
    - Systematically limited by uncertain astrophysics
- Weak-lensing-to-mass relation is known within few percents

Idealized (exaggerated) situation

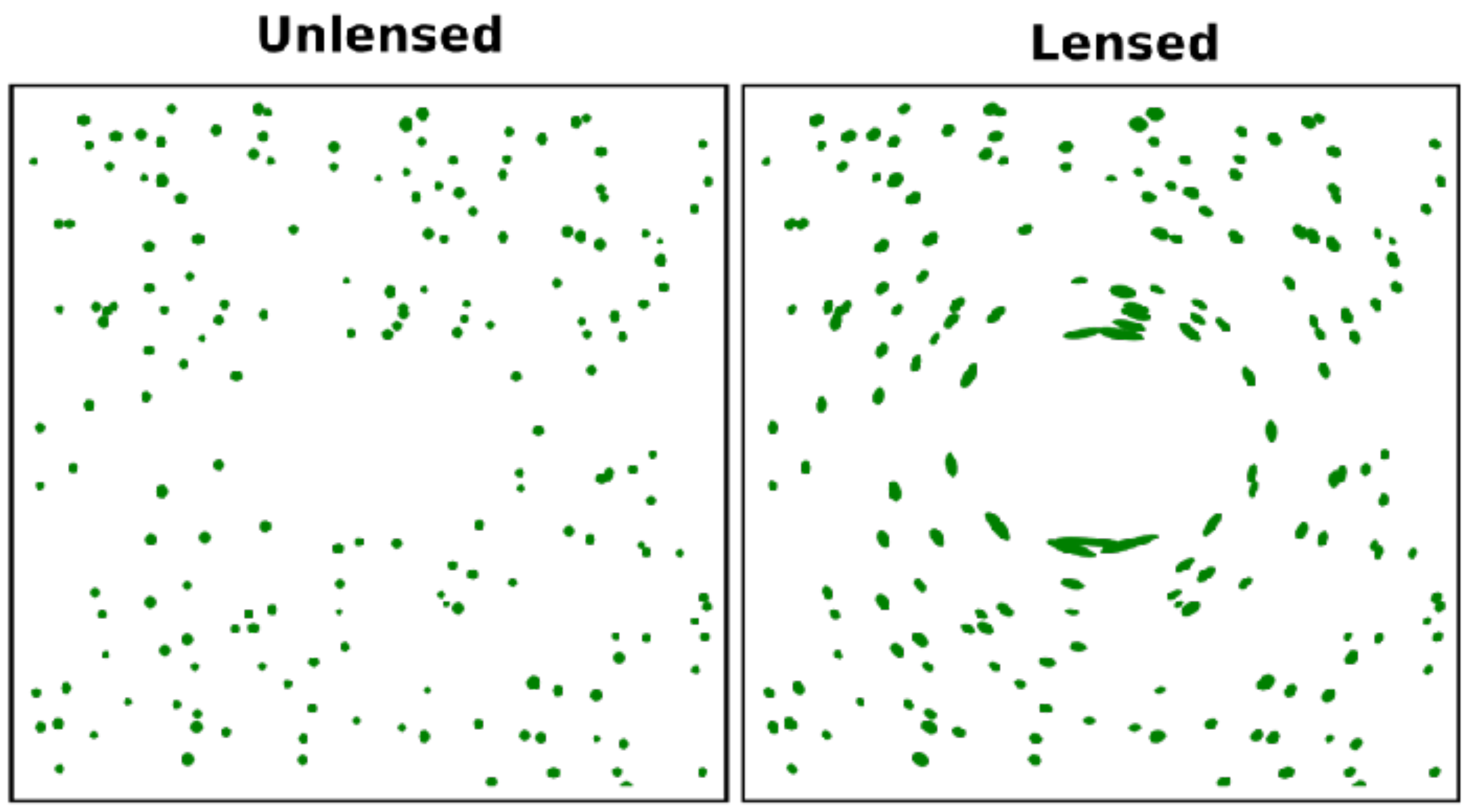

By TallJimbo - Own work, CC BY-SA 3.0, https://commons.wikimedia.org/w/index.php?curid=4150002

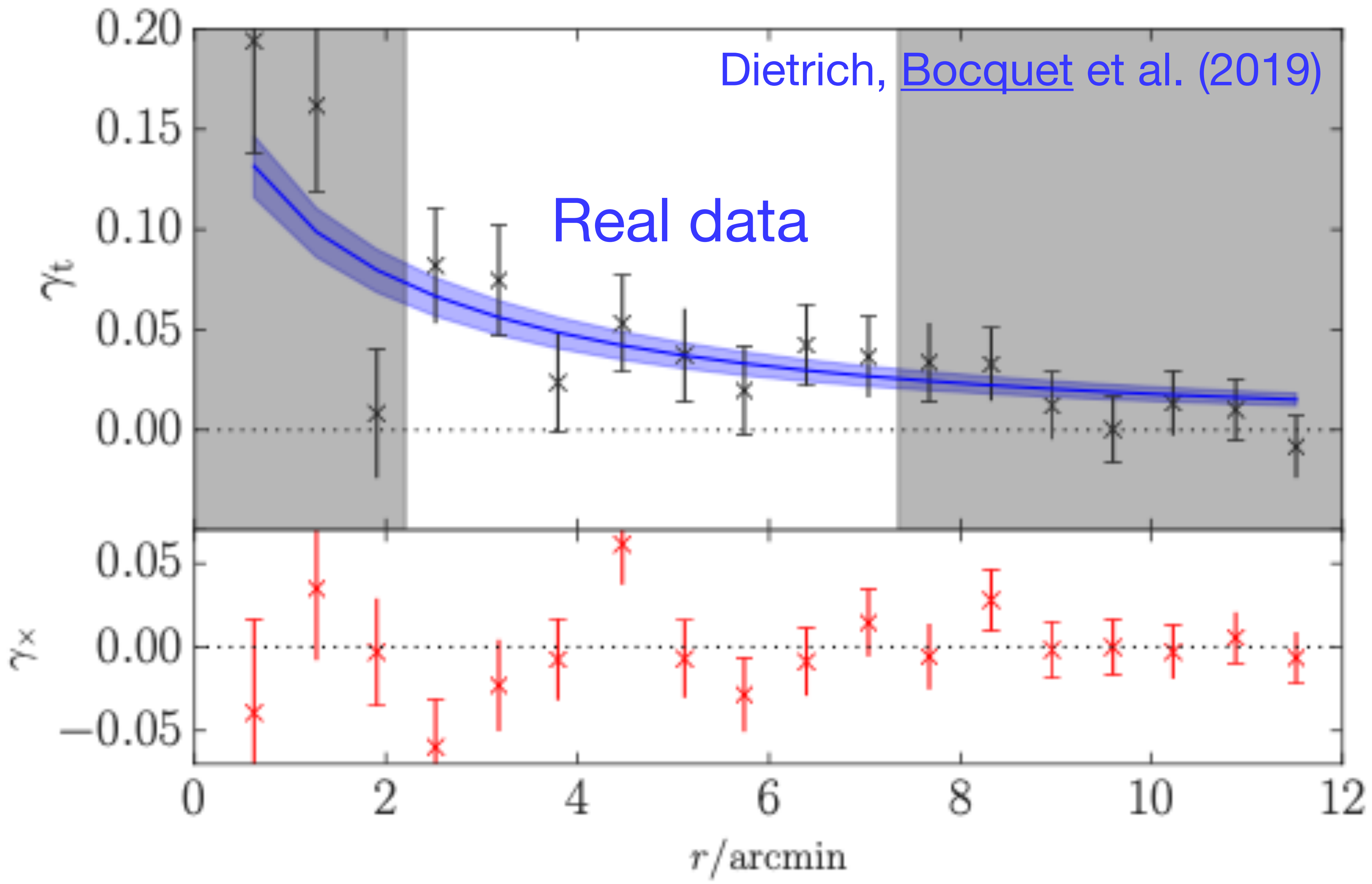
Dietrich, Bocquet et al. (2019)

Real data

(b) Tangential shear profile of SPT-CL J0254−5857.

Weak-Lensing Mass Calibration

Robust observable—mass relations

- We *could* use predictions from first principles (e.g., hydrostatic equilibrium) or numerical simulations
    - Systematically limited by uncertain astrophysics
- Weak-lensing-to-mass relation is known within few percents
    - Used to demonstrate that **hydrostatic mass ≠ halo mass**
    - **With lensing** measurements of sample clusters, **we *empirically* calibrate the observable—mass relations**

Medezinski+ 18

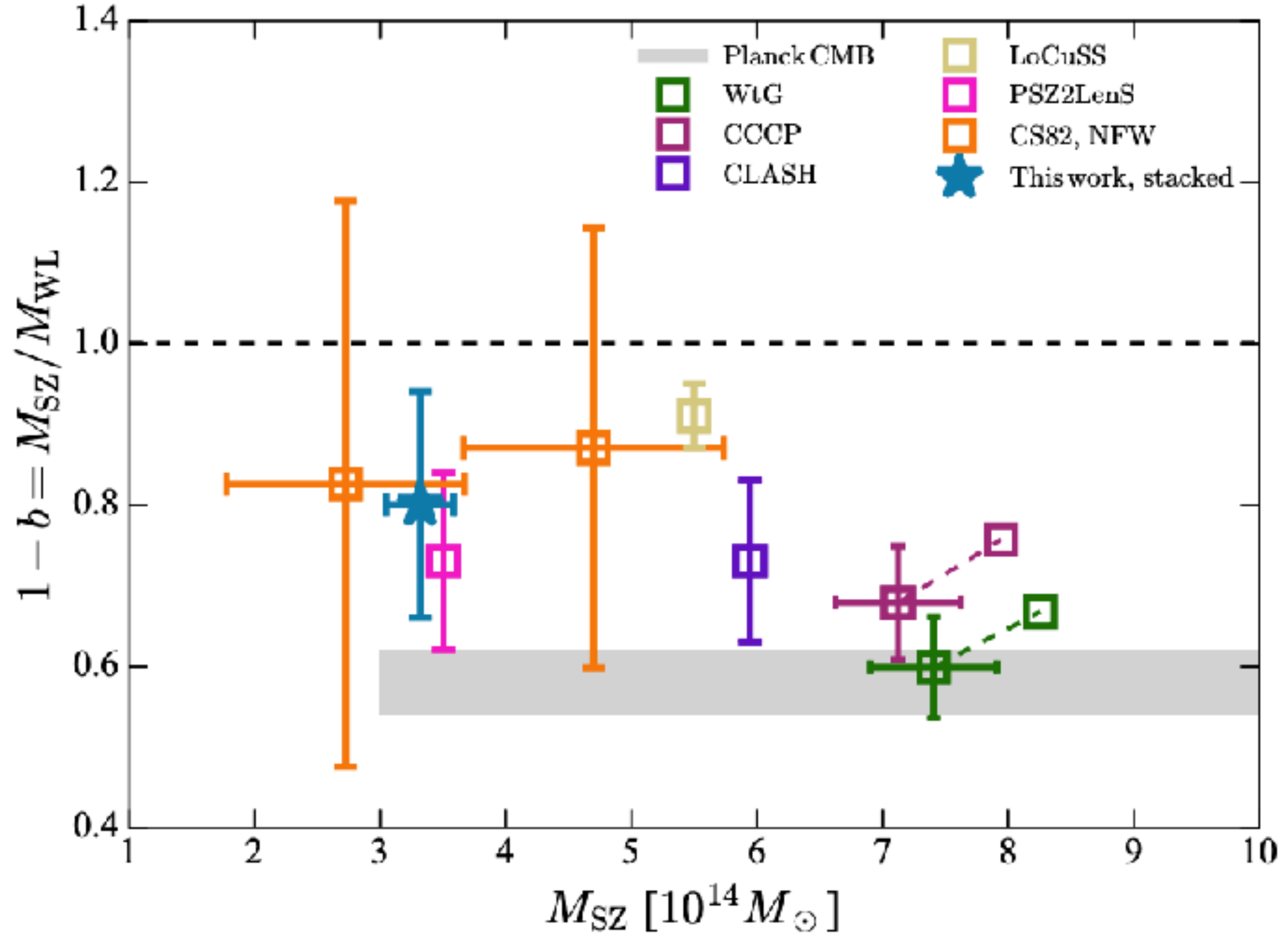

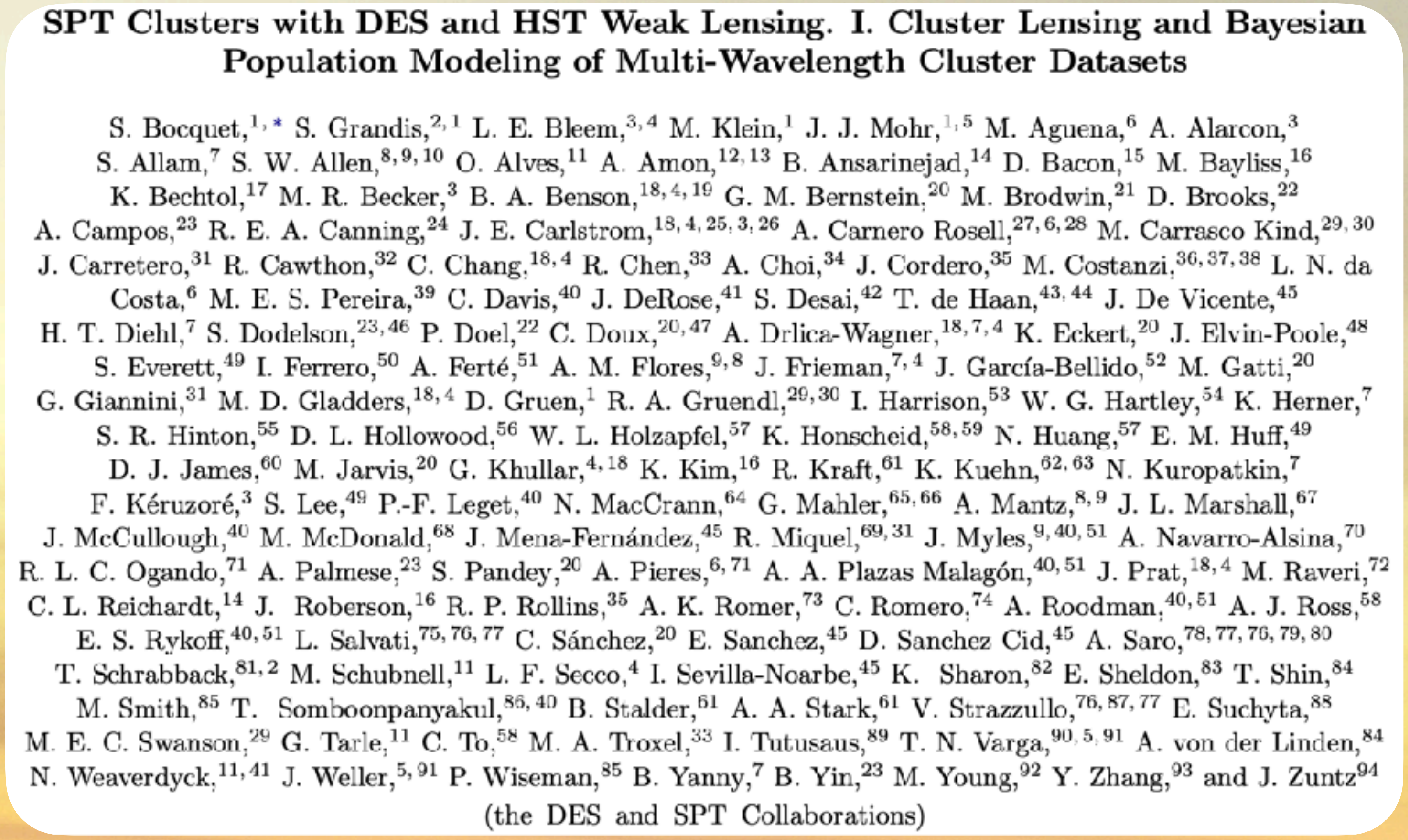

SPT Clusters with DES and HST Weak Lensing. I. Cluster Lensing and Bayesian Population Modeling of Multi-Wavelength Cluster Datasets

S. Bocquet,[1,*] S. Grandis,[2,1] L. E. Bleem,[3,4] M. Klein,[1] J. J. Mohr,[1,5] M. Aguena,[6] A. Alarcon,[3] S. Allam,[7] S. W. Allen,[8,9,10] O. Alves,[11] A. Amon,[12,13] B. Ansarinejad,[14] D. Bacon,[15] M. Bayliss,[16] K. Bechtol,[17] M. R. Becker,[3] B. A. Benson,[18,4,19] G. M. Bernstein,[20] M. Brodwin,[21] D. Brooks,[22] A. Campos,[23] R. E. A. Canning,[24] J. E. Carlstrom,[18,4,25,3,26] A. Carnero Rosell,[27,6,28] M. Carrasco Kind,[29,30] J. Carretero,[31] R. Cawthon,[32] C. Chang,[18,4] R. Chen,[33] A. Choi,[34] J. Cordero,[35] M. Costanzi,[36,37,38] L. N. da Costa,[6] M. E. S. Pereira,[39] C. Davis,[40] J. DeRose,[41] S. Desai,[42] T. de Haan,[43,44] J. De Vicente,[45] H. T. Diehl,[7] S. Dodelson,[23,46] P. Doel,[22] C. Doux,[20,47] A. Drlica-Wagner,[18,7,4] K. Eckert,[20] J. Elvin-Poole,[48] S. Everett,[49] I. Ferrero,[50] A. Ferté,[51] A. M. Flores,[9,8] J. Frieman,[7,4] J. García-Bellido,[52] M. Gatti,[20] G. Giannini,[31] M. D. Gladders,[18,4] D. Gruen,[1] R. A. Gruendl,[29,30] I. Harrison,[53] W. G. Hartley,[54] K. Herner,[7] S. R. Hinton,[55] D. L. Hollowood,[56] W. L. Holzapfel,[57] K. Honscheid,[58,59] N. Huang,[57] E. M. Huff,[49] D. J. James,[60] M. Jarvis,[20] G. Khullar,[4,18] K. Kim,[16] R. Kraft,[61] K. Kuehn,[62,63] N. Kuropatkin,[7] F. Kéruzoré,[3] S. Lee,[49] P.-F. Leget,[40] N. MacCrann,[64] G. Mahler,[65,66] A. Mantz,[8,9] J. L. Marshall,[67] J. McCullough,[40] M. McDonald,[68] J. Mena-Fernández,[45] R. Miquel,[69,31] J. Myles,[9,40,51] A. Navarro-Alsina,[70] R. L. C. Ogando,[71] A. Palmese,[23] S. Pandey,[20] A. Pieres,[6,71] A. A. Plazas Malagón,[40,51] J. Prat,[18,4] M. Raveri,[72] C. L. Reichardt,[14] J. Roberson,[16] R. P. Rollins,[35] A. K. Romer,[73] C. Romero,[74] A. Roodman,[40,51] A. J. Ross,[58] E. S. Rykoff,[40,51] L. Salvati,[75,76,77] C. Sánchez,[20] E. Sanchez,[45] D. Sanchez Cid,[45] A. Saro,[78,77,76,79,80] T. Schrabback,[81,2] M. Schubnell,[11] L. F. Secco,[4] I. Sevilla-Noarbe,[45] K. Sharon,[82] E. Sheldon,[83] T. Shin,[84] M. Smith,[85] T. Somboonpanyakul,[86,40] B. Stalder,[61] A. A. Stark,[61] V. Strazzullo,[76,87,77] E. Suchyta,[88] M. E. C. Swanson,[29] G. Tarle,[11] C. To,[58] M. A. Troxel,[33] I. Tutusaus,[89] T. N. Varga,[90,5,91] A. von der Linden,[84] N. Weaverdyck,[11,41] J. Weller,[5,91] P. Wiseman,[85] B. Yanny,[7] B. Yin,[23] M. Young,[92] Y. Zhang,[93] and J. Zuntz[94]
(the DES and SPT Collaborations)

arXiv:2310:12213 — PRD accepted

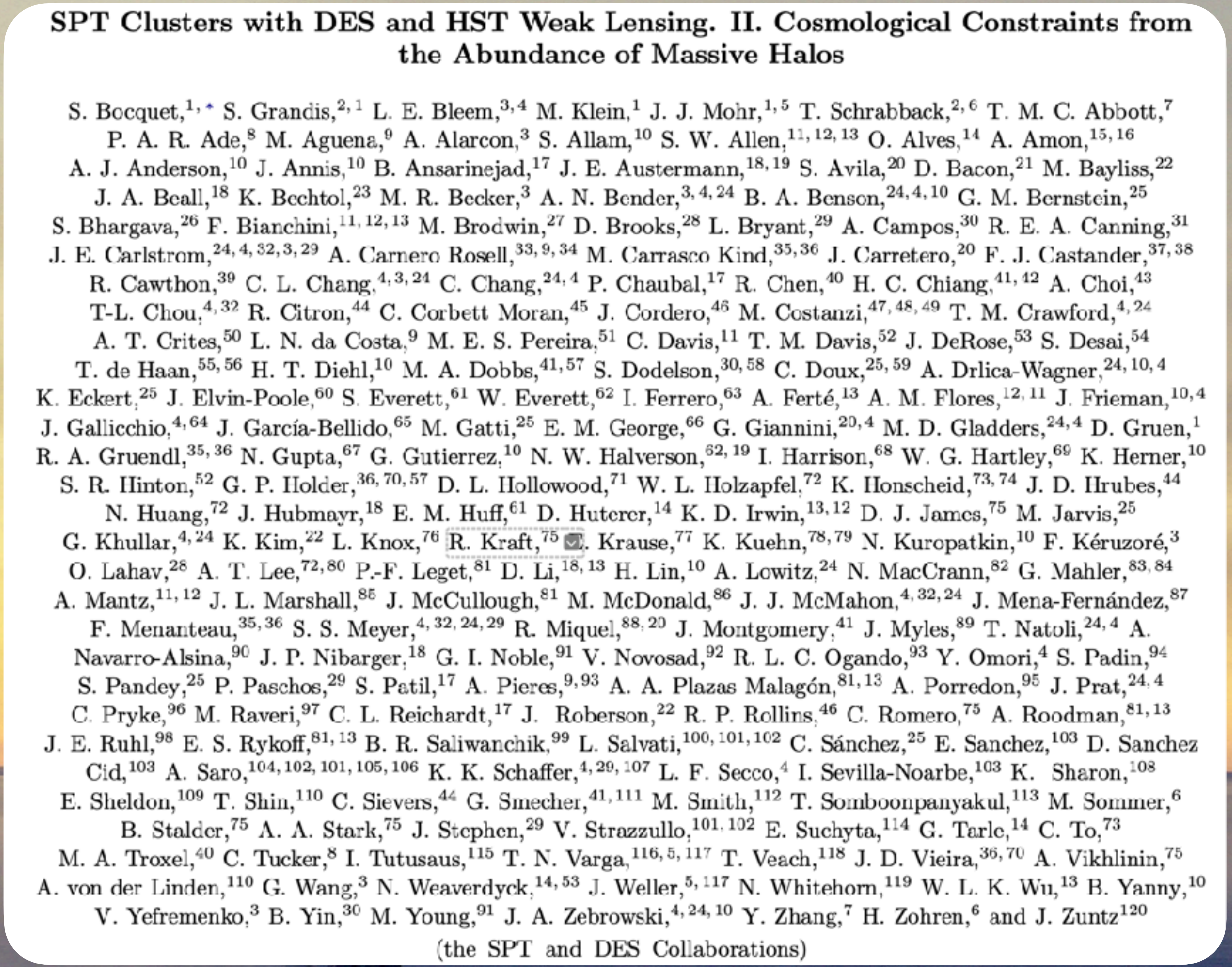

SPT Clusters with DES and HST Weak Lensing. II. Cosmological Constraints from the Abundance of Massive Halos

S. Bocquet,[1,*] S. Grandis,[2,1] L. E. Bleem,[3,4] M. Klein,[1] J. J. Mohr,[1,5] T. Schrabback,[2,6] T. M. C. Abbott,[7] P. A. R. Ade,[8] M. Aguena,[9] A. Alarcon,[3] S. Allam,[10] S. W. Allen,[11,12,13] O. Alves,[14] A. Amon,[15,16] A. J. Anderson,[10] J. Annis,[10] B. Ansarinejad,[17] J. E. Austermann,[18,19] S. Avila,[20] D. Bacon,[21] M. Bayliss,[22] J. A. Beall,[18] K. Bechtol,[23] M. R. Becker,[3] A. N. Bender,[3,4,24] B. A. Benson,[24,4,10] G. M. Bernstein,[25] S. Bhargava,[26] F. Bianchini,[11,12,13] M. Brodwin,[27] D. Brooks,[28] L. Bryant,[29] A. Campos,[30] R. E. A. Canning,[31] J. E. Carlstrom,[24,4,32,3,29] A. Carnero Rosell,[33,9,34] M. Carrasco Kind,[35,36] J. Carretero,[20] F. J. Castander,[37,38] R. Cawthon,[39] C. L. Chang,[4,3,24] C. Chang,[24,4] P. Chaubal,[17] R. Chen,[40] H. C. Chiang,[41,42] A. Choi,[43] T-L. Chou,[4,32] R. Citron,[44] C. Corbett Moran,[45] J. Cordero,[46] M. Costanzi,[47,48,49] T. M. Crawford,[4,24] A. T. Crites,[50] L. N. da Costa,[9] M. E. S. Pereira,[51] C. Davis,[11] T. M. Davis,[52] J. DeRose,[53] S. Desai,[54] T. de Haan,[55,56] H. T. Diehl,[10] M. A. Dobbs,[41,57] S. Dodelson,[30,58] C. Doux,[25,59] A. Drlica-Wagner,[24,10,4] K. Eckert,[25] J. Elvin-Poole,[60] S. Everett,[61] W. Everett,[62] I. Ferrero,[63] A. Ferté,[13] A. M. Flores,[12,11] J. Frieman,[10,4] J. Gallicchio,[4,64] J. García-Bellido,[65] M. Gatti,[25] E. M. George,[66] G. Giannini,[20,4] M. D. Gladders,[24,4] D. Gruen,[1] R. A. Gruendl,[35,36] N. Gupta,[67] G. Gutierrez,[10] N. W. Halverson,[62,19] I. Harrison,[68] W. G. Hartley,[69] K. Herner,[10] S. R. Hinton,[52] G. P. Holder,[36,70,57] D. L. Hollowood,[71] W. L. Holzapfel,[72] K. Honscheid,[73,74] J. D. Hrubes,[44] N. Huang,[72] J. Hubmayr,[18] E. M. Huff,[61] D. Huterer,[14] K. D. Irwin,[13,12] D. J. James,[75] M. Jarvis,[25] G. Khullar,[4,24] K. Kim,[22] L. Knox,[76] R. Kraft,[75] ☑. Krause,[77] K. Kuehn,[78,79] N. Kuropatkin,[10] F. Kéruzoré,[3] O. Lahav,[28] A. T. Lee,[72,80] P.-F. Leget,[81] D. Li,[18,13] H. Lin,[10] A. Lowitz,[24] N. MacCrann,[82] G. Mahler,[83,84] A. Mantz,[11,12] J. L. Marshall,[85] J. McCullough,[81] M. McDonald,[86] J. J. McMahon,[4,32,24] J. Mena-Fernández,[87] F. Menanteau,[35,36] S. S. Meyer,[4,32,24,29] R. Miquel,[88,20] J. Montgomery,[41] J. Myles,[89] T. Natoli,[24,4] A. Navarro-Alsina,[90] J. P. Nibarger,[18] G. I. Noble,[91] V. Novosad,[92] R. L. C. Ogando,[93] Y. Omori,[4] S. Padin,[94] S. Pandey,[25] P. Paschos,[29] S. Patil,[17] A. Pieres,[9,93] A. A. Plazas Malagón,[81,13] A. Porredon,[95] J. Prat,[24,4] C. Pryke,[96] M. Raveri,[97] C. L. Reichardt,[17] J. Roberson,[22] R. P. Rollins,[46] C. Romero,[75] A. Roodman,[81,13] J. E. Ruhl,[98] E. S. Rykoff,[81,13] B. R. Saliwanchik,[99] L. Salvati,[100,101,102] C. Sánchez,[25] E. Sanchez,[103] D. Sanchez Cid,[103] A. Saro,[104,102,101,105,106] K. K. Schaffer,[4,29,107] L. F. Secco,[4] I. Sevilla-Noarbe,[103] K. Sharon,[108] E. Sheldon,[109] T. Shin,[110] C. Sievers,[44] G. Smecher,[41,111] M. Smith,[112] T. Somboonpanyakul,[113] M. Sommer,[6] B. Stalder,[75] A. A. Stark,[75] J. Stephen,[29] V. Strazzullo,[101,102] E. Suchyta,[114] G. Tarle,[14] C. To,[73] M. A. Troxel,[40] C. Tucker,[8] I. Tutusaus,[115] T. N. Varga,[116,5,117] T. Veach,[118] J. D. Vieira,[36,70] A. Vikhlinin,[75] A. von der Linden,[110] G. Wang,[3] N. Weaverdyck,[14,53] J. Weller,[5,117] N. Whitehorn,[119] W. L. K. Wu,[13] B. Yanny,[10] V. Yefremenko,[3] B. Yin,[30] M. Young,[91] J. A. Zebrowski,[4,24,10] Y. Zhang,[7] H. Zohren,[6] and J. Zuntz[120]
(the SPT and DES Collaborations)

arXiv:2401.02075 — PRD accepted

Image credit: SPT 2018 winter-overs Adam & Joshua

Image credit: SPT 2018 winter-overs Adam & Joshua

The South Pole Telescope (SPT)

10-meter sub-mm quality wavelength telescope

90, 150, 220 GHz and
1.6, 1.2, 1.0 arcmin resolution

2007: SPT-SZ
960 detectors
90,150,220 GHz

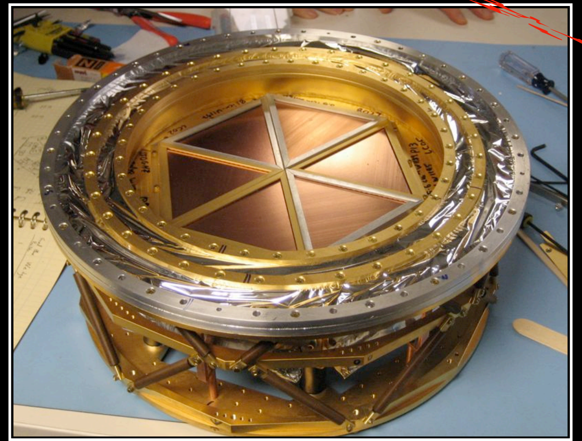

2012: SPTpol
1600 detectors
90,150 GHz
+Polarization

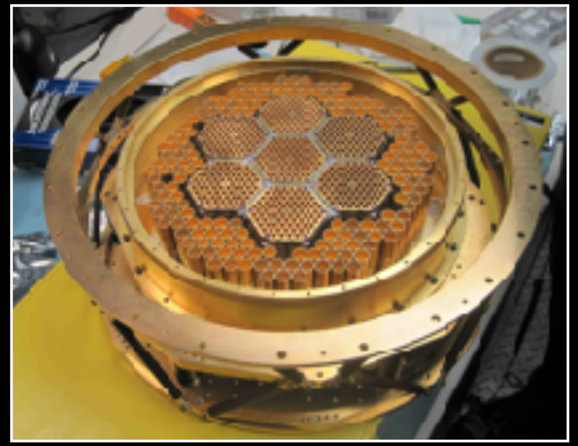

2017: SPT-3G
~15,200 detectors
90,150,220 GHz
+Polarization

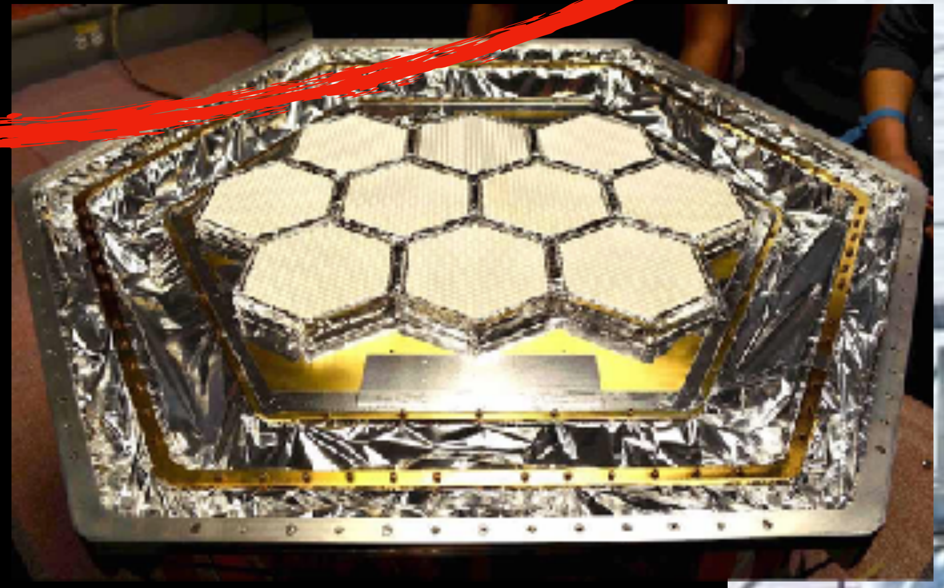

Funded By:

Funded by:

mm-wave map

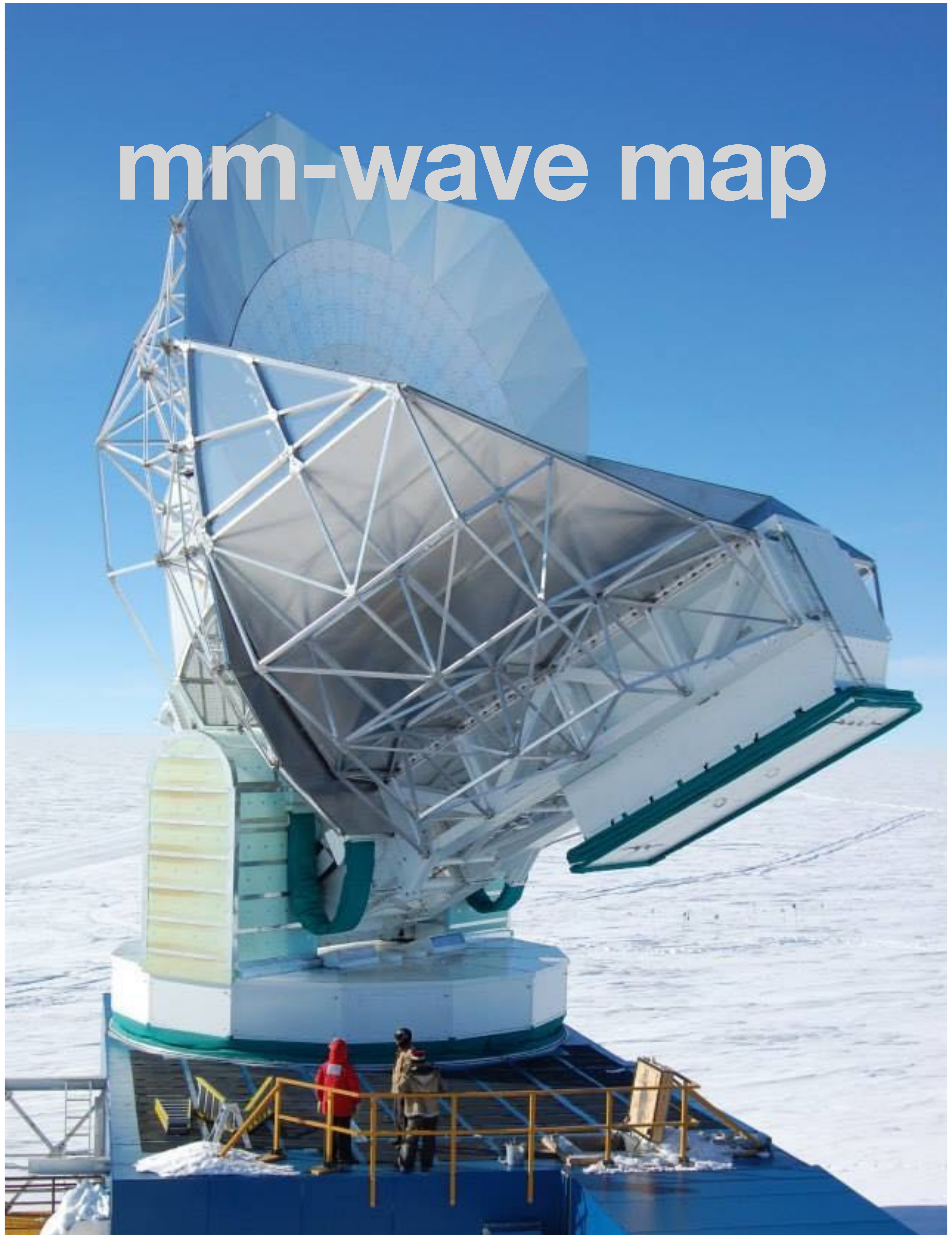

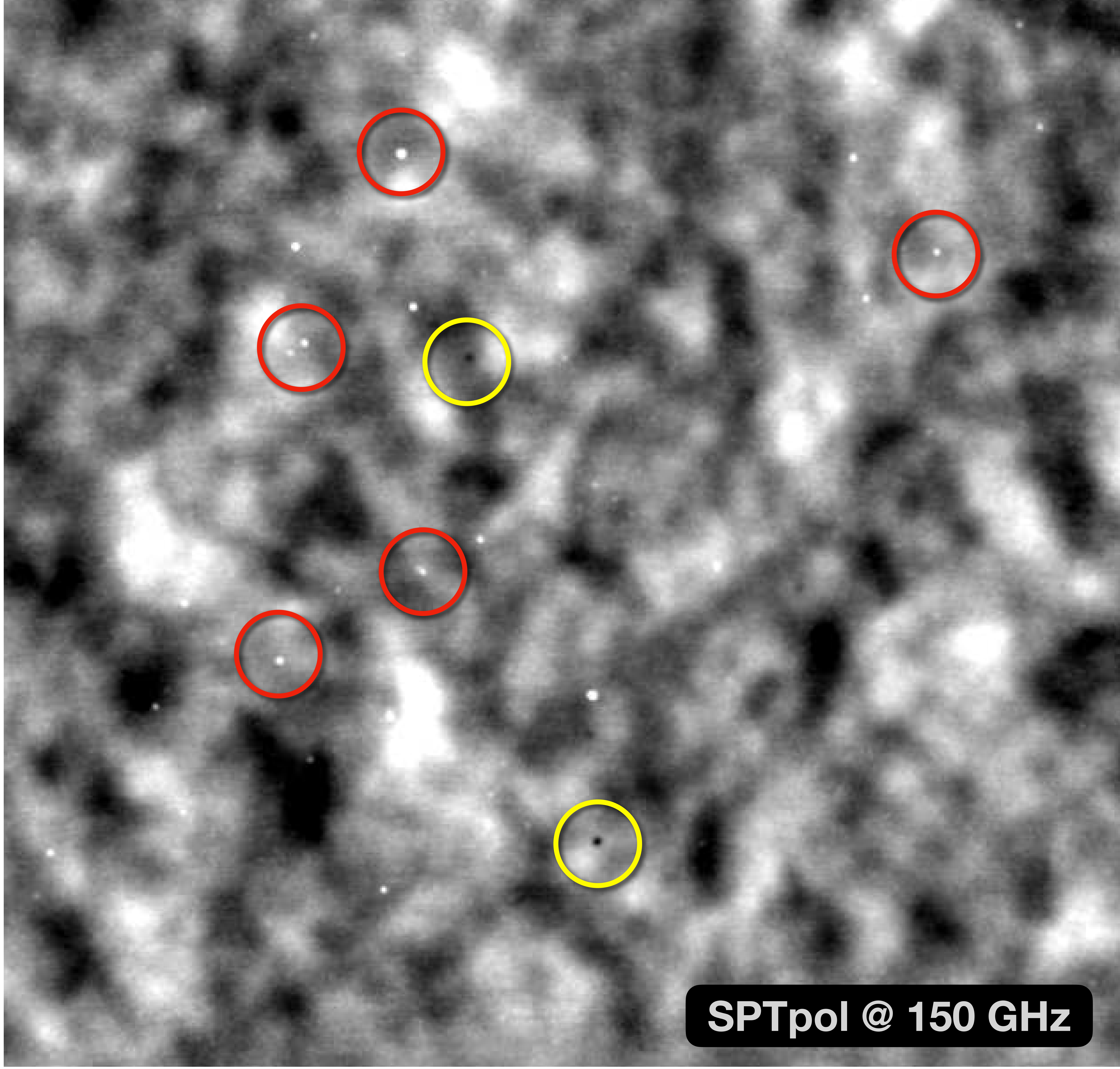

Find clusters

Sunyaev-Zel’dovich (SZ) Effect

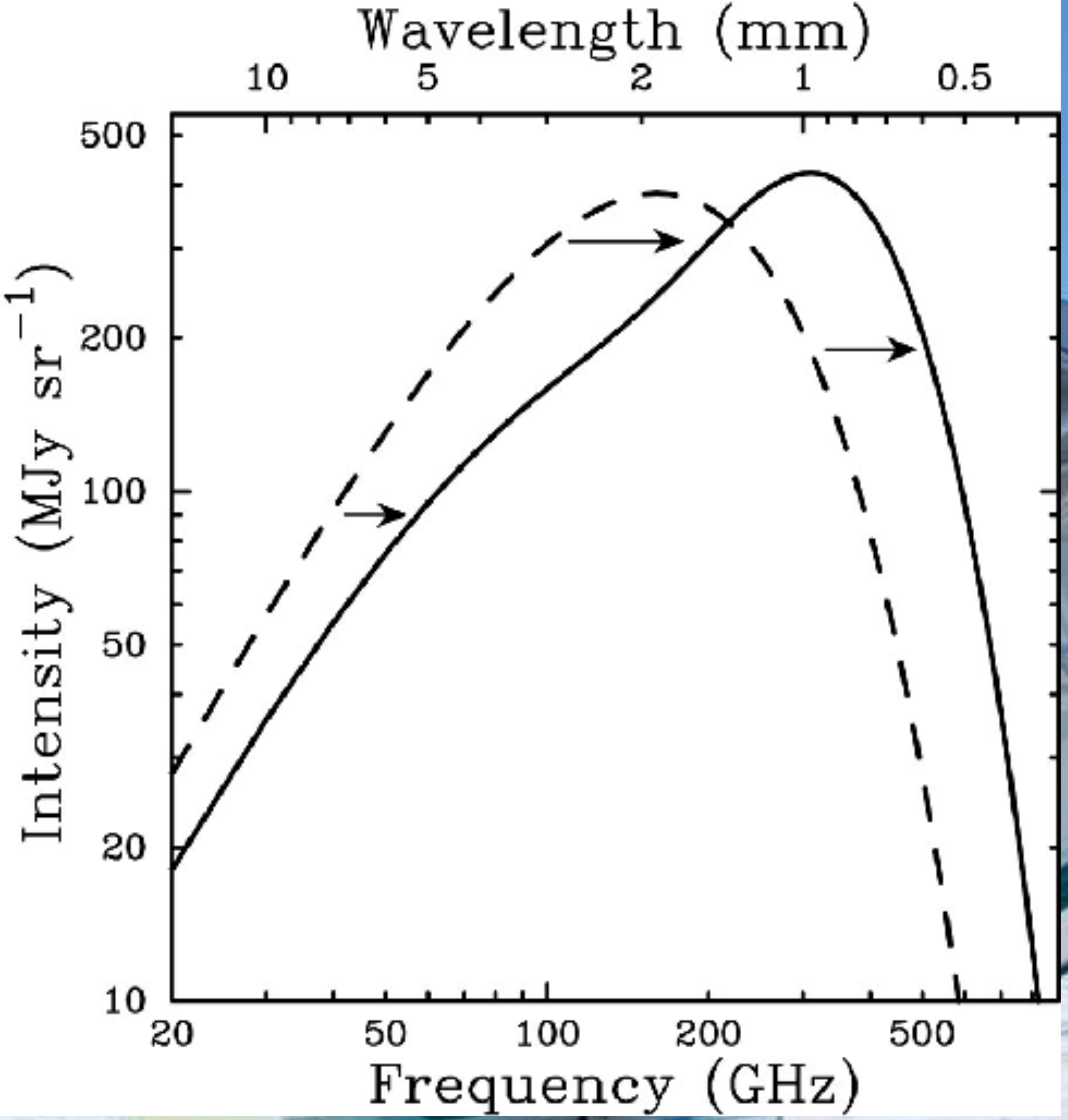

CMB spectrum

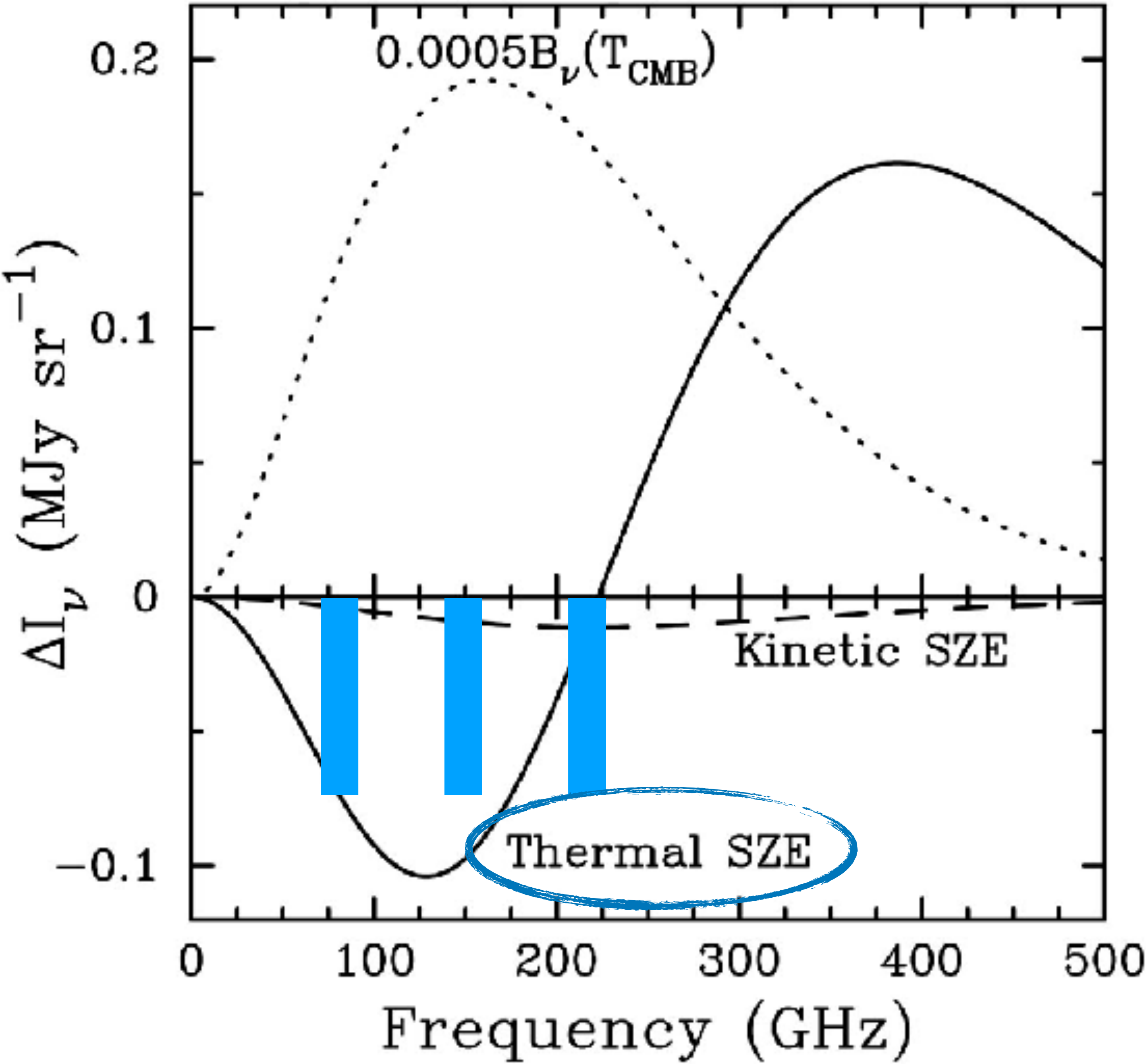

SZ spectrum

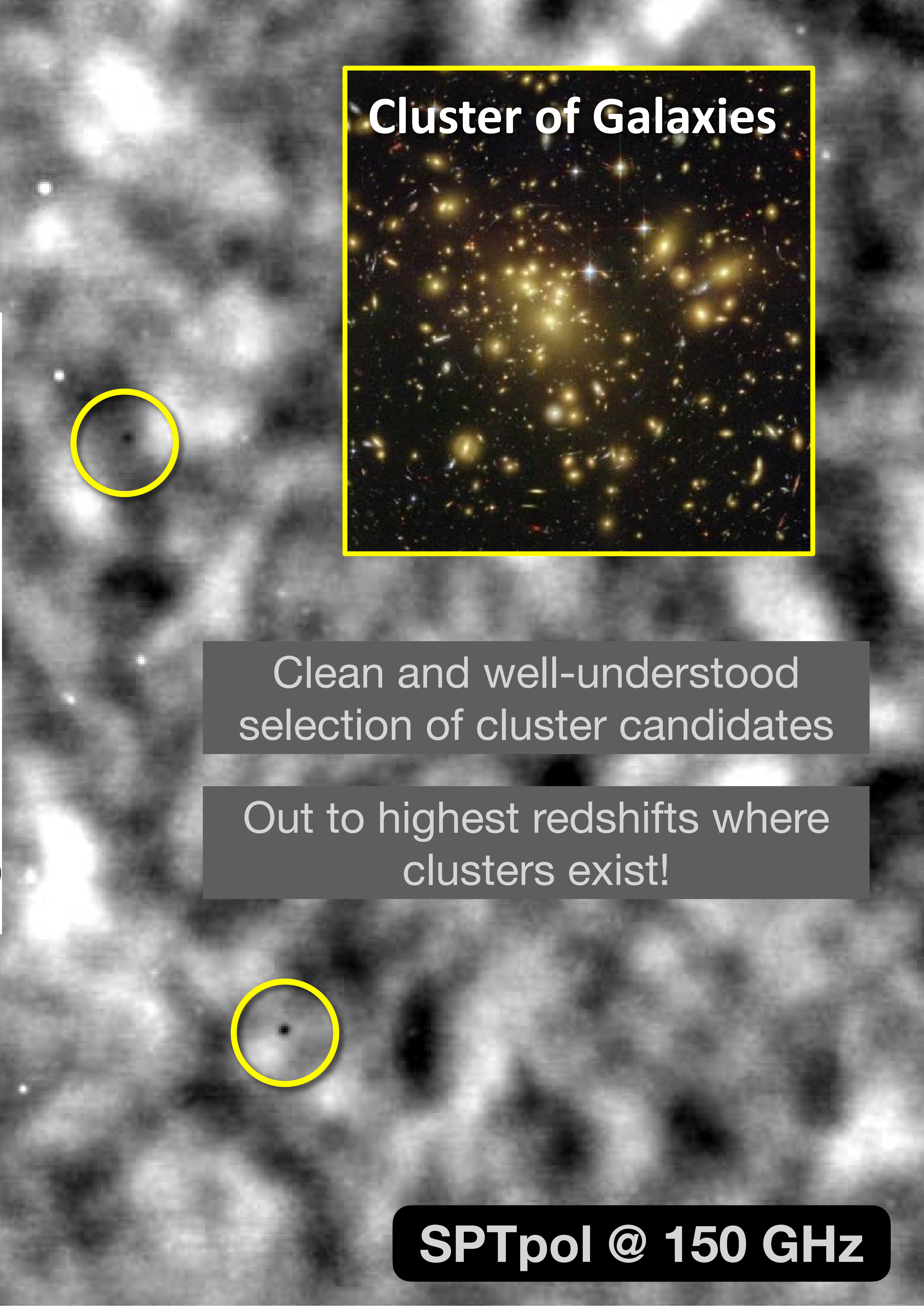

Clean and well-understood selection of cluster candidates

Out to highest redshifts where clusters exist!

Why use SZ-selected clusters?

Three approaches: X-ray, Optical, SZ

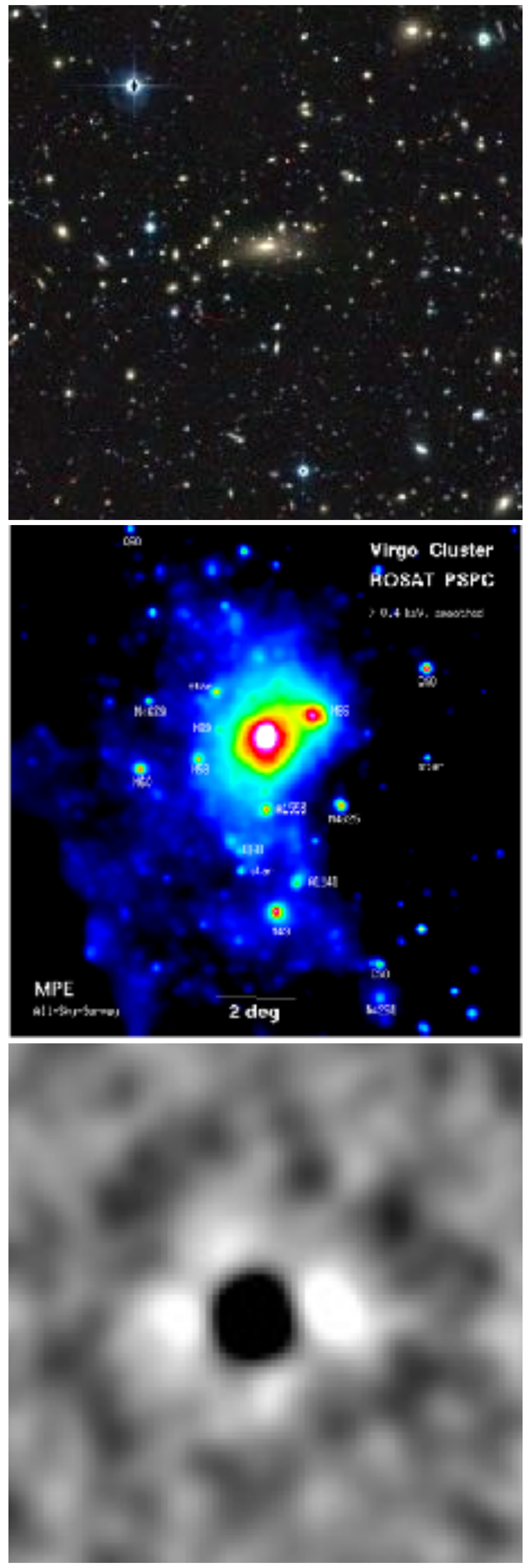

Weinberg et al. 2013

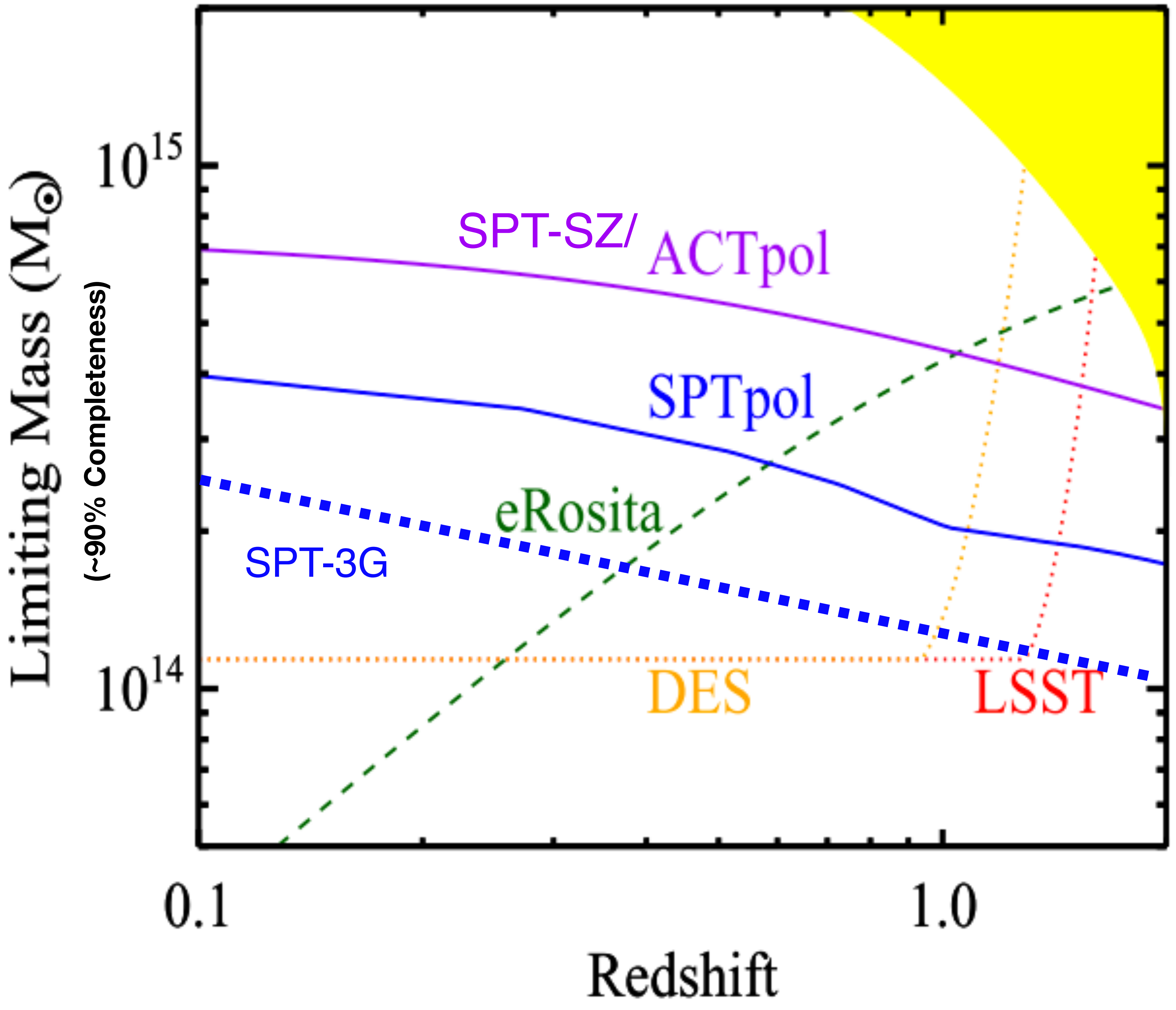

SZ: clean, well-understood selection

Complementarity with other methods

Kéruzoré et al. 2023

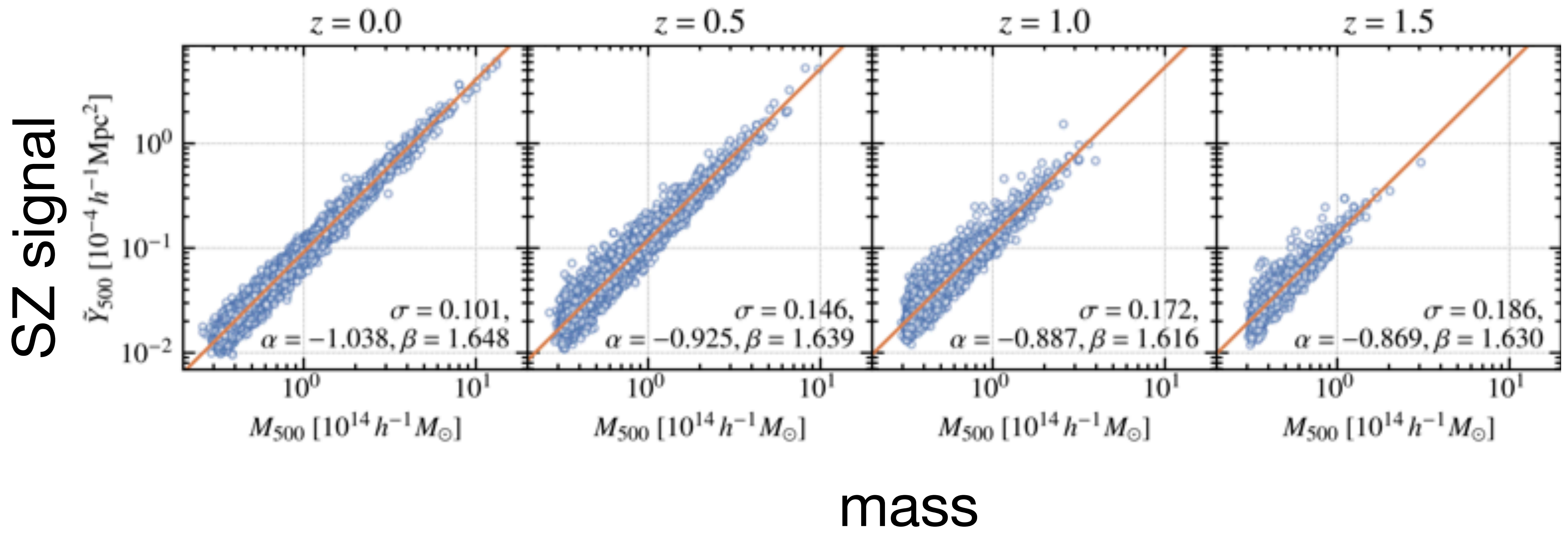

The Dark Energy Survey

5000 deg^2 galaxies & weak lensing

Catalog of SPT-selected cluster candidates needs

- Confirmation
- Cluster redshifts
- Weak-lensing (mass) measurement

all of which DES was designed for

(here we use DES Year 3 data = Y3)

Image credit: CTIO/NOIRLab/NSF/AURA/D. Munizaga

SZ Cluster Selection + Optical Confirmation

—> clean and deep cluster catalog

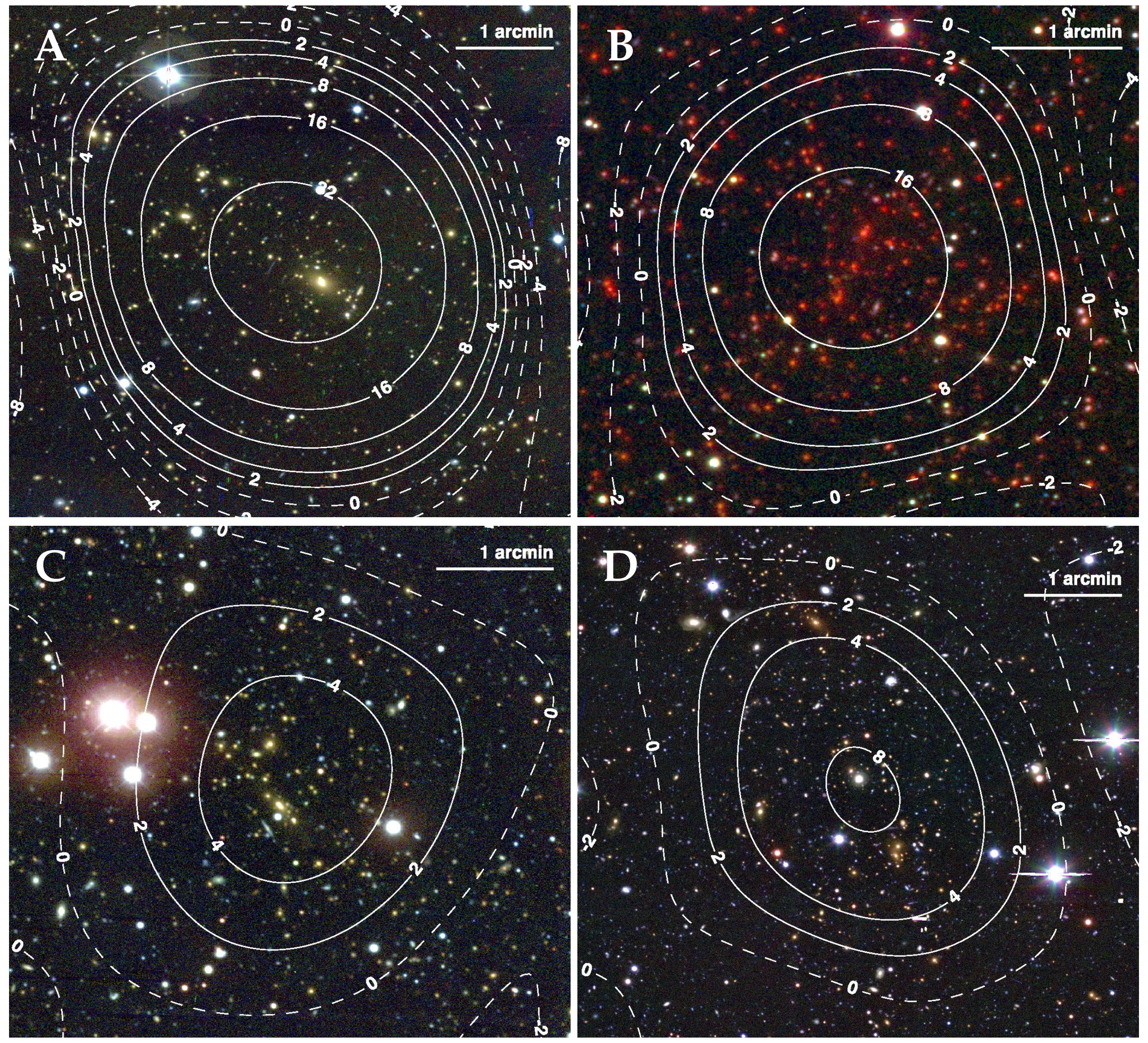

- Confirm SPT cluster candidates by measuring redshift (photo-*z*) and optical richness λ
- For the experts:
  - Get rid of chance associations (with SPT noise fluctuation)
    - Calibrate probability of chance association by measuring (λ, *z*) at random locations
    - Establish $\lambda_{\mathrm{min}}(z)$ to achieve target purity (> 98%)

MCMF machinery (Klein+18,23; Bleem+24)

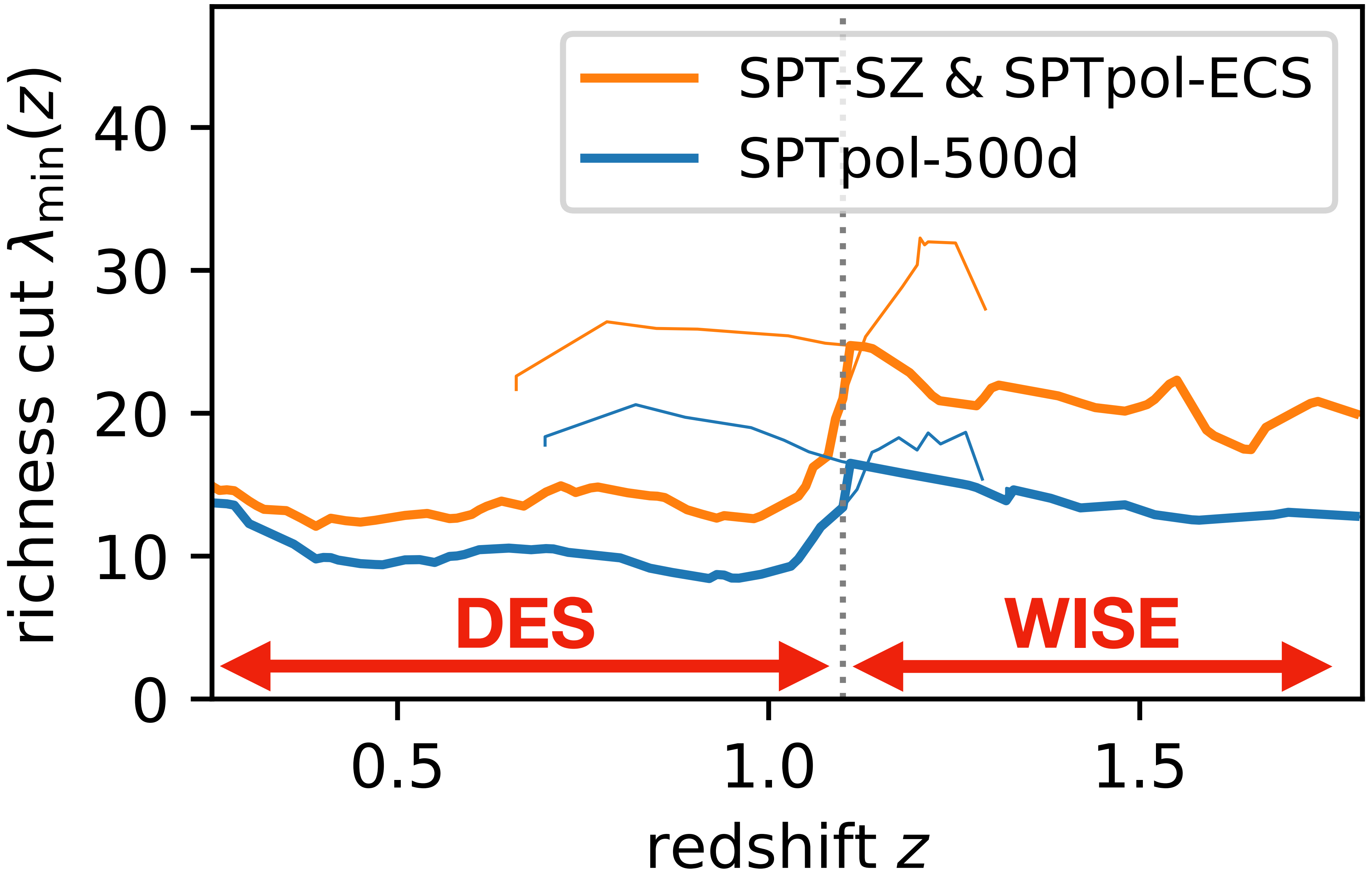

SPT(SZ+pol) Cluster Sample

1,005 confirmed clusters above *z* > 0.25 over 5,200 deg²

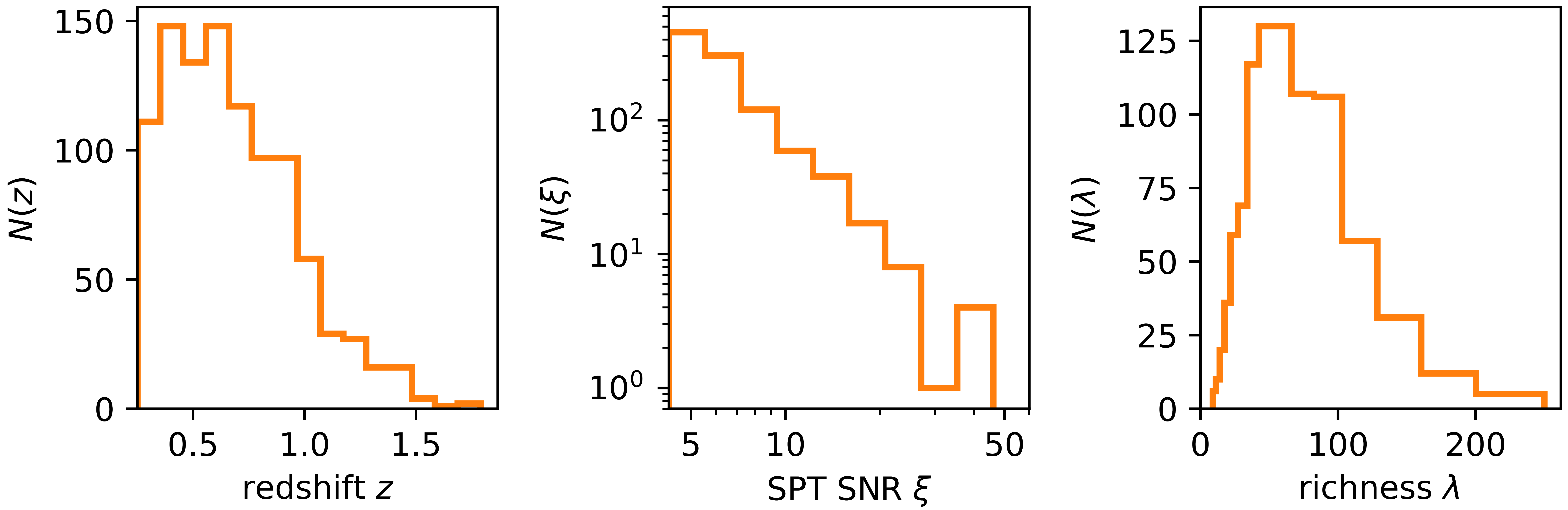

SPT Clusters and the Dark Energy Survey

3,600 deg² overlap

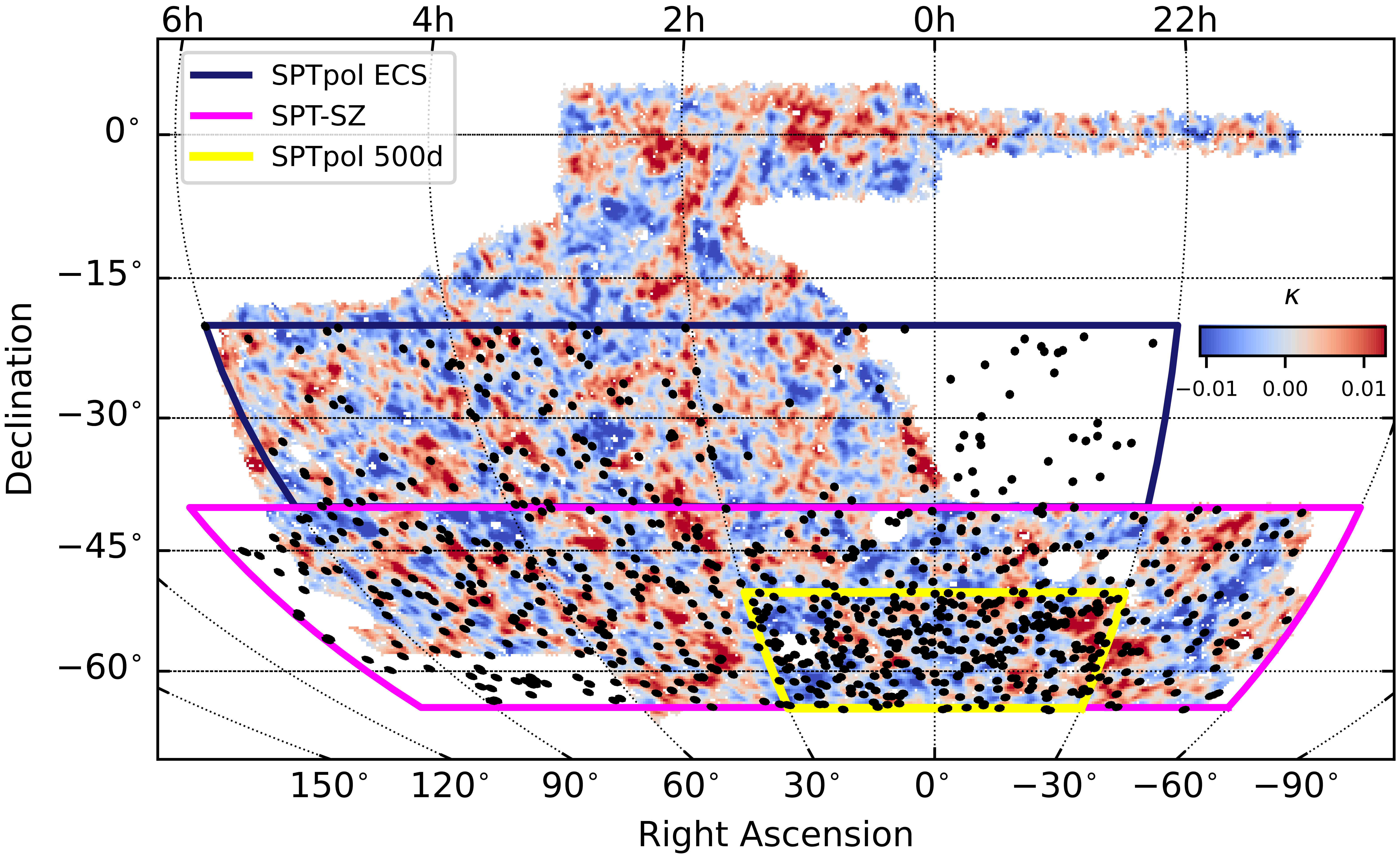

Bleem+15,20,24
Klein+24
Bocquet+24II

Cluster lensing analysis

Shear profiles

- Almost 700 SPT clusters (redshift 0.25—0.95) with DES Y3 shear
  - Analysis uses individual cluster shear profiles
  - Stacked for visualization purposes
  - For the experts:
    - Same source selection as in DES Y3 3x2pt
      - Same photo-*z* and shear calibrations
    - Radial range: $0.5 < r\ [h^{-1}\mathrm{Mpc}] < 3.2 / (1 + z)$
      (avoid cluster centers, stay in 1-halo term regime)
- 39 high-redshift clusters (redshift 0.6—1.7) with
  the Hubble Space Telescope
  Schrabback+18, Schrabback,Bocquet+21, Zohren,Schrabback,Bocquet+22

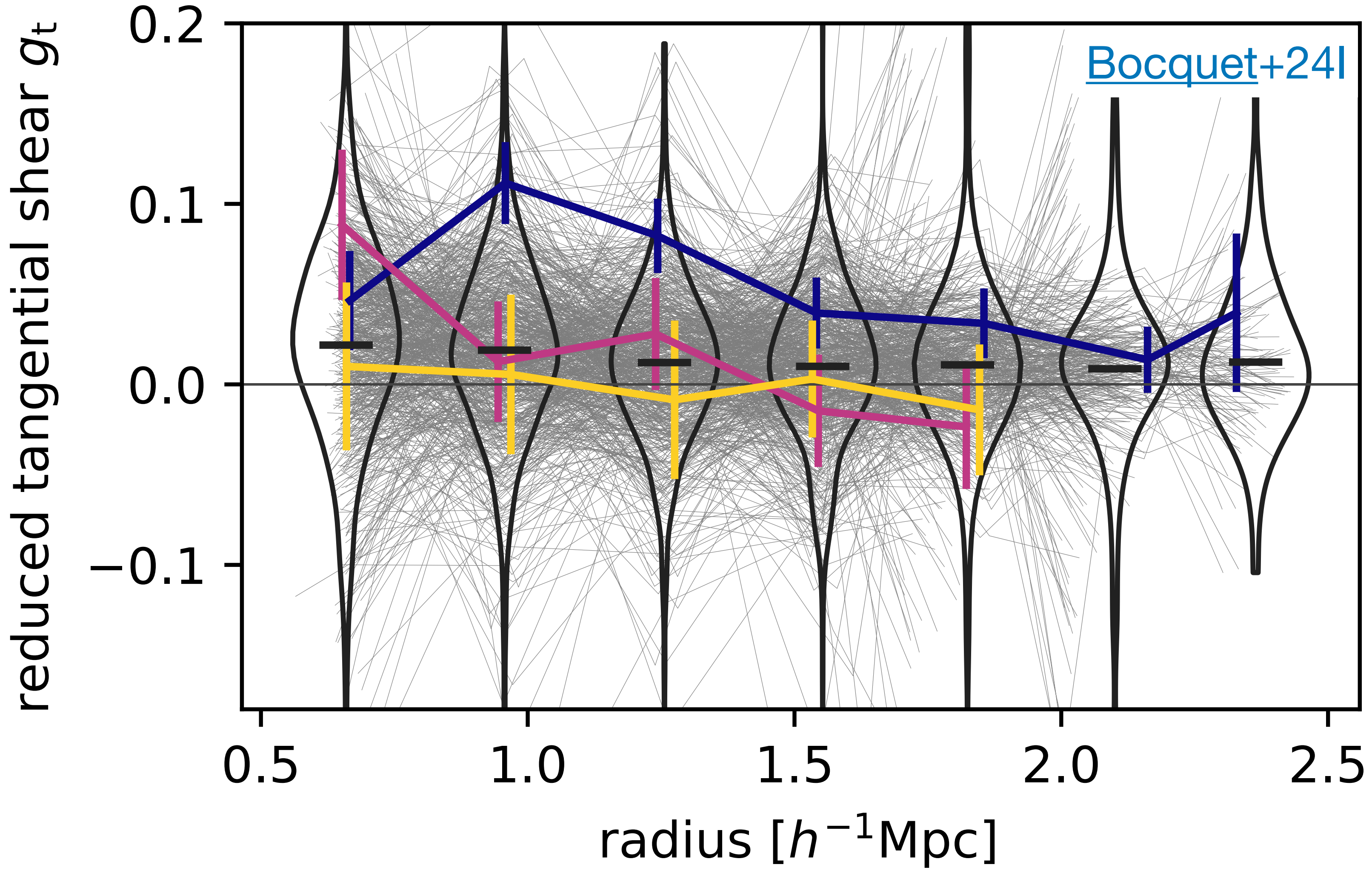

Bocquet+24I

Bocquet+24II

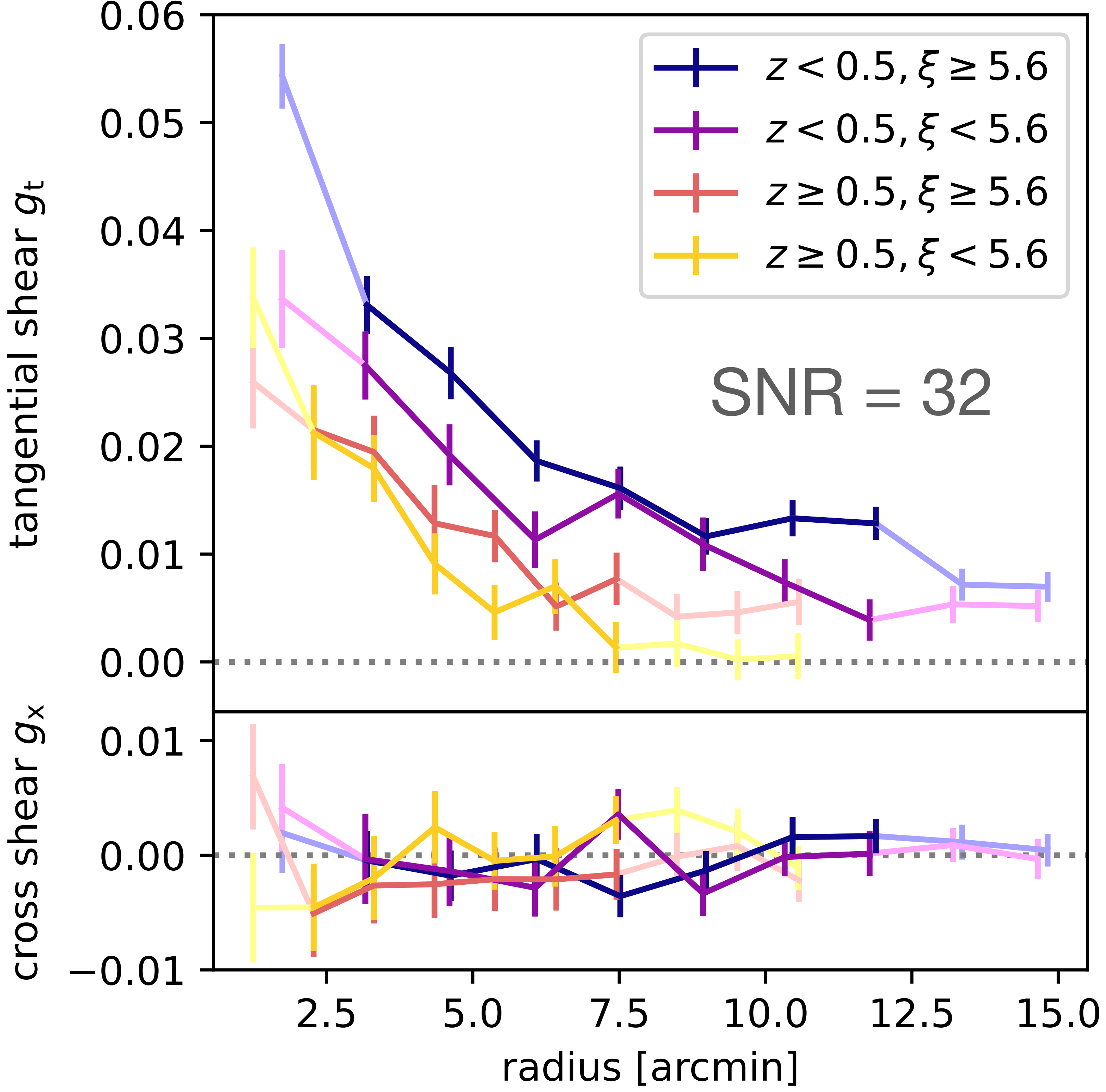

Likelihood Function I

Bayesian Population Modeling

Let us generate a cluster dataset!

cosmological

halo mass function

astrophysical

observable—mass relation

observational

telescope, detector, atmosphere, etc.

$$\frac{d^3N(\boldsymbol{p})}{dM\,dz\,dV}\,\frac{dV(z,\boldsymbol{p})}{d\Omega_\mathrm{s}} \xrightarrow{\text{Poisson draw}} \{M,z\} \xrightarrow{\text{OMR + scatter}} \{\zeta,\lambda,M_\mathrm{WL},z\} \xrightarrow{\text{measurement noise}} \{\xi,\lambda,\boldsymbol{g}_\mathrm{t},z\}$$

Likelihood Function I

Bayesian Population Modeling

Let us generate a cluster dataset!

cosmological

halo mass function

astrophysical

observable—mass relation

observational

telescope, detector, atmosphere, etc.

$$\frac{d^3N(\boldsymbol{p})}{dM\,dz\,dV}\,\frac{dV(z,\boldsymbol{p})}{d\Omega_\mathrm{s}} \xrightarrow{\text{Poisson draw}} \{M, z\} \xrightarrow{\text{OMR + scatter}} \{\zeta, \lambda, M_\mathrm{WL}, z\} \xrightarrow{\text{measurement noise}} \{\xi, \lambda, \boldsymbol{g}_\mathrm{t}, z\}$$

Differential multi-observable cluster abundance

$$\boxed{\frac{d^4N(\boldsymbol{p})}{d\xi\,d\lambda\,d\boldsymbol{g}_\mathrm{t}\,dz}} = \boxed{\int \dots \int dM\,d\zeta\,d\tilde{\lambda}\,dM_\mathrm{WL}}\,d\Omega_\mathrm{s}\,\boxed{P(\xi\,|\,\zeta)P(\lambda\,|\,\tilde{\lambda})P(\boldsymbol{g}_\mathrm{t}\,|\,M_\mathrm{WL})}\boxed{P(\zeta, \lambda, M_\mathrm{WL}\,|\,M, z, \boldsymbol{p})}\boxed{\frac{d^2N(\boldsymbol{p})}{dM\,dV}\,\frac{d^2V(z,\boldsymbol{p})}{dz\,d\Omega_\mathrm{s}}}$$

marginalize over

latent variables

Likelihood Function II

Poisson likelihood function: $\mathscr{L}(k\,\textbf{events}\mid\textbf{rate}\,\mu) \propto \mu^k e^{-\mu} \Rightarrow \ln\mathscr{L} = k\ln(\mu) - \mu$

$$\ln\mathscr{L}(\boldsymbol{p}) = \sum_i \ln \frac{d^4N(\boldsymbol{p})}{d\xi\, d\lambda\, d\boldsymbol{g}_\mathrm{t}\, dz}\bigg|_{\xi_i,\lambda_i,g_{\mathrm{t},i},z_i} - \int\ldots\int d\xi\, d\lambda\, d\boldsymbol{g}_\mathrm{t}\, dz\, \frac{d^4N(\boldsymbol{p})}{d\xi\, d\lambda\, d\boldsymbol{g}_\mathrm{t}\, dz}\Theta_\mathrm{s}(\xi,\lambda,z) + \mathrm{const}\,.$$

Likelihood Function II

Poisson likelihood function: $\mathscr{L}(k$ **events** | **rate** $\mu) \propto \mu^k e^{-\mu} \Rightarrow \ln \mathscr{L} = k \ln(\mu) - \mu$

$$\ln \mathscr{L}(\boldsymbol{p}) = \sum_i \ln \boxed{\frac{d^4N(\boldsymbol{p})}{d\xi\, d\lambda\, d\boldsymbol{g}_\mathrm{t}\, dz}}\Bigg|_{\xi_i,\lambda_i,g_{\mathrm{t},i},z_i} - \int \dots \int d\xi\, d\lambda\, d\boldsymbol{g}_\mathrm{t}\, dz\, \boxed{\frac{d^4N(\boldsymbol{p})}{d\xi\, d\lambda\, d\boldsymbol{g}_\mathrm{t}\, dz}} \Theta_\mathrm{s}(\xi, \lambda, z) + \mathrm{const}\,.$$

Likelihood Function II

Poisson likelihood function: $\mathscr{L}(k\,\textbf{events}\mid\textbf{rate}\,\mu) \propto \mu^k\, e^{-\mu} \Rightarrow \ln\mathscr{L} = k\ln(\mu) - \mu$

$$\ln\mathscr{L}(\boldsymbol{p}) = \sum_i \ln \frac{d^4N(\boldsymbol{p})}{d\xi\, d\lambda\, d\boldsymbol{g}_\mathrm{t}\, dz}\bigg|_{\xi_i,\lambda_i,g_{\mathrm{t},i},z_i} - \int\ldots\int d\xi\, d\lambda\, d\boldsymbol{g}_\mathrm{t}\, dz\, \frac{d^4N(\boldsymbol{p})}{d\xi\, d\lambda\, d\boldsymbol{g}_\mathrm{t}\, dz}\Theta_\mathrm{s}(\xi,\lambda,z) + \mathrm{const}\,.$$

can be re-written as

Likelihood Function II

Poisson likelihood function: $\mathscr{L}(k\ \textbf{events}\,|\,\textbf{rate}\ \mu) \propto \mu^k e^{-\mu} \Rightarrow \ln\mathscr{L} = k\ln(\mu) - \mu$

$$\ln\mathscr{L}(\boldsymbol{p}) = \sum_i \ln \left.\frac{d^4N(\boldsymbol{p})}{d\xi\,d\lambda\,d\boldsymbol{g}_\mathrm{t}\,dz}\right|_{\xi_i,\lambda_i,g_{\mathrm{t},i},z_i} - \int\dots\int d\xi\,d\lambda\,d\boldsymbol{g}_\mathrm{t}\,dz\,\frac{d^4N(\boldsymbol{p})}{d\xi\,d\lambda\,d\boldsymbol{g}_\mathrm{t}\,dz}\Theta_\mathrm{s}(\xi,\lambda,z) + \mathrm{const}\,.$$

can be re-written as

$$\ln\mathscr{L}(\boldsymbol{p}) = \underbrace{\sum_i \ln\int_{\lambda_\mathrm{cut}}^{\infty} d\lambda \left.\frac{d^3N(\boldsymbol{p})}{d\xi\,d\lambda\,dz}\right|_{\xi_i,z_i} - \int_{z_\mathrm{cut}}^{\infty} dz \int_{\xi_\mathrm{cut}}^{\infty} d\xi \int_{\lambda_\mathrm{cut}}^{\infty} d\lambda \frac{d^3N(\boldsymbol{p})}{d\xi\,d\lambda\,dz}}_{\text{cluster abundance likelihood}} + \sum_i \ln \boxed{\frac{\left.\frac{d^4N(\boldsymbol{p})}{d\xi\,d\lambda\,d\boldsymbol{g}_\mathrm{t}\,dz}\right|_{\xi_i,\lambda_i,\boldsymbol{g}_{\mathrm{t},i},z_i}}{\int_{\lambda_\mathrm{cut}}^{\infty} d\lambda \left.\frac{d^3N(\boldsymbol{p})}{d\xi\,d\lambda\,dz}\right|_{\xi_i,z_i}}} + \mathrm{const}\,.$$

$$\underbrace{\boxed{\frac{\frac{d^4N(\boldsymbol{p})}{d\xi\,d\lambda\,d\boldsymbol{g}_\mathrm{t}\,dz}}{\int_{\lambda_\mathrm{cut}}^{\infty} d\lambda \frac{d^3N(\boldsymbol{p})}{d\xi\,d\lambda\,dz}}}}_{\text{conditional “mass calibration likelihood”}} = \frac{P(\lambda,\boldsymbol{g}_\mathrm{t},\xi,z\,|\,\boldsymbol{p})}{P(\lambda>\lambda_\mathrm{cut},\xi,z\,|\,\boldsymbol{p})} \equiv P(\lambda,\boldsymbol{g}_\mathrm{t}\,|\,\lambda>\lambda_\mathrm{cut},\xi,z,\boldsymbol{p})$$

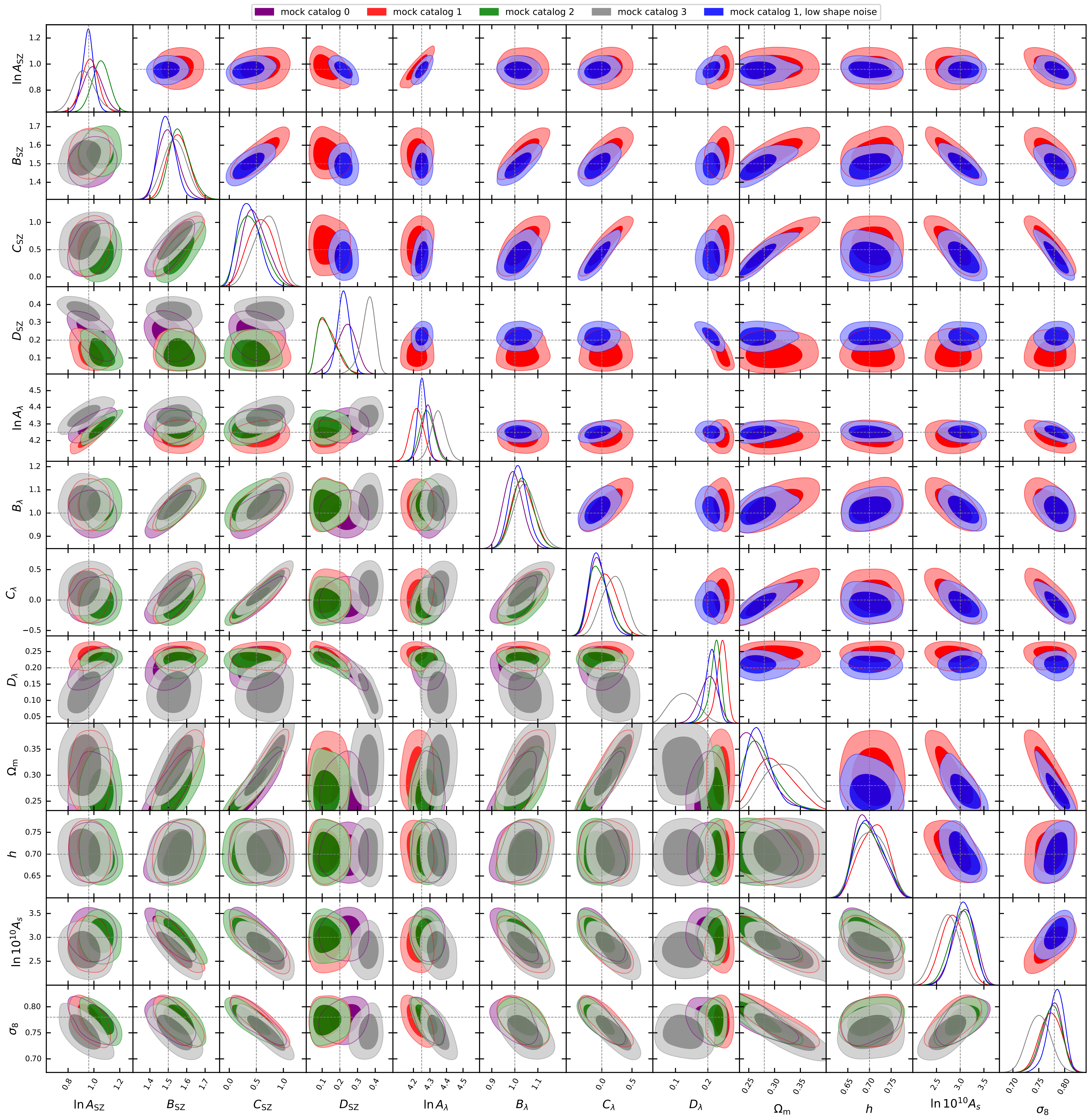

Bocquet+24l

Pipeline Verification

using mock datasets created from the model

- Create synthetic clusters from the halo mass function using observable—mass relations
- Analyze several statistically independent mock realizations
- Pipeline recovers input values
- We correctly implemented the analysis framework!

Robustness Tests during Blind Analysis Phase

All chains were blinded by applying the same unknown parameter offset

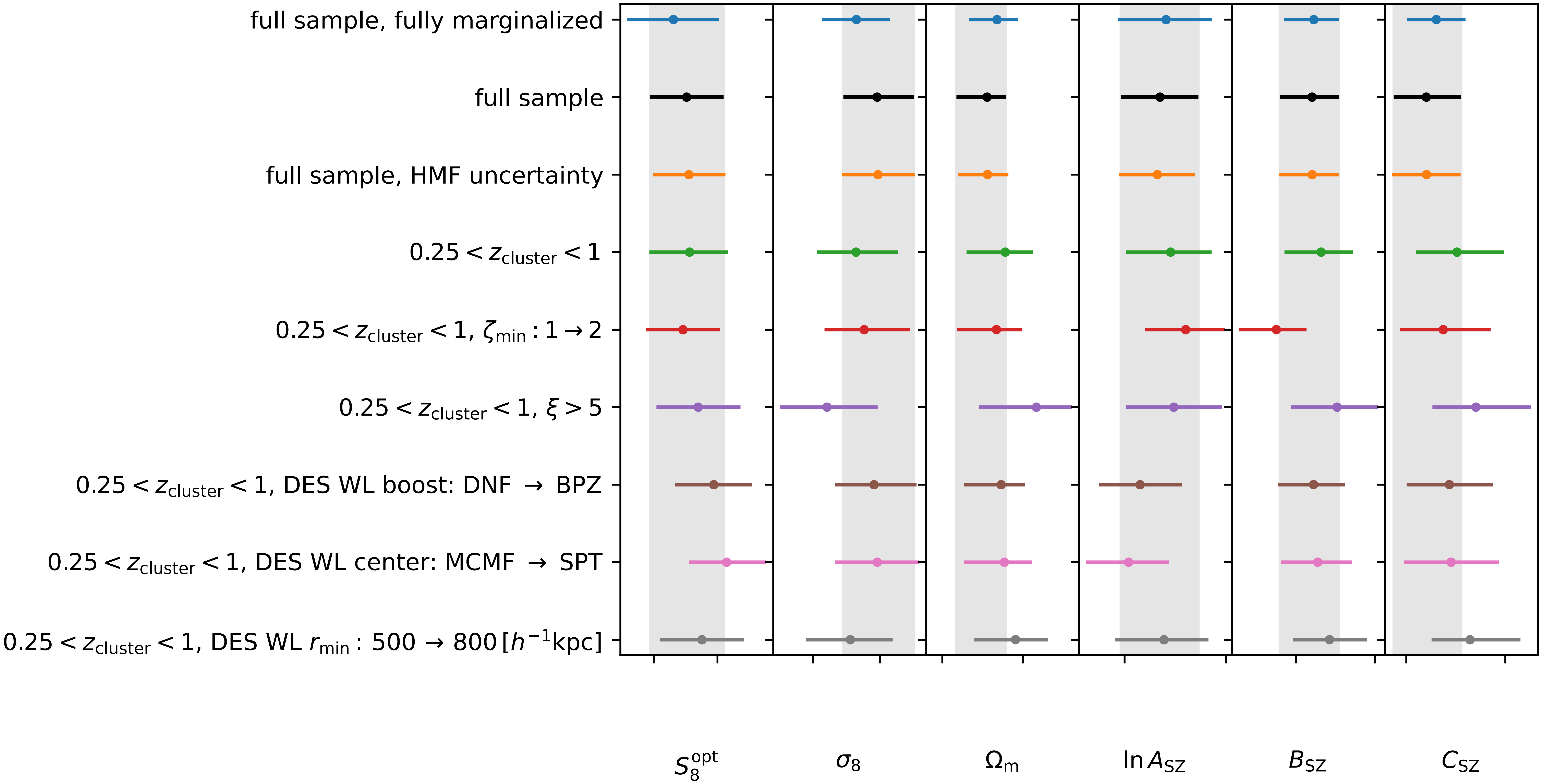

Bocquet+24II

Robustness Tests during Blind Analysis Phase

All chains were blinded by applying the same unknown parameter offset

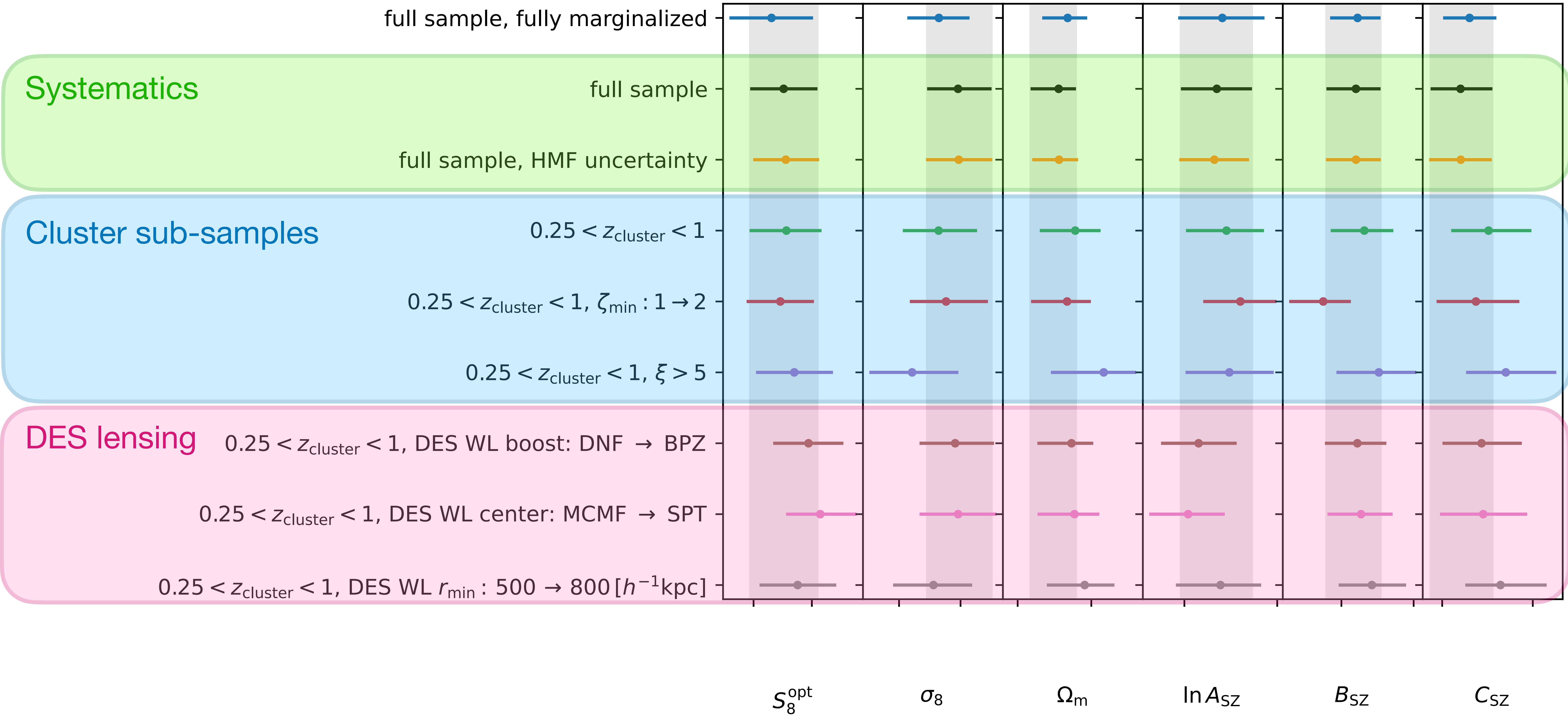

Bocquet+24II

Does the model describe the data?

Binned and stacked data for visualization

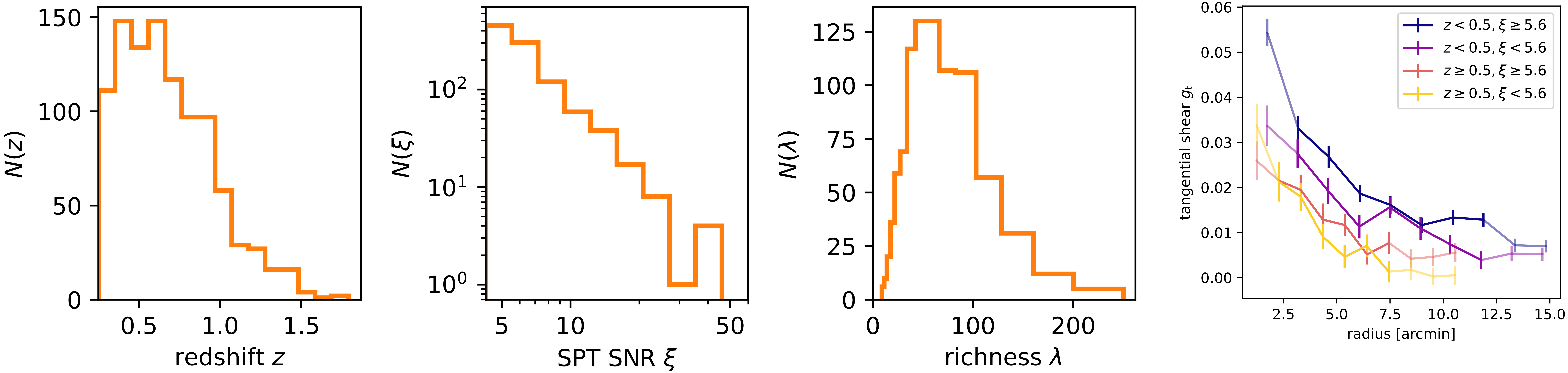

Bocquet+24II

Does the model describe the data?

Binned and stacked data for visualization

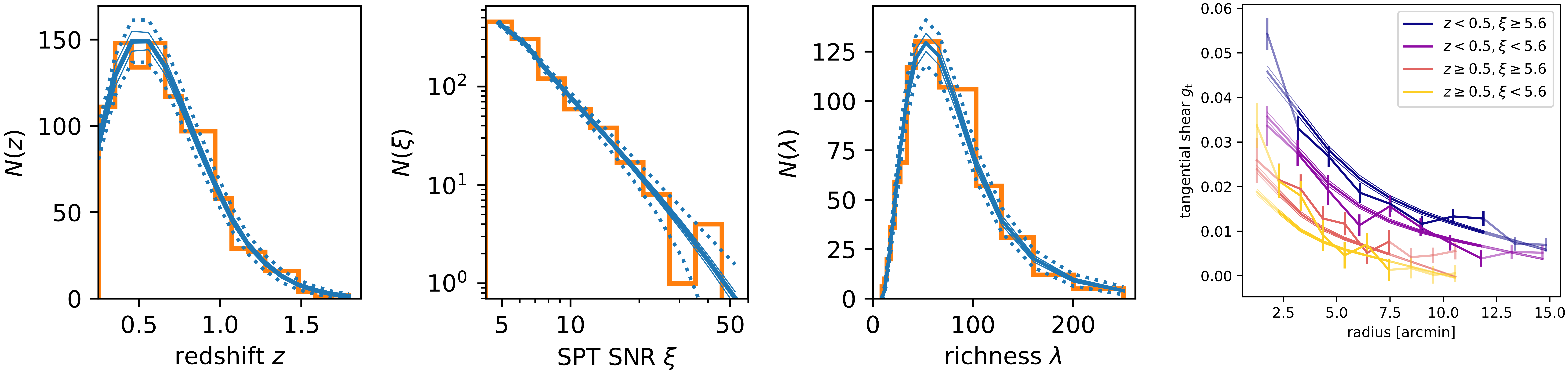

Bocquet+24II

Mean recovered model (and uncertainties) from full analysis.
No significant signs of problems.

ΛCDM with massive neutrinos

amplitude of fluctuation in matter density field

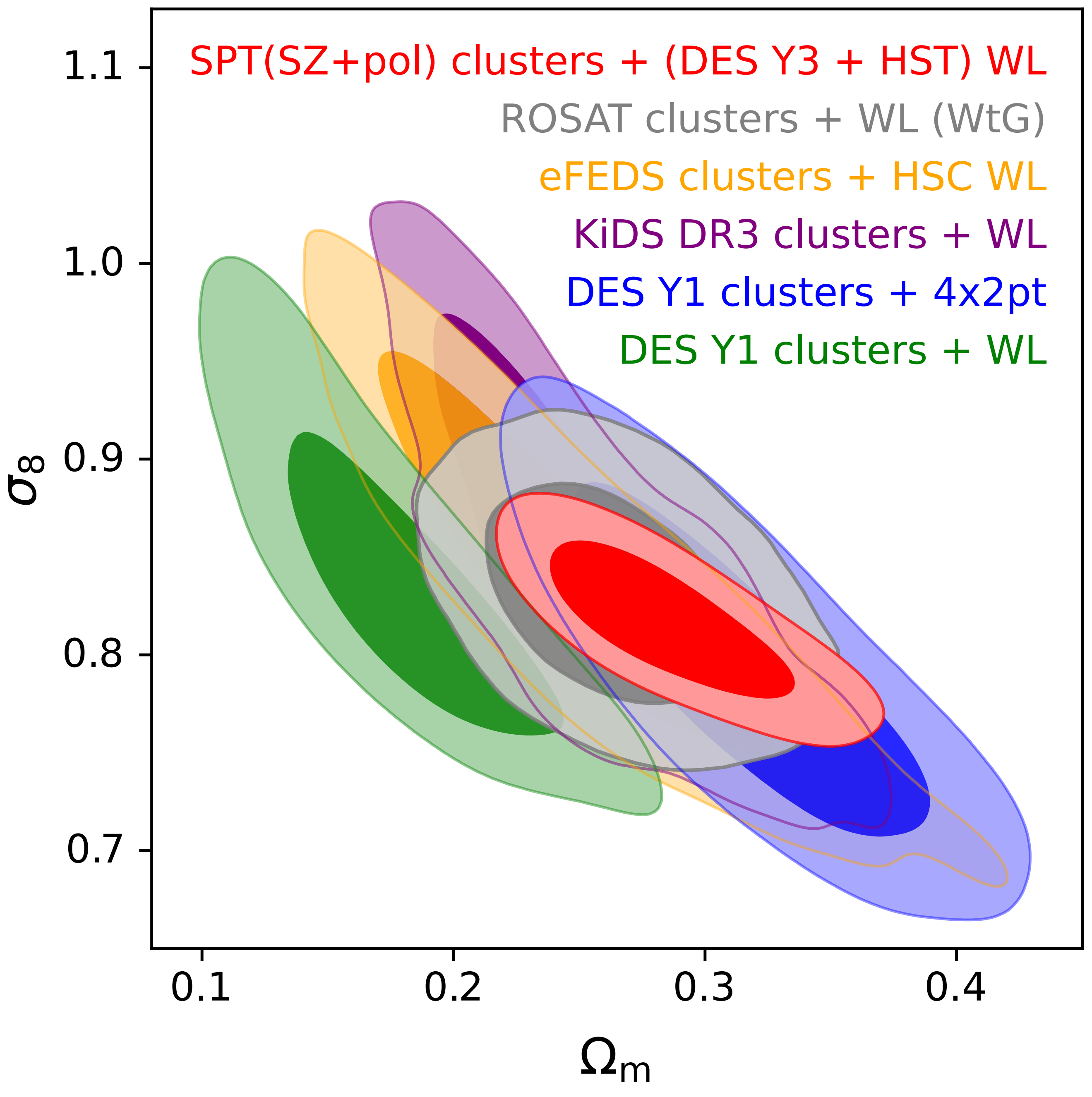

matter density

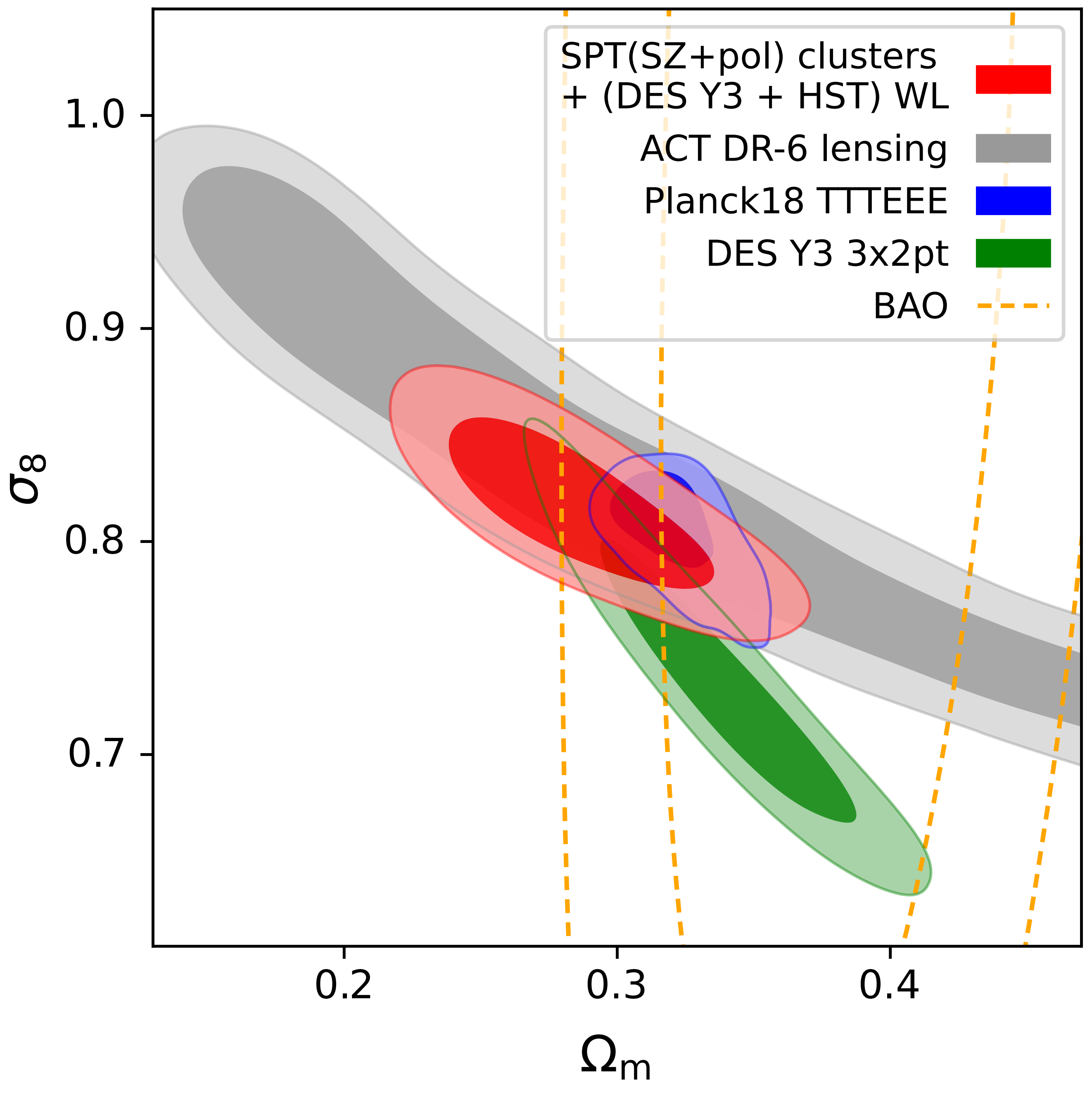

Bocquet+24II

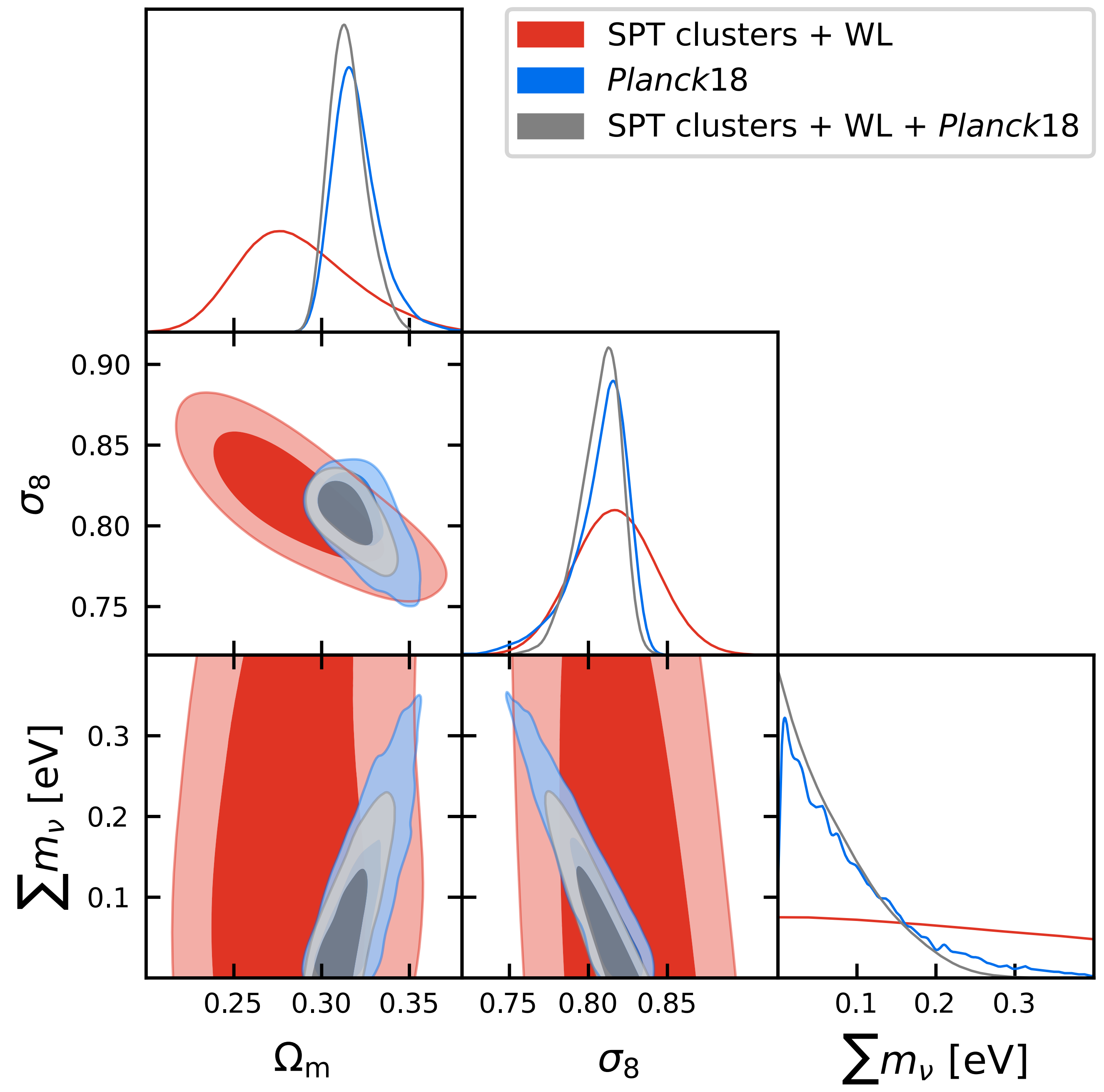

- Competitive constraints, especially on $S_8^{\rm opt} \equiv \sigma_8 \left(\Omega_{\rm m}/0.3\right)^{0.25}$
- No evidence for "S_8 tension" with Planck (1.1 σ)
- In combination with Planck $\sum m_\nu < 0.18\,{\rm eV}\,(95\,\%\,{\rm C.L.})$

Tracing the Growth of Structure

Phenomenological test

- Five bins in redshift with equal number of clusters
- Fit for independent amplitudes $\sigma_8(z)$
- With loose prior on Ω_m from the sound horizon at recombination θ_*
- Good agreement with ΛCDM model and *Planck* parameters from $z = 0.25$ to $z = 1.8$

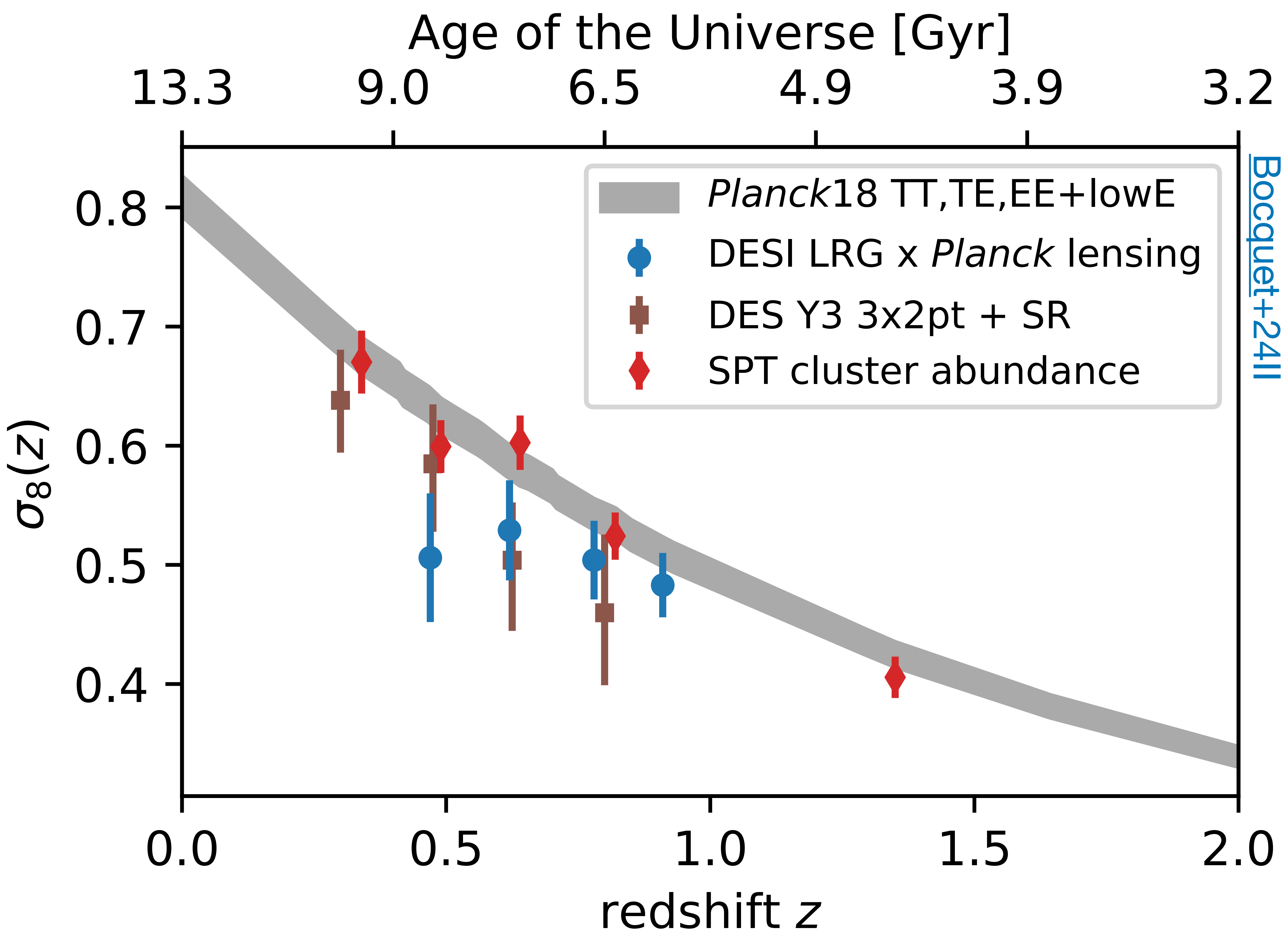

Outlook

select work by PhD students

Mazoun, Bocquet, Garny, Mohr, Rubira, Vogt 24

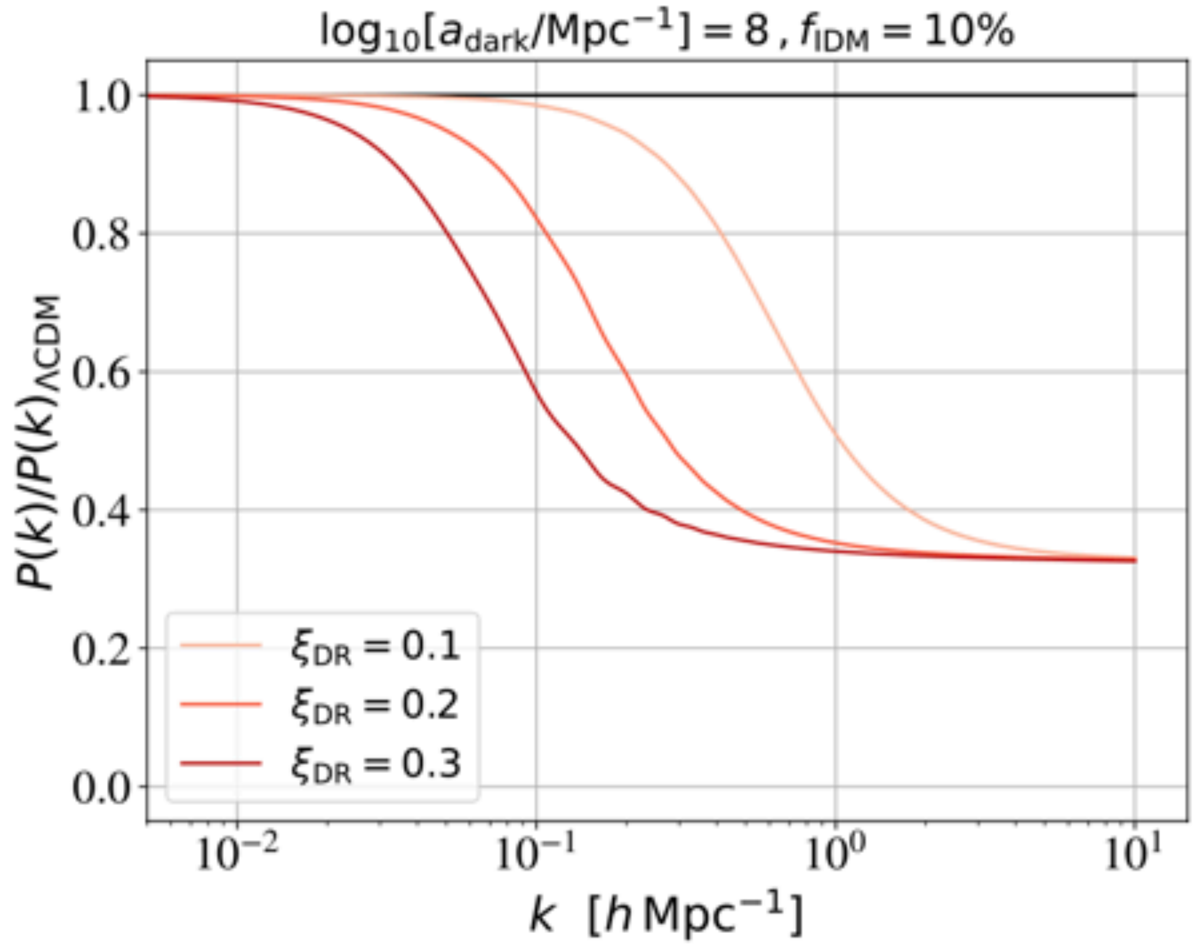

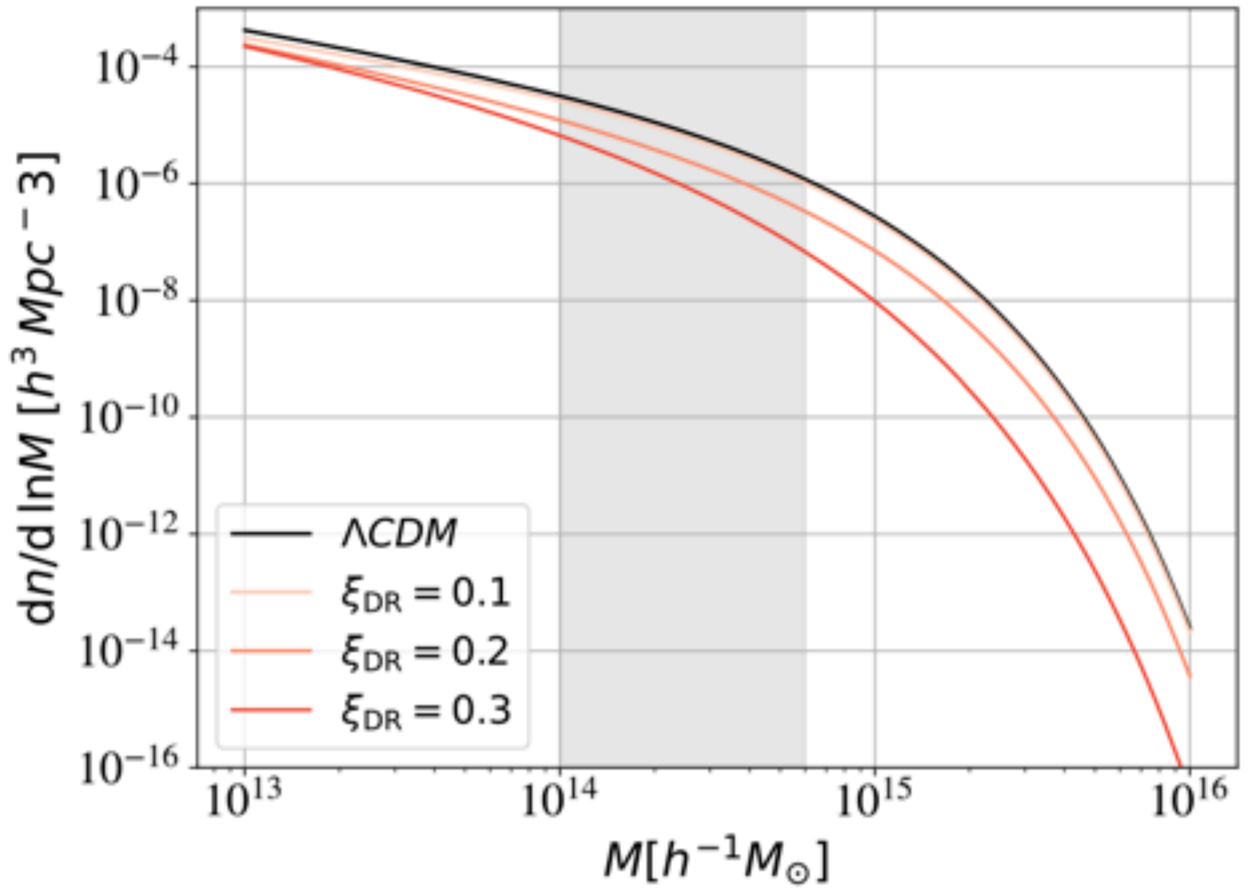

Asmaa Mazoun

Interacting dark sector models

Analysis of SPT+DES dataset ongoing
(Mazoun+ in prep.)

Sophie Vogt

f(R) and nDGP models

Analysis of SPT+DES dataset done
(Vogt+ in prep.)

Vogt, Bocquet, Davies, Mohr, Schmidt 24

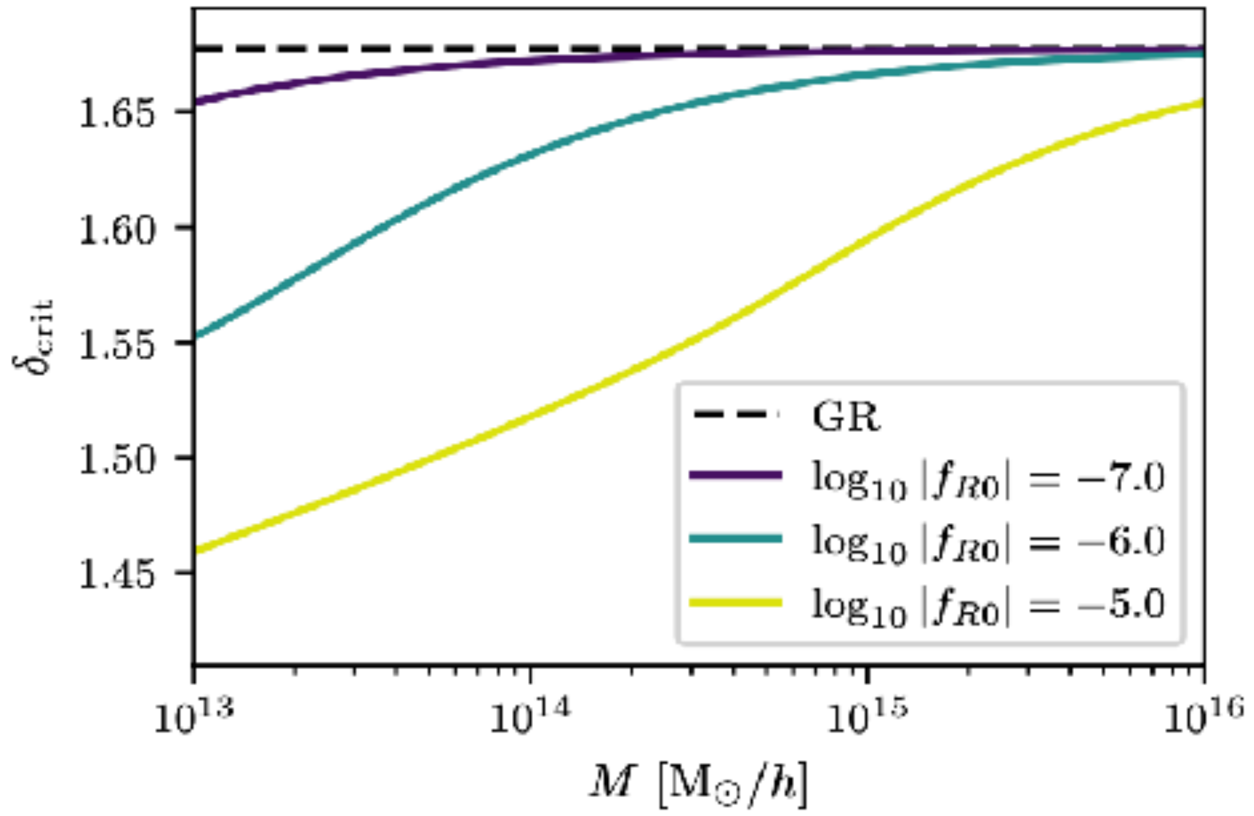

FIG. 1. The critical overdensity $\delta_{\rm crit}$ for spherical collapse in $f(R)$ gravity (Eq. (12)) for different values of $\log_{10}|f_{R0}|$ at collapse redshift $z_c = 0$ in colored solid lines. The dashed black line represents $\delta_{\rm crit}$ in a corresponding GR cosmology (Eq. (13)).

Outlook: Joint Constraints

SPT Cluster Abundance + DES 3x2 pt

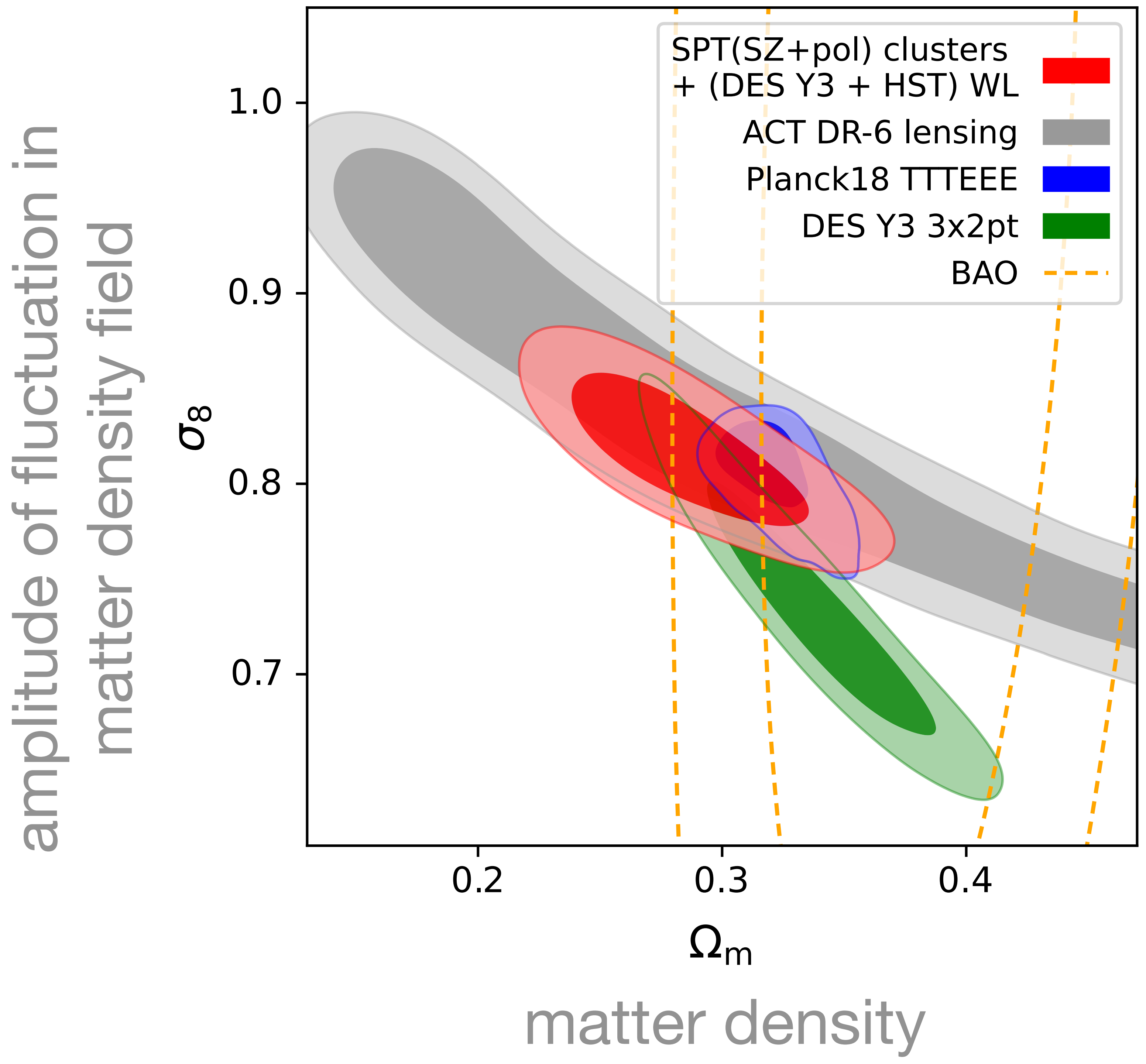

- Joint analysis
  - Cosmological covariance
  - Shared (lensing) systematics
  - Addressed w/
    Chun-Hao To, Elisabeth Krause, Sebastian Grandis
- Expect powerful constraints on z < 2 large-scale structure
- Ideal complement to high-redshift CMB measurements by *Planck*

Outlook: Joint Constraints

SPT Cluster Abundance + DES 3x2 pt

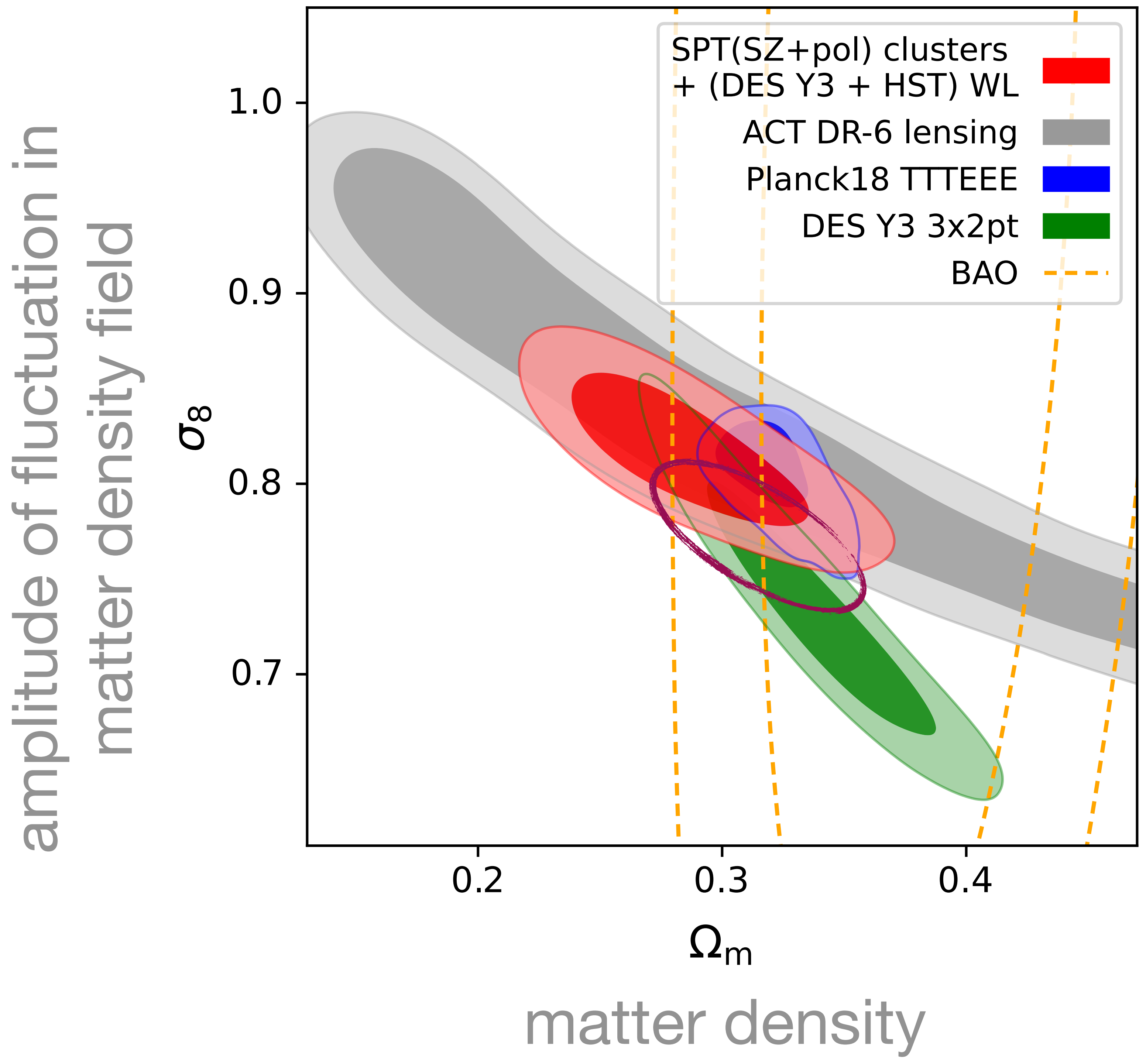

- Joint analysis
  - Cosmological covariance
  - Shared (lensing) systematics
  - Addressed w/
    Chun-Hao To, Elisabeth Krause, Sebastian Grandis
- Expect powerful constraints on $z < 2$ large-scale structure
- Ideal complement to high-redshift CMB measurements by *Planck*

The South Pole Telescope (SPT)

10-meter sub-mm quality wavelength telescope

90, 150, 220 GHz and
1.6, 1.2, 1.0 arcmin resolution

2007: SPT-SZ
960 detectors
90,150,220 GHz

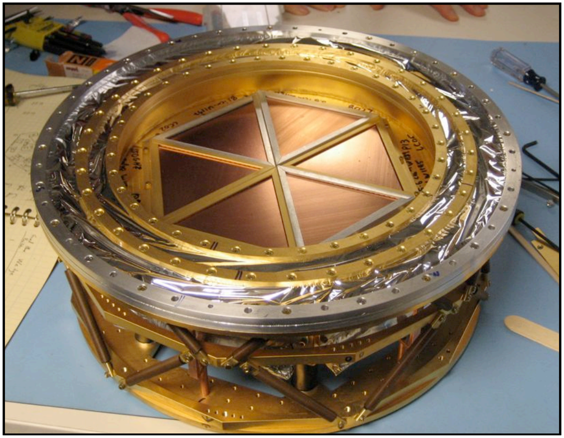

2012: SPTpol
1600 detectors
90,150 GHz
+Polarization

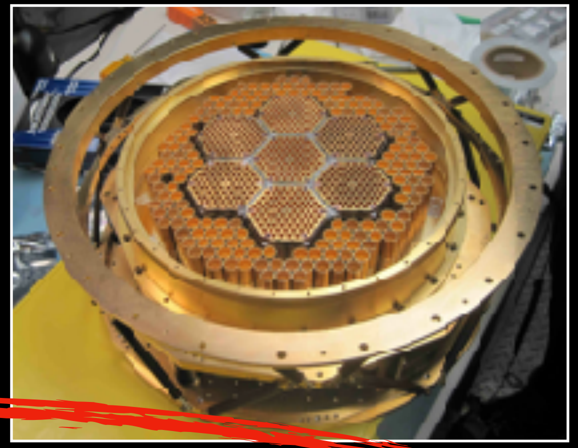

2017: SPT-3G
~15,200 detectors
90,150,220 GHz
+Polarization

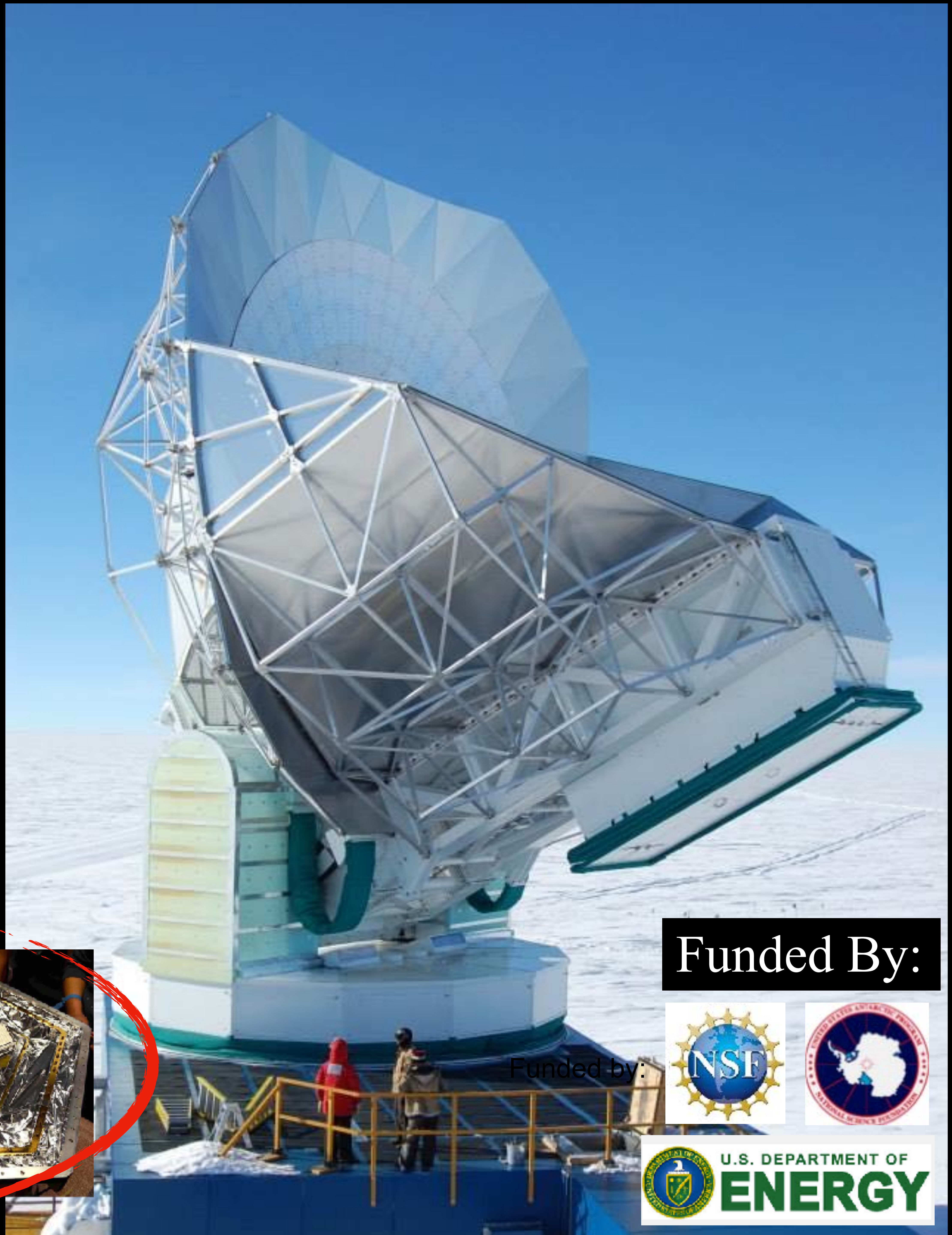

Funded By:

Funded by:

NSF

UNITED STATES ANTARCTIC PROGRAM · NATIONAL SCIENCE FOUNDATION

U.S. DEPARTMENT OF ENERGY

The 10,000 deg² SPT-3G Survey(s)

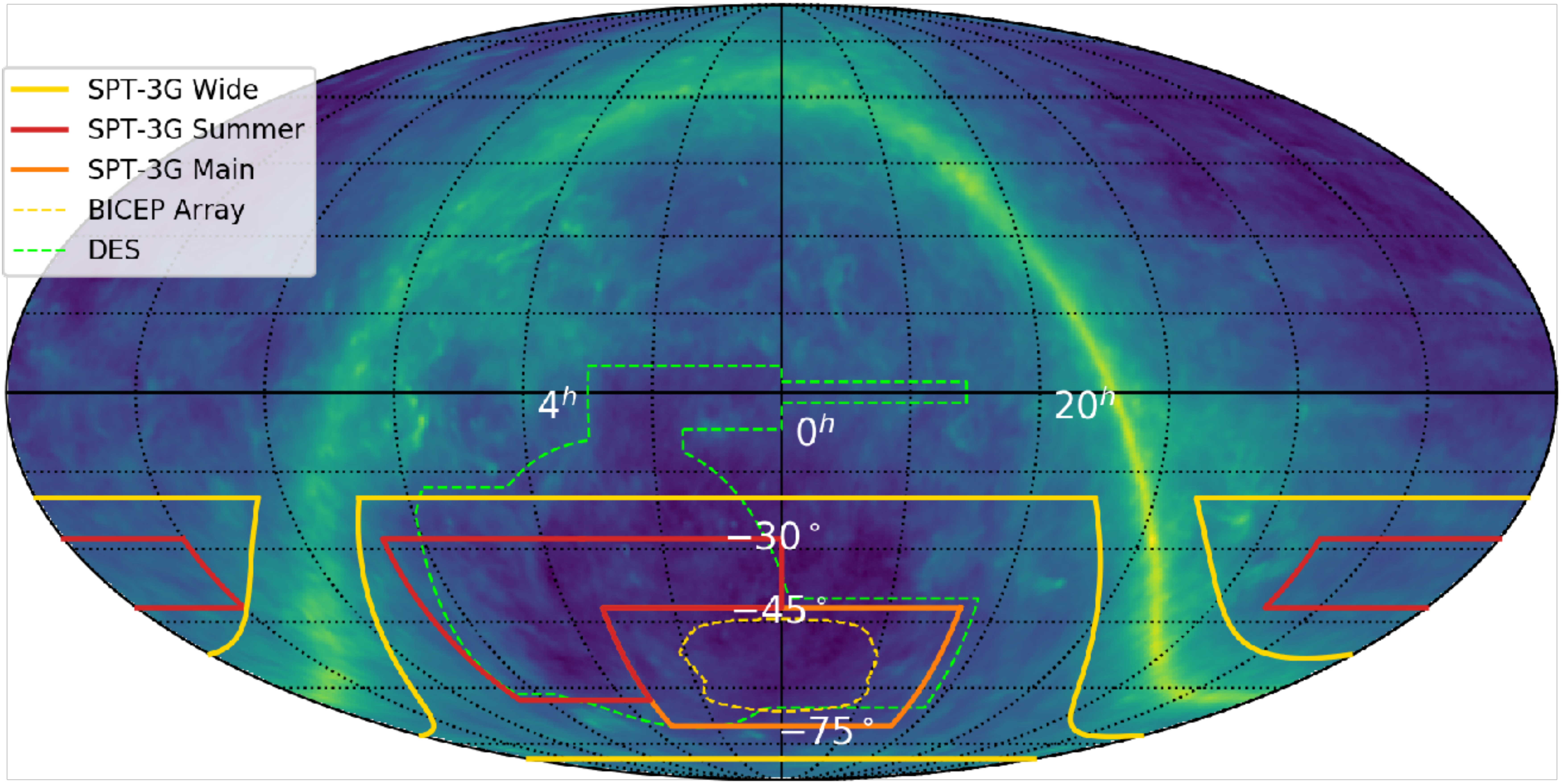

Survey	Area [deg^2]	Years observed	Noise level (T) [μK-arcmin] 95 GHz	150 GHz	220 GHz	Coadded
SPT-3G Main	1500	2019-2023, 2025-2026	2.5	2.1	7.6	1.6
SPT-3G Summer	2600	2019-2023	8.5	9.0	31	6.1
SPT-3G Wide	6000	2024	14	12	42	8.8

Wide is still 2—3 times deeper than SPT-SZ!

Slide from Lindsey Bleem

The 10,000 deg² SPT-3G Survey(s)

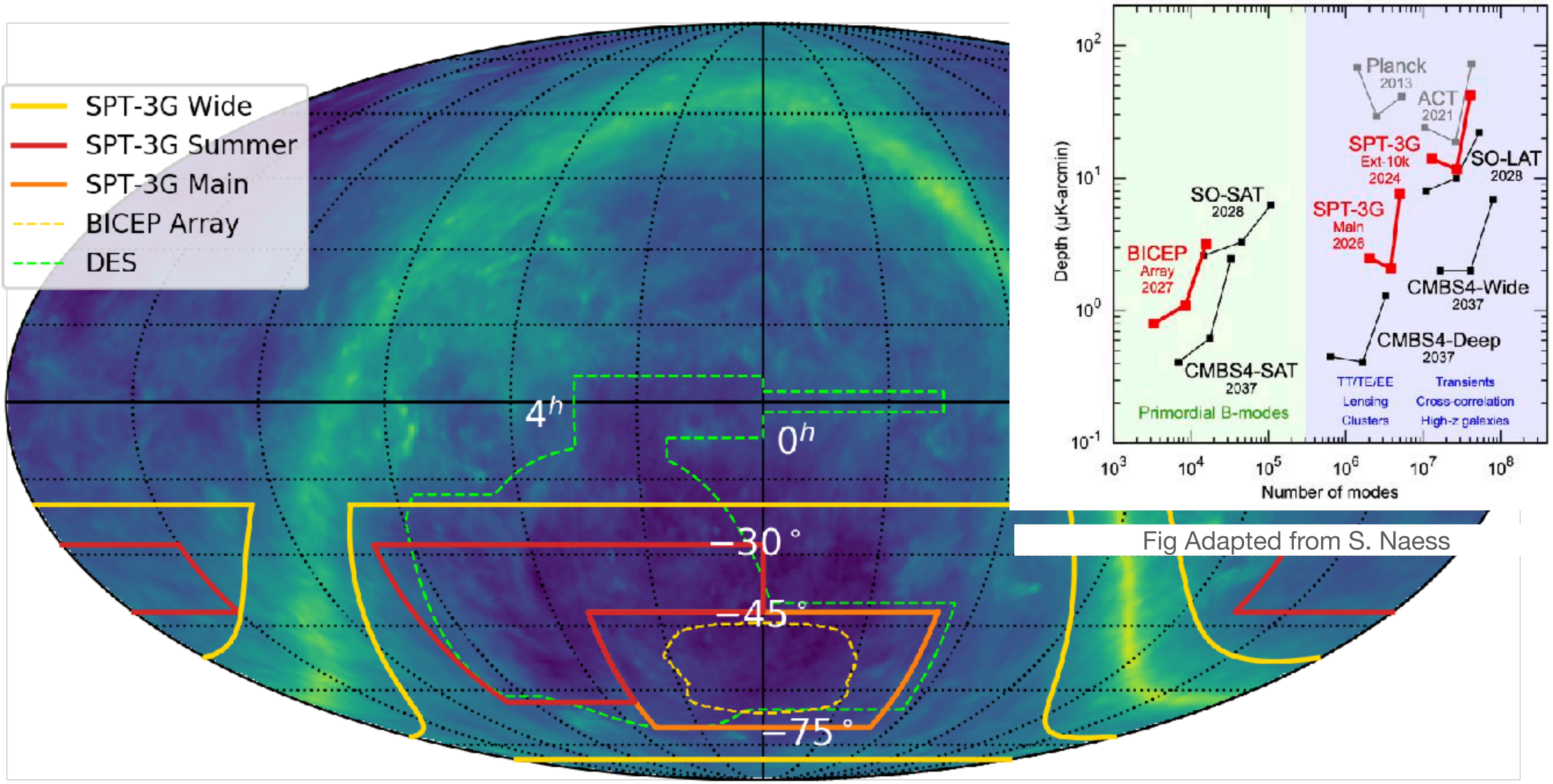

Fig Adapted from S. Naess

Survey	Area [deg^2]	Years observed	Noise level (T) [μK-arcmin]			
			95 GHz	150 GHz	220 GHz	Coadded
SPT-3G Main	1500	2019-2023, 2025-2026	2.5	2.1	7.6	1.6
SPT-3G Summer	2600	2019-2023	8.5	9.0	31	6.1
SPT-3G Wide	6000	2024	14	12	42	8.8

Wide is still 2—3 times deeper than SPT-SZ!

Slide from Lindsey Bleem

Summary

- Cluster abundance as a cosmological probe
- SZ-selection + weak-lensing mass calibration = excellent control over systematics
- Latest analysis of SPT (SZ+pol) clusters with DES Y3 + HST lensing is competitive and compatible with other probes
- Next few years will be spectacular (SPT-3G, advACT, SO, eROSITA, DES Y6, KiDS, HSC, Euclid, LSST, CMB-S4, etc.)

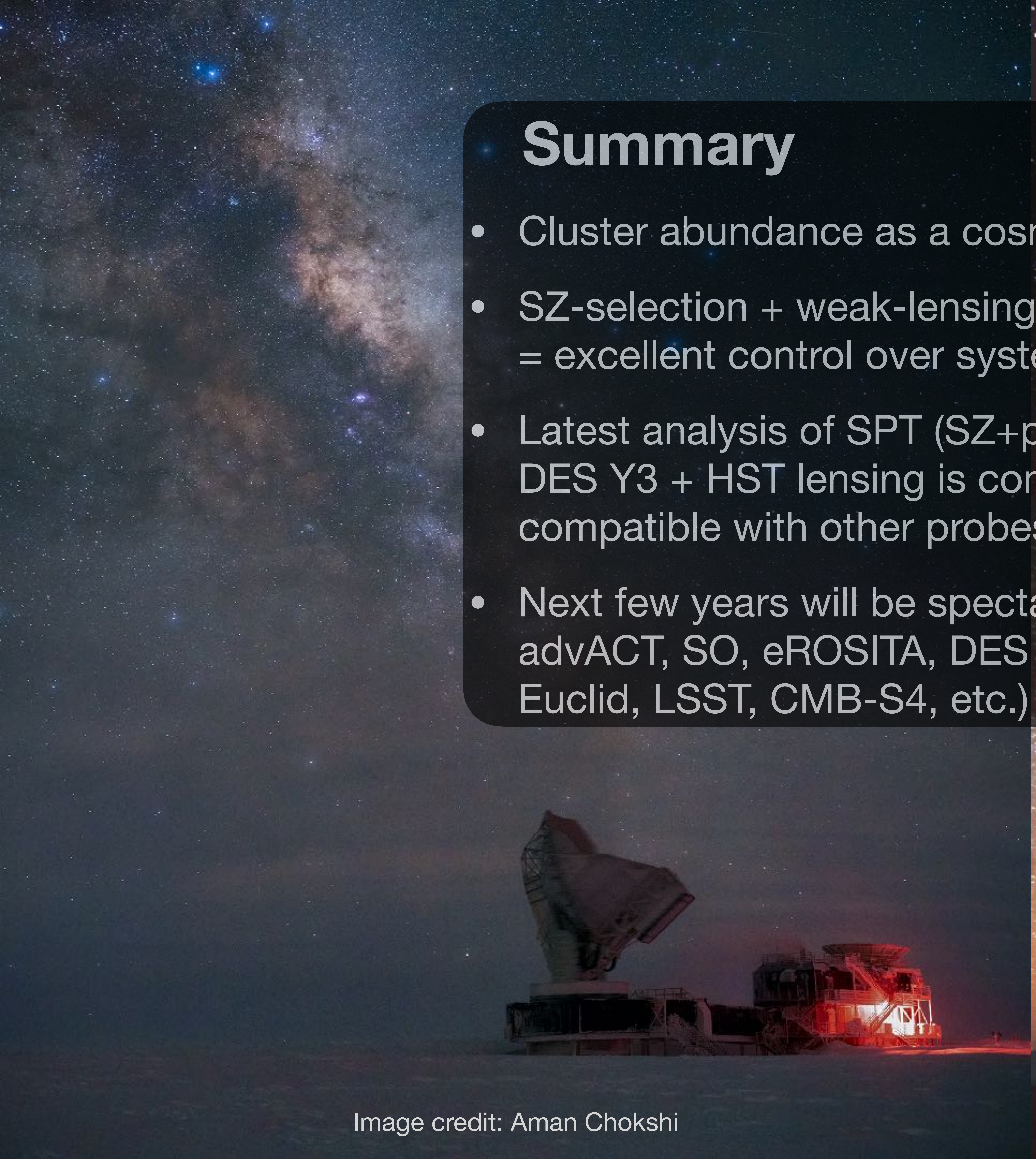

Image credit: Aman Chokshi

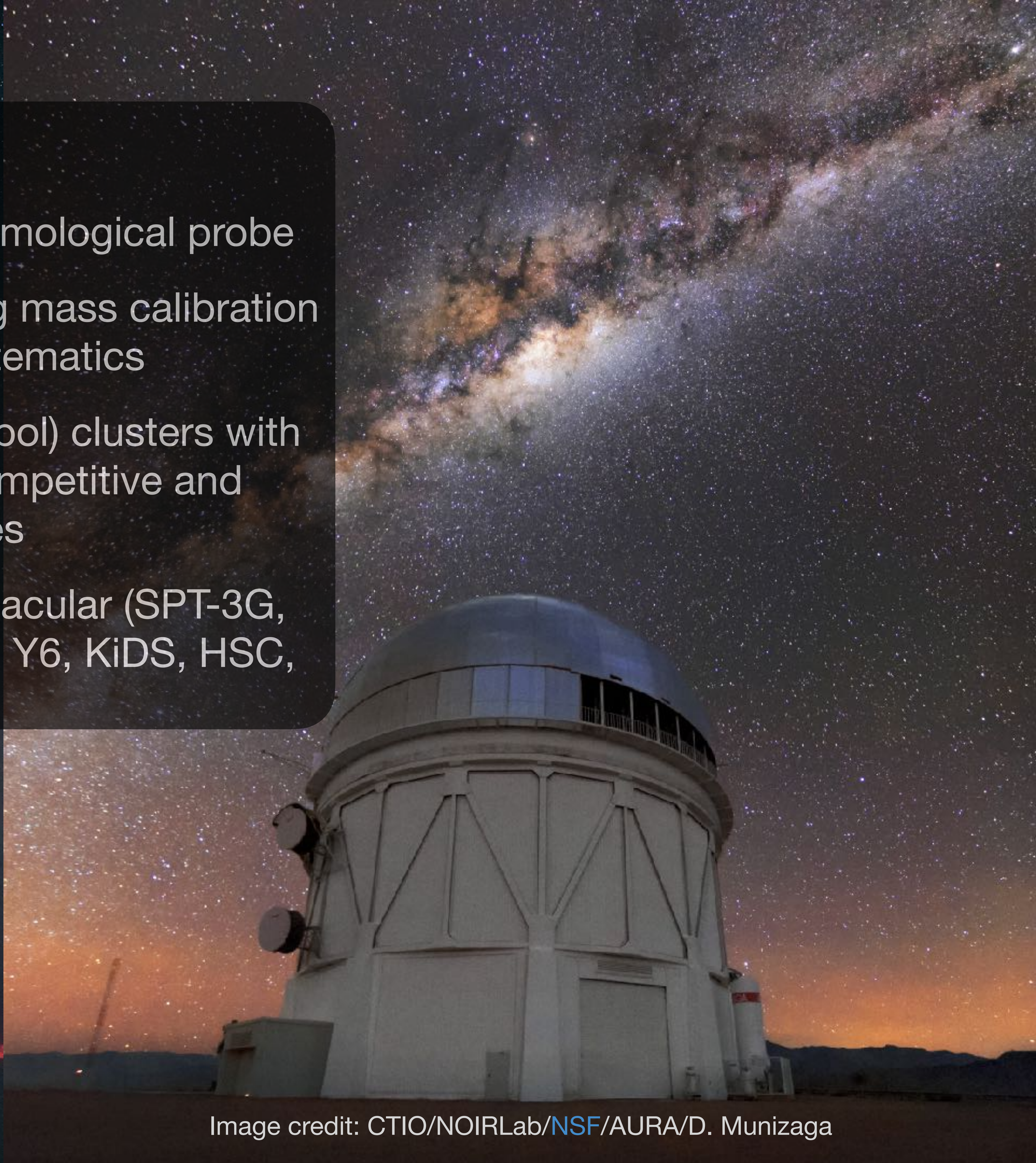

Image credit: CTIO/NOIRLab/NSF/AURA/D. Munizaga

Cluster Lensing Model

Grandis, Bocquet+21

- Simple model shear(*Mass*) based on NFW profile
- Biased and noisy estimator
  (e.g., Becker&Kravtsov 11)
- Solution: Introduce latent variable M_WL and establish M_WL—M_halo relation such that shear(M_WL) is unbiased
- establish M_WL—M_halo relation using hydrodynamic simulations to capture baryonic effects
- Incorporate all known sources of uncertainty in lensing measurements into M_WL—M_halo

Calibrate mean M_WL—M_halo relation and intrinsic scatter

$$\langle \ln\left(\frac{M_\mathrm{WL}}{M_0}\right)\rangle = b_\mathrm{WL}(z) + b_M \ln\left(\frac{M_{200c}}{M_0}\right)$$

$$\ln \sigma_{\ln M_\mathrm{WL}} = \frac{1}{2}\left[s_\mathrm{WL}(z) + s_M \ln\left(\frac{M_{200c}}{M_0}\right)\right]$$

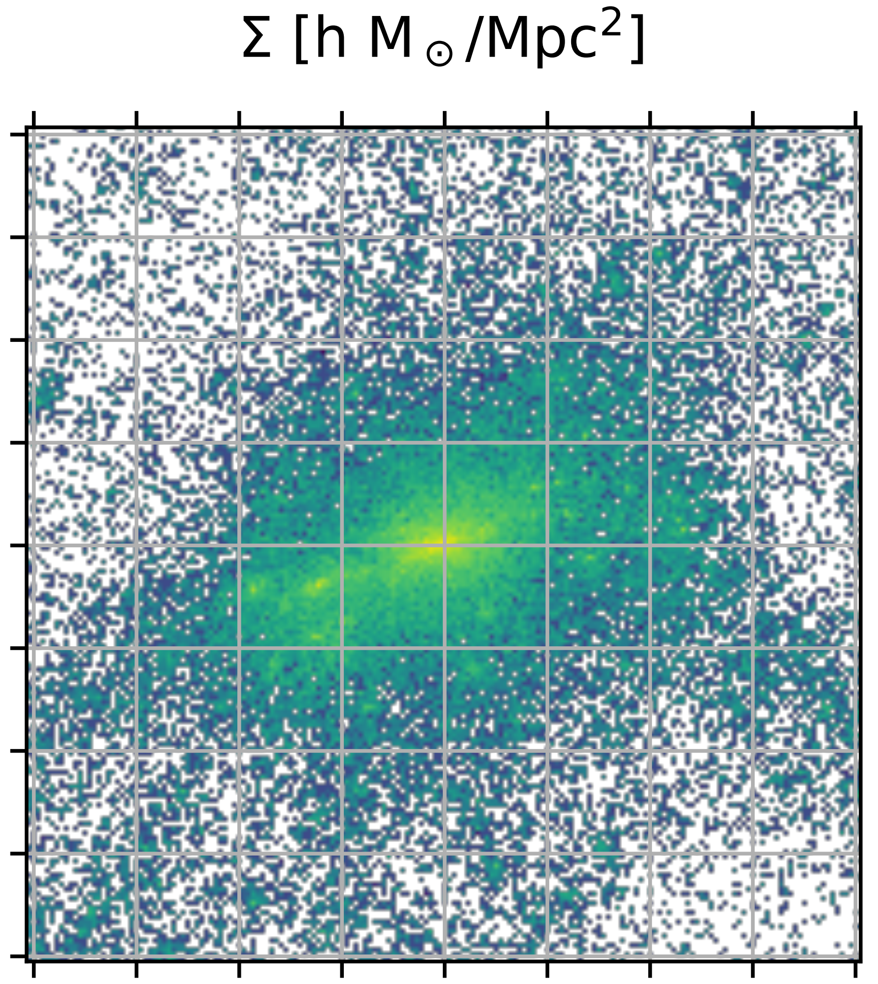

halo mass map
from hydro simulation

synthetic shear profile

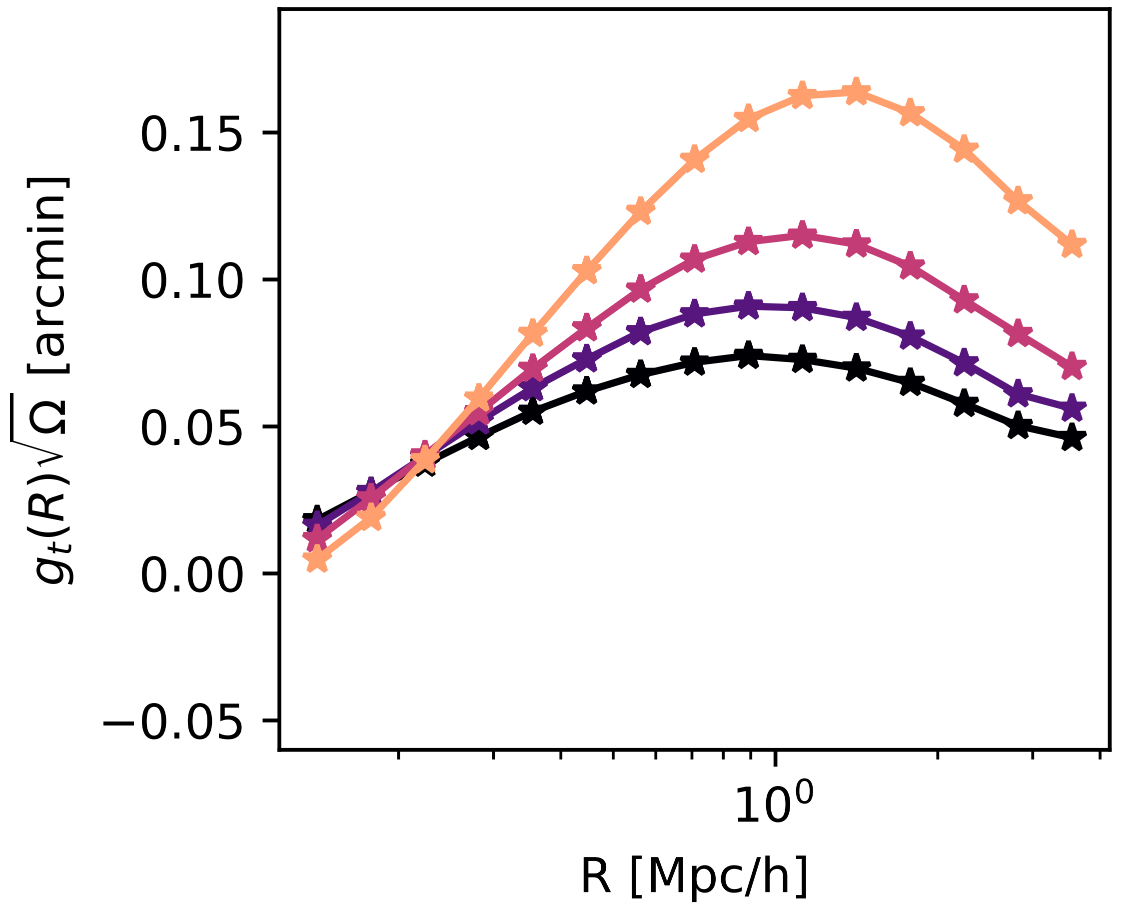

lensing mass

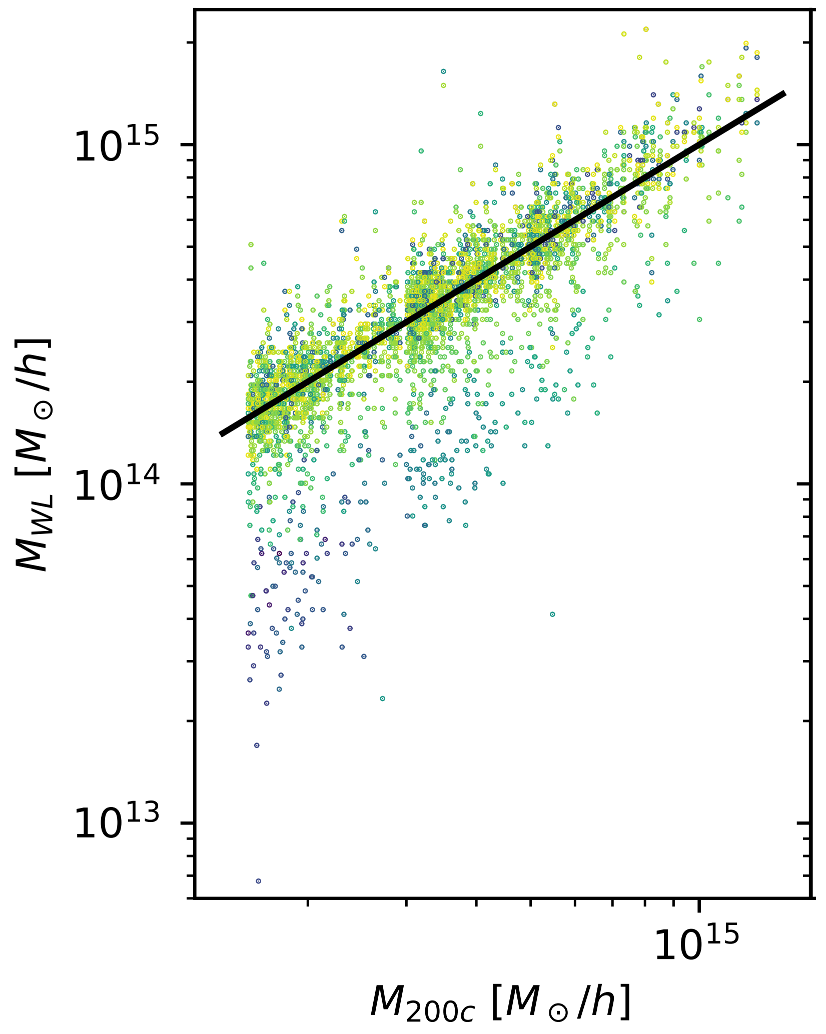

halo mass

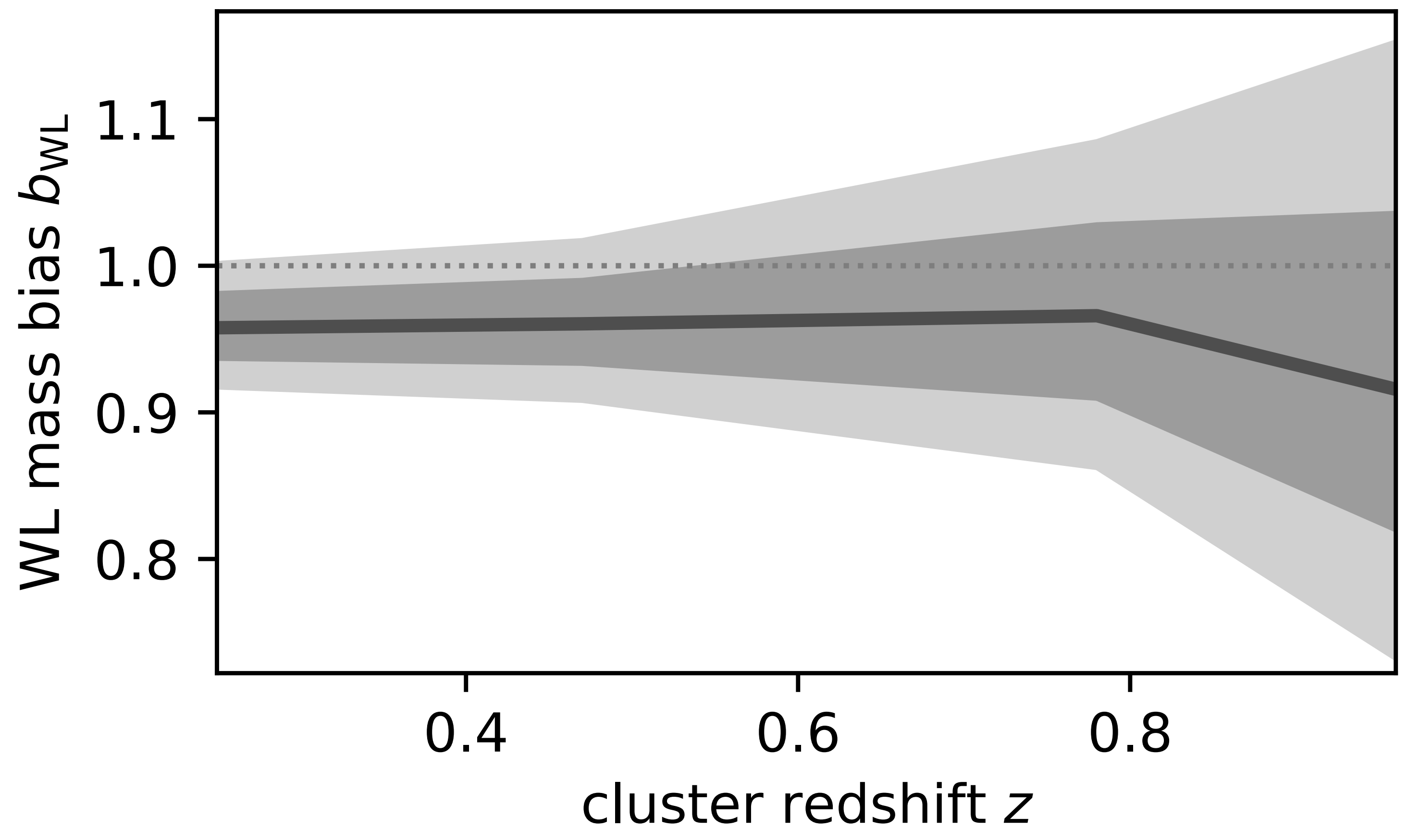


SRG/eROSITA
0.3-2.3 keV - RGB
IKI
MPE

Ghirardini+24

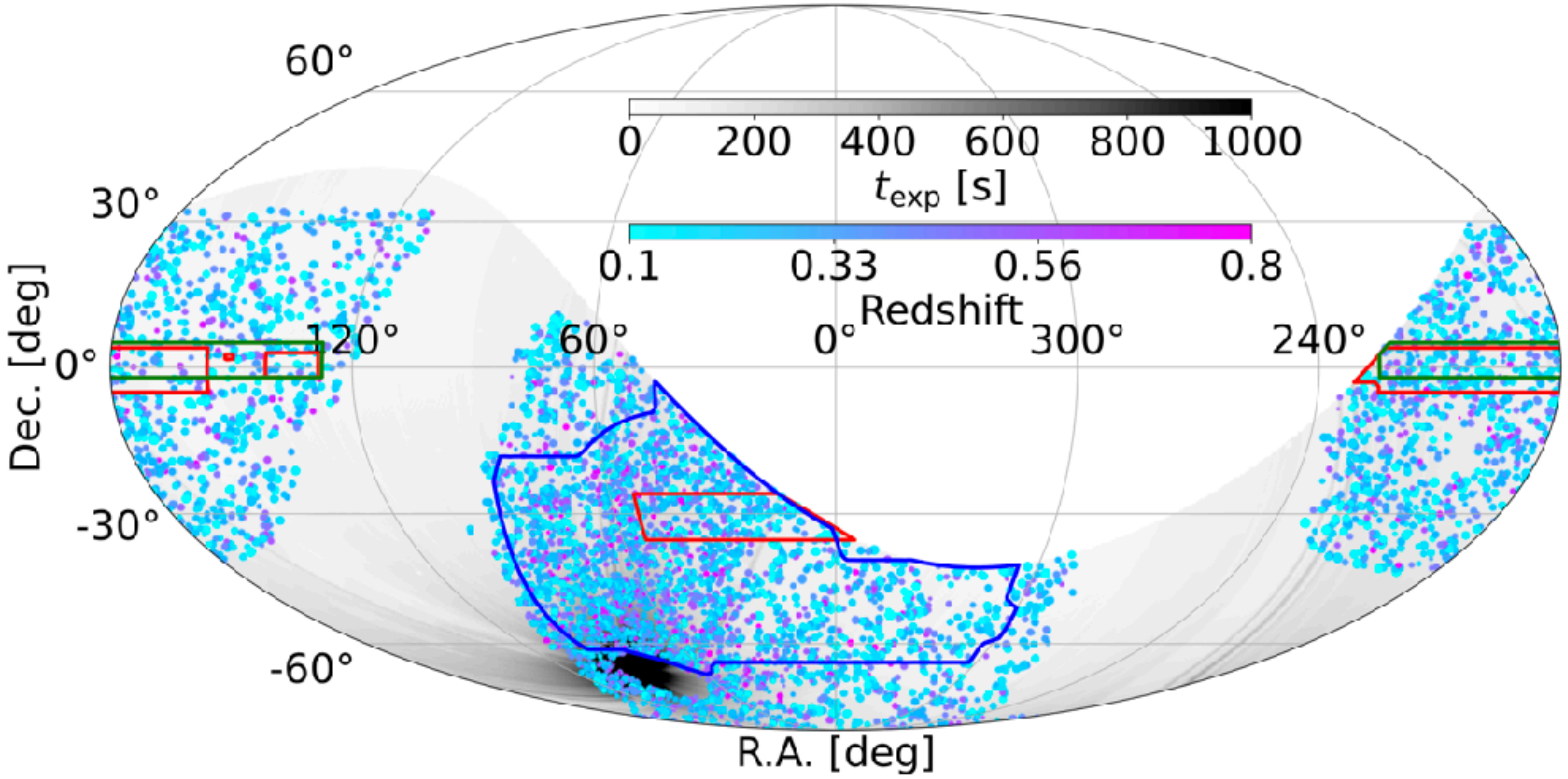

- 5,259 clusters over 12,791 deg2
- Low-redshift lenses
- DES Y3 lensing SNR = 65

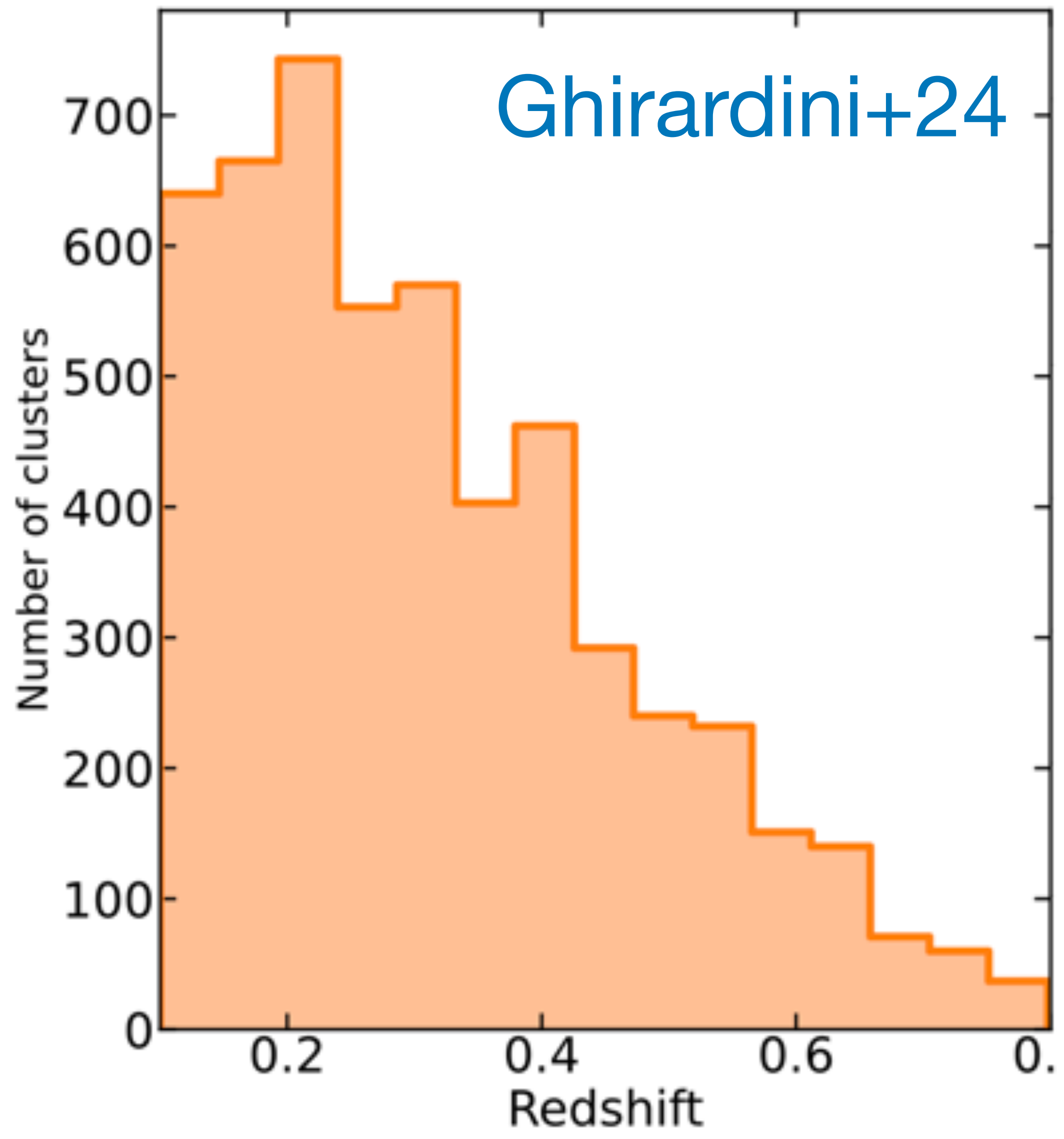

Ghirardini+24

EDSU Tools 2024

Grandis, Ghirardini, Bocquet+24

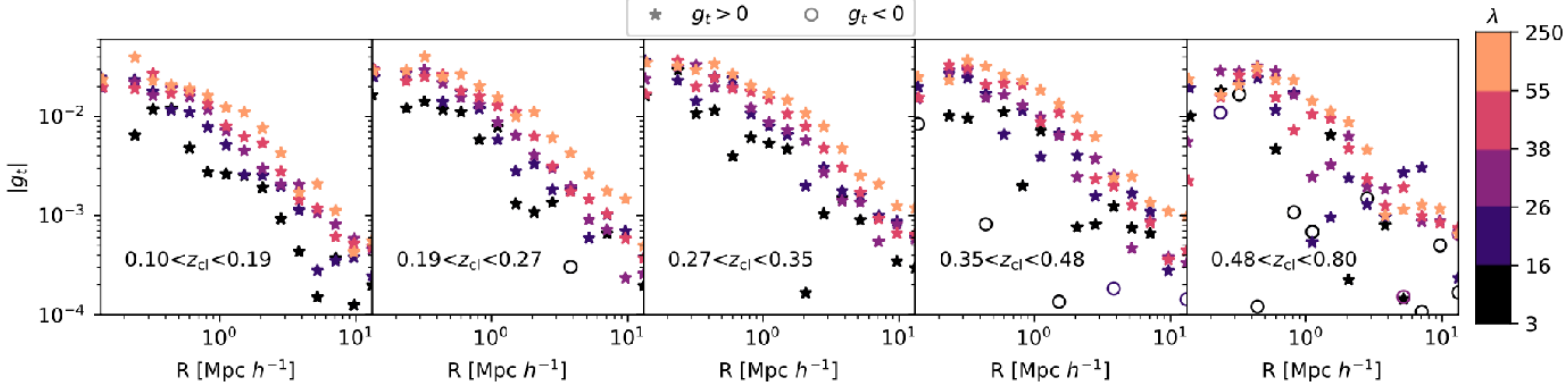

eRASS1 cluster abundance

>5,000 X-ray selected clusters

- Mass calibration driven by DES Year 3 lensing data (SNR 65) (Grandis, Ghirardini, Bocquet+24)
- eROSITA largely follows our approach
  - Individual cluster likelihoods
  - *M*wl—*M*halo relation
  - DES Year 3 lensing analysis
(but they also use KiDS and HSC data)
- Simultaneous constraints on Ω_m, σ_8, w, $\sum m_\nu$
- Cluster cosmology using ICM-selected clusters works!

Ghirardini+24

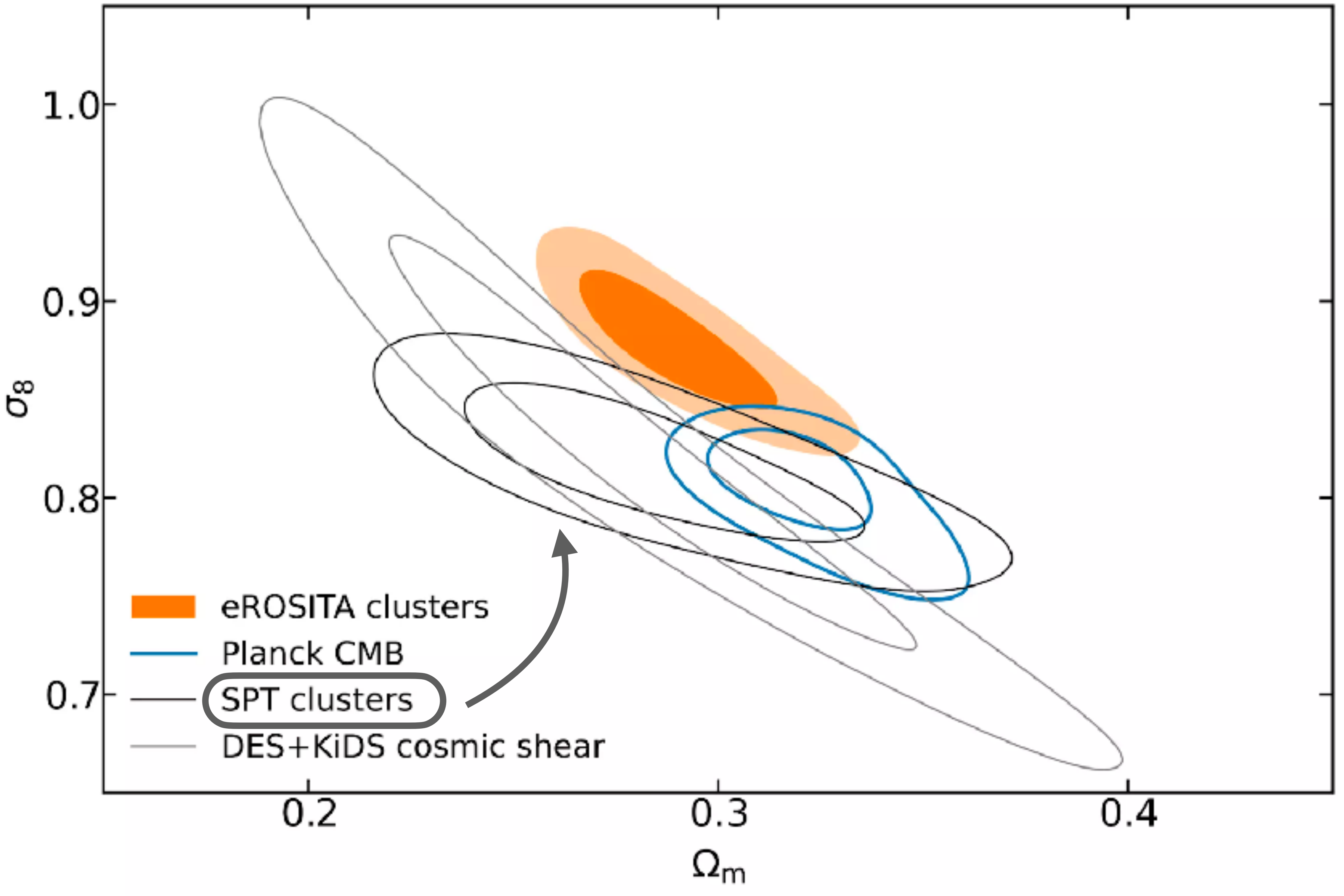

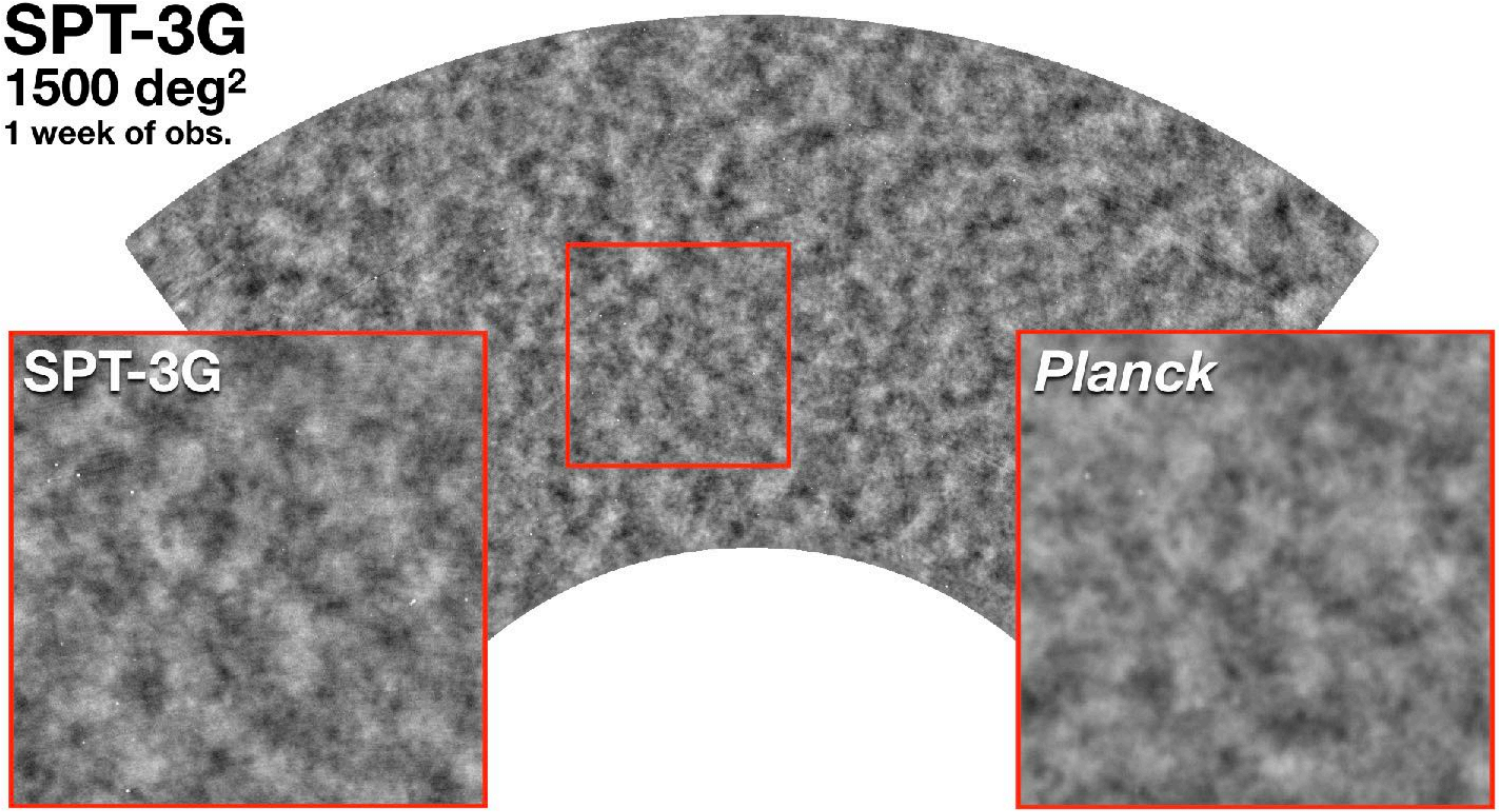

- ***SPT-3G data gets to ~Planck depth on 1500d field with a ~week of data.***
- ***Observe 1500d field every ~2 days for 6 years***

The SPT-3G SZ Catalog

- First catalog from 2019-2020 data
- Preliminary cluster run: > 2,400 cluster candidates at $\xi > 5$ (>99% purity)
- 5891 candidates at $3.85 < \xi <$ **130.2**(!)
- Candidates screened through DES, promising targets flagged for additional followup. A total of 12 nights of NIR followup with Magellan/FourStar of SPTpol 500d/SPT-3G cluster candidates has resulted in 124 SPT-3G cluster candidates with NIR imaging, analysis of these systems is ongoing

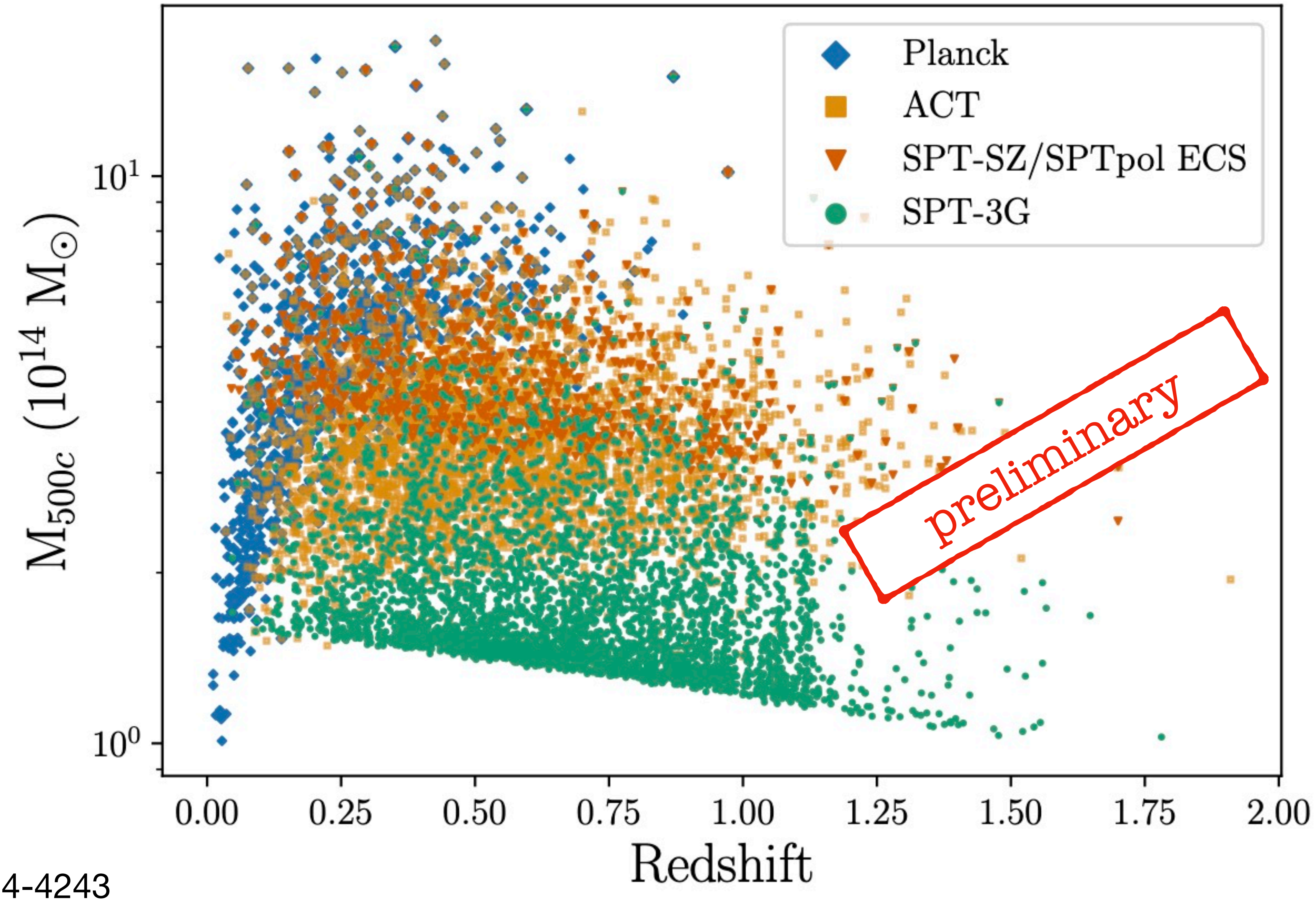

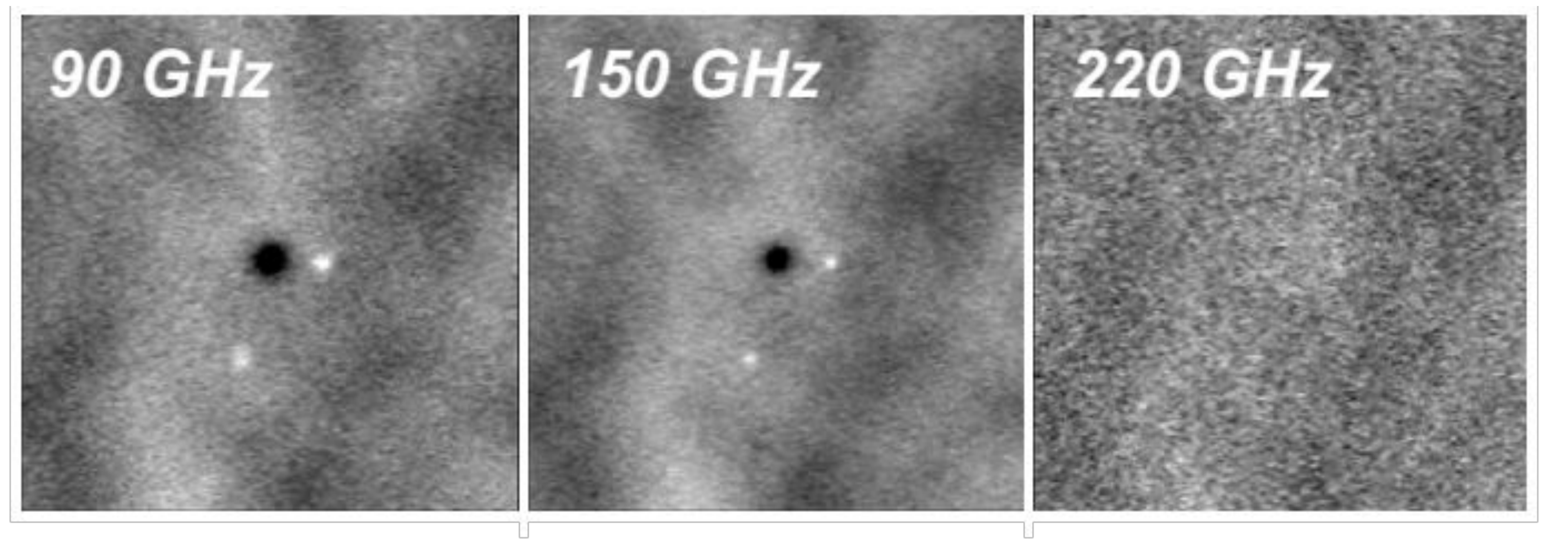

SPT-CL J2344-4243 (Phoenix Cluster, z=0.6) see in SPT-3G data at S/N>120

Slide adapted from Lindsey Bleem

SPT-3G

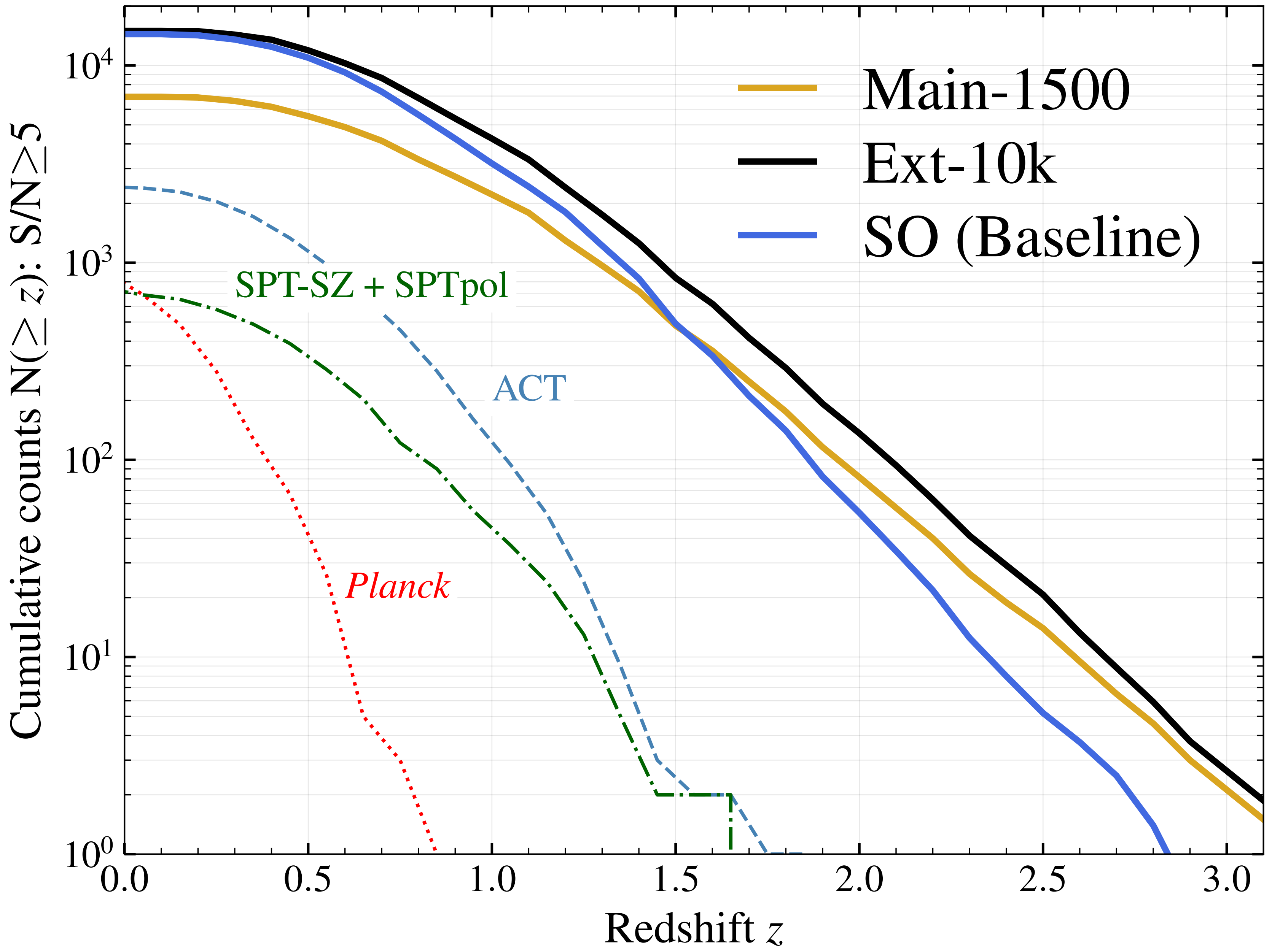

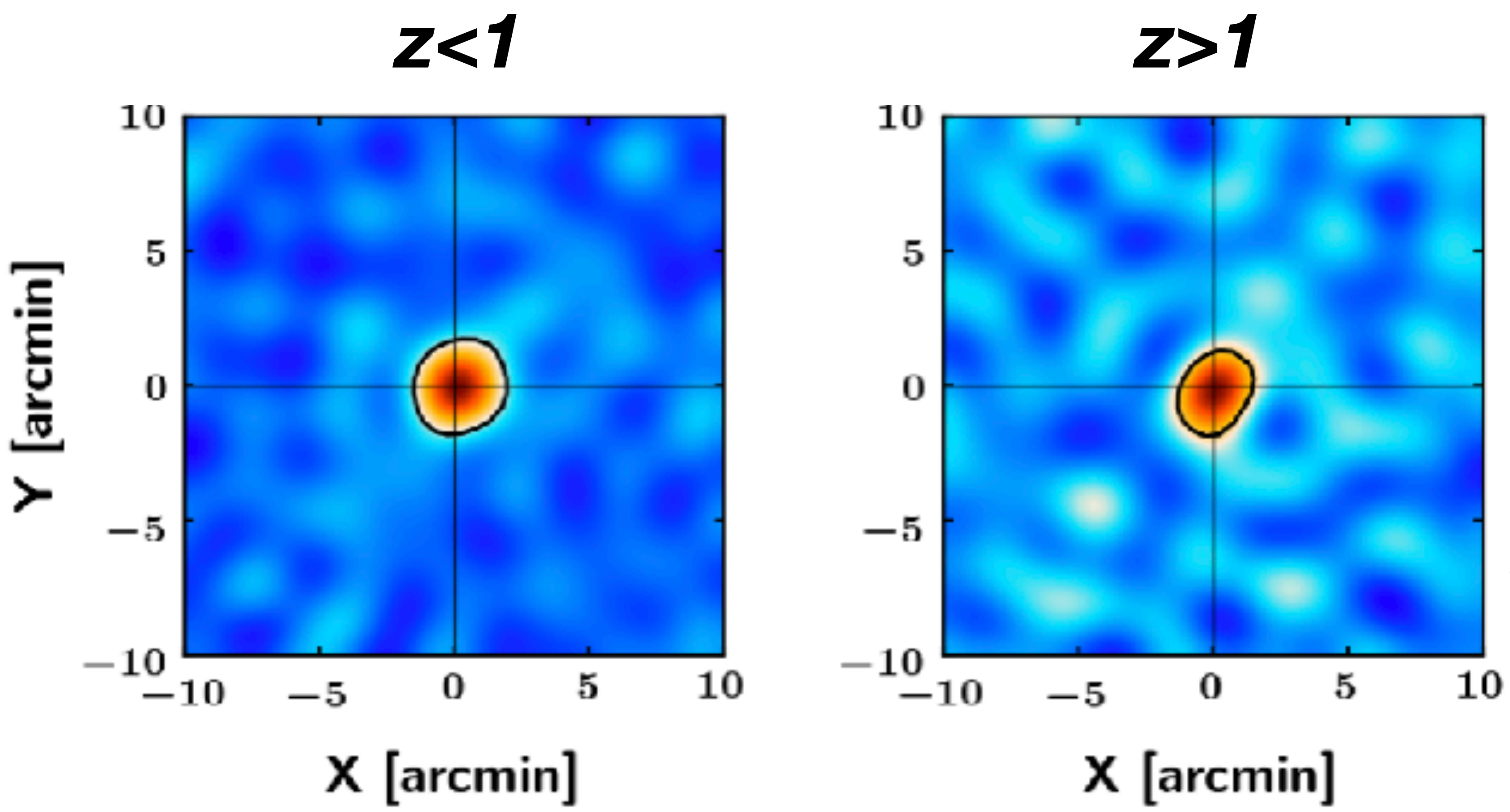

S. Raghunathan

High S/N (>30σ) detection of CMB cluster lensing!

S.Bocquet+L. Bleem

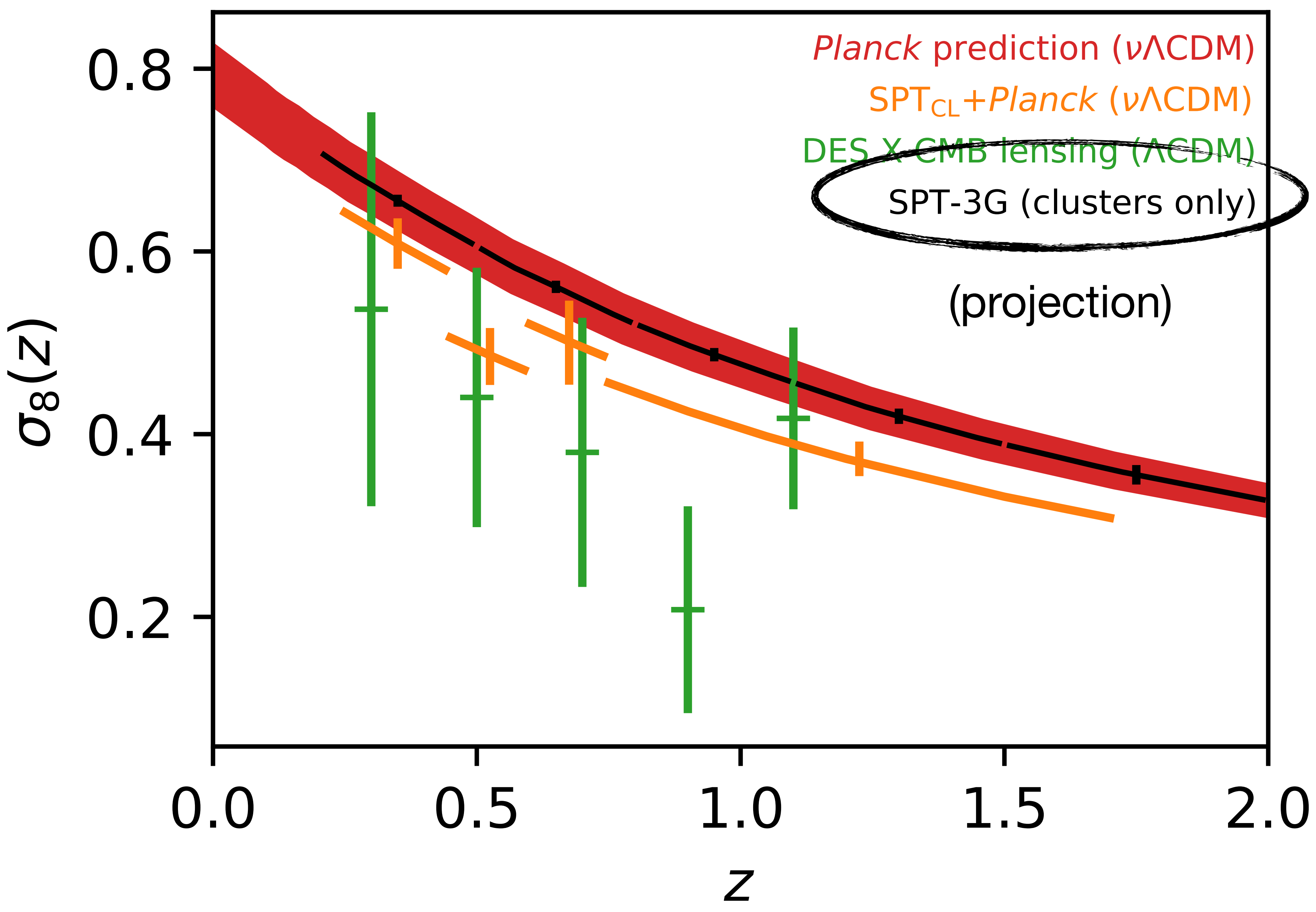

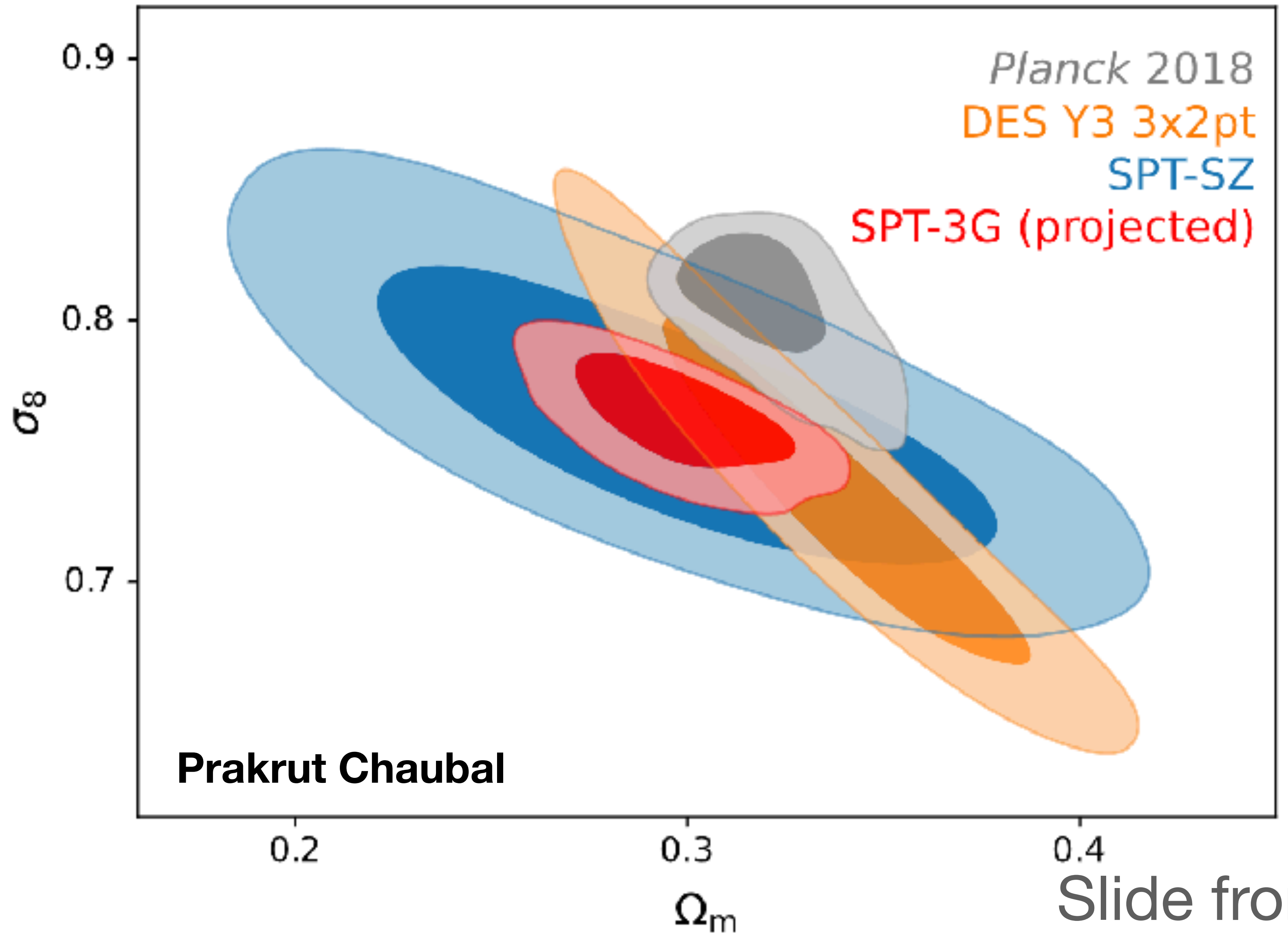

Prakrut Chaubal

Slide from Lindsey Bleem